PROBABILISTIC METHODS FOR ESTIMATING THE SEISMIC DEFORMATIONS OF UNDERGROUND STRUCTURES

A THESIS SUBMITTED TO
THE GRADUATE SCHOOL OF NATURAL AND APPLIED SCIENCES
OF
MIDDLE EAST TECHNICAL UNIVERSITY

BY

KADİR BUĞRA SOYMAN

IN PARTIAL FULFILLMENT OF THE REQUIREMENTS
FOR
THE DEGREE OF MASTER OF SCIENCE
IN
CIVIL ENGINEERING

JUNE 2018

Approval of the thesis:

PROBABILISTIC METHODS FOR ESTIMATING THE SEISMIC DEFORMATIONS OF UNDERGROUND STRUCTURES

submitted by **KADİR BUĞRA SOYMAN** in partial fulfillment of the requirements for the degree of **Master of Science in Civil Engineering Department, Middle East Technical University** by,

Prof. Dr. Halil Kalıpçılar _____
Dean, Graduate School of **Natural and Applied Sciences**

Prof. Dr. İsmail Özgür Yaman _____
Head of Department, **Civil Engineering Dept., METU**

Assoc. Prof. Dr. Zeynep Gülerce _____
Supervisor, **Civil Engineering Dept., METU**

Examining Committee Members:

Prof. Dr. Kemal Önder Çetin _____
Civil Engineering Department, METU

Assoc. Prof. Dr. Zeynep Gülerce _____
Civil Engineering Deptartment, METU

Asst. Prof. Dr. Onur Pekcan _____
Civil Engineering Department, METU

Asst. Prof. Dr. Nabi Kartal Toker _____
Civil Engineering Department, METU

Assoc. Prof . Dr. Berna Unutmaz _____
Civil Engineering Department, Hacettepe University

DATE: 12.06.2018

I hereby declare that all information in this document has been obtained and presented in accordance with academic rules and ethical conduct. I also declare that, as required by these rules and conduct, I have fully cited and referenced all material and results that are not original to this work.

Name, Last name: Kadir Buğra, Soyman

Signature :

ABSTRACT

PROBABILISTIC METHODS FOR ESTIMATING THE SEISMIC DEFORMATIONS OF UNDERGROUND STRUCTURES

Soyman, Kadir Buğra

MS., Department of Civil Engineering

Supervisor: Assoc. Prof. Dr. Zeynep Gülerce

June 2018, 100 pages

In seismic design of underground structures, simplified semi-deterministic methods based on the stiffness of the soil and the underground structure are used to estimate the seismic deformations. Generally, peak ground acceleration (PGA) value for different hazard levels are provided by the probabilistic seismic hazard assessment (PSHA) analysis, but a single (and deterministic) PGA value is employed in deformation calculations. The objective of this study is to propose a fully probabilistic framework for estimating the free field deformations (Δ_{ff}) of underground infrastructure, especially the metro stations. For this purpose, stations of two metro lines planned to be constructed in Istanbul are used as case studies. A new seismic source characterization model (SSC) is developed for the segments of North Anatolian Fault Zone that are close to metro stations. This SSC model is combined with current global and regionalized ground motion prediction models in PSHA framework to estimate the design ground motions. Simplified soil profiles of metro stations are developed and incorporated into 1-D equivalent linear (EQL) analysis. Using analysis results, two prediction models are developed for estimation of Δ_{ff}. According to performance-based earthquake engineering framework (PBEE), these models are incorporated into the hazard integral to provide annual rate of exceedance for specified Δ_{ff} levels and 475-year return period Δ_{ff} values are estimated for each station. Analysis results show that the 475-year return period Δ_{ff} values are significantly different than the Δ_{ff} values

calculated by current semi-deterministic methods, indicating that fully probabilistic approach should be utilized in seismic design of underground structures.

Keywords: Underground structures seismic deformations, Probabilistic Seismic Hazard Analysis, Equivalent Linear Analysis, Performance Based Earthquake Engineering.

ÖZ

GÖMÜLÜ YAPILARIN SİSMİK DEFORMASYONUNUN BELİRLENMESİ İÇİN OLASILIKSAL YÖNTEMLER

Soyman, Kadir Buğra

Yüksek Lisans, İnşaat Mühendisliği Bölümü

Tez Yöneticisi: Doç. Dr. Zeynep Gülerce

Haziran 2018, 100 sayfa

Gömülü yapılar için sismik deformasyonların belirlenmesinde zeminin ve gömülü yapıların esneklik ve esnemezlik faktörlerine dayanan basit yarı deterministik methodlar yaygın olarak kullanılmaktadır. Genel olarak, farklı tehlike seviyeleri için maksimum yer ivmesi değerleri (PGA) olasılıksal sismik tehlike analizi (OSTA) ile elde edilmesine rağmen deplasman hesaplarında tek (deterministik) PGA değeri kullanılmaktadır. Bu çalışmanın amacı, gömülü yapılar için sismik deplasman hesaplanmasında kullanılabilecek olasıksal bir yaklaşım önermektir. Bu amaçla İstanbul Bölgesinde inşaası planlanan iki adet metro hattının istasyonları örnek çalışma olarak ele alınmıştır. Metro istasyonlarına yakın olan Kuzey Anadolu Fay Zonu bölümleri için yeni bir sismik kaynak modeli geliştirilmiştir. Bu sismik kaynak modeli, mevcut global ve yerelleştirilmiş yer hareketi tahmin modelleri ile birleştirilerek metro istasyonları için OSTA yapılmış ve tasarım yer hareketleri belirlenmiştir. Metro istasyonları için basitleştirilmiş zemin profilleri geliştirilmiş ve profiller 1-D Eşdeğer Doğrusal Zemin Tepki Analizlerinde kullanılmıştır. Analiz sonuçları kullanılarak serbest yer deplasmanı (Δ_{ff}) için iki adet tahmin denklemi geliştirilmiştir. Bu modeller, performansa dayalı deprem mühendisliği çerçevesine göre, çeşitli Δ_{ff} seviyeleri için yıllık aşılma oranını belirlemek amacıyla sismik tehlike integraline dahil edilmiştir ve her istasyon için 475 yıllık aşılma olasılığına denk gelen

Δ_{ff} değerleri belirlenmiştir. Analiz sonuçlarına göre 475 yıllık aşılma olasılığına denk gelen Δ_{ff} değerlerinin, yarı deterministik mevcut metodlar kullanılarak belirlenen Δ_{ff} değerlerinden oldukça farklı olduğu belirlendiğinden, gömülü yapıların sismik dizaynında tamamen olasıksal yaklaşımların kullanılması önerilmektedir.

Anahtar kelimeler: Gömülü yapıların sismik davranışı, Olasılıksal Sismik Tehlike Analizi , Eşdeğer Doğrusal Analizler, Performansa Dayalı Deprem Mühendisliği.

To my beloved family

To my second mother (grandmother), Müzeyyen Uğurlu

ACKNOWLEDGEMENTS

First of all I would like to thank to my supervisor Assoc. Prof. Dr. Zeynep Gülerce for her limitless patience and support during my study. I would like to thank to Prof. Dr. Nuretdin Kaymakçı for his guidance and understanding during preparation of two academic papers which are published about this thesis.

I am very thankful to Yuksel Project International Company for whole support during my studies, especially my chief Cihat Güner. All the employees of the company have contributed to this thesis by sharing their experience, studies and informations about the projects. I would also like to express my respect for Dr. Zeynep Çekinmez Bayram for her constructive comments and suggestions on my study.

The other committee members: Prof. Dr. Kemal Önder Çetin, Assist. Prof. Dr. Nabi Kartal Toker, Asst. Prof. Dr. Onur Pekcan, Assoc. Prof . Dr. Berna Unutmaz greatly assisted me through their insightful comments in shaping the final draft of this study. I am very thankful to them for spending their time and efforts.

My family deserves the greatest thanks for supporting me to start master degree after graduation and helping me in my most difficult times.

I would like to give special thanks to my friend, Şeyda Bağcıl for all support during my studies and her beliefe that I will complete my studies. It is my greatest gratitude to have one of the greatest thanks for bringing me the position to complete this work from the situation which we met.

Finally, I would like to give my thanks to one of the most important women in my life, Müzeyyen Uğurlu, my second mother (grandmother) who I lost during my studies, for her all support of during my bachelor and master studies in my life. If she does not believe me, it is impossible to complete my study in METU. You will be with me all my life. This study has been dedicated to her.

TABLE OF CONTENTS

LIST OF TABLES

TABLES

LIST OF FIGURES

FIGURES

CHAPTER 1

INTRODUCTION

International Association of Public Transport defines the metro systems as passenger transport systems that are *"operated on their own right of way and segregated from general road and pedestrian traffic"*. The difference of metro from other line systems is that the metro always runs on a grade-seperated exclusive right-of-way which does not have any access from pedestrians and other traffic. Additionally, metro systems have higher service frequencies, higher passenger volumes, and different type of cars compared to other rail systems. The oldest metro line was opened in London in 1863. Although London is known to have the longest metro network (402 kilometers in line and 270 metro stations), the longest metro network actually exists in Shangai with 632.1 kilometers of rail line and 394 metro stations. The first metro system was constructed in Istanbul in 1875, only 12 years after the London Metro Line. After the construction of Beyoğlu-Karaköy Tunnel Füniküler Line, the second metro line, İstiklal Street Tramway was opened 115 years later. According to Metro Istanbul (accessed through http://www.istanbulunmetrosu.com), Turkey owned 45.10 kilometres rail lines until 2004 and it is planned that Turkey will have 160.55 kilometers of metro lines until 2018. According to Metrobits, Turkey currently has 105.9 kilometers of metro lines with 82 stations and these numbers are increasing rapidly, mostly in Istanbul.

Cut and cover box structures are generally used in the transportation projects for mass transit such as metro stations. These structures are generally embedded and surrounded by soil in three or more sides. The behaviour of this type of structures under seismic loads is controlled by deformations and inertial response of soil that encloses the structure (Wang, 1993; Wu and Penzien, 1994; Hashash et al., 2001). Compared to the seismic response of other structures, performance of cut and cover

structures is better during seismic events (Arango, 2008; Hashash et al., 2001). The Bay Area Rapid Transit in San Francisco and the Los Angeles Metro did not suffer significantly from the 1989 Loma Prieta and 1994 Northridge earthquakes in terms "of permanent damage. Until 1995, there was no evidence of underground structures experiencing seismic damage. In 1995, Daikai Station collapsed during the Hyogoken-Nambu (Kobe) earthquake. Investigations after the earthquake showed that the failure was attributed to insufficiency in the reinforcement of the columns (Iida et al., 1996; Parra-Montesinos et al., 2006). According to Iida et al. (1996), high relative displacement between the top and bottom slabs induced a larger horizontal shear force over the central column than expected and the overburdened soil mass influenced the seismic response of structure by increasing the inertial forces. Although underground structures have a relatively good performance during seismic events, collapse of Daikai Subway Station shows that the seismic loads have to be considered in the design stage of underground structures.

Istanbul is under significant seismic hazard and risk, expecting the next big earthquake in the next 20 years (Parsons, 2004). Therefore, new metro lines and station infrastructures have to be designed considering the seismic hazards and design ground motions. Recently, the Turkish Earthquake Code had been updated by the Department of Earthquake Directorate of AFAD and the new Turkish Seismic Hazard Map will enter into force on January 1, 2019 (accessed through https://www.afad.gov.tr/en/26735/Turkeys-New-Earthquake-Hazard-Map-is-Published). The new Turkish Seismic Hazard Map is developed using a fully probabilistic seismic hazard analyses (PSHA) approach and it provides the design ground motions for 475 and 2475-year return periods for different site classes. On the other hand, the earthquake resistant design practice for underground structures, especially Level 1 and Level 2 Methods are mostly deterministic (as explained below) and requires an adjustment to fit in to the new and probabilistic seismic design practice of Turkey.

1.1 Level 1 Methods for Earthquake Resisting Design of Metro Tunnels and Stations

Underground tunnels are exposed to three primary modes of deformation according to Owen and Scholl (1981): i) axial deformation, ii) curvature deformation, iii) the ovaling / racking deformation. Axial and curvature deformation is observed in the horizontal or nearly horizontal linear tunnels (Figure 1.1). Seismic waves that propogate in parallel or in transverse to the tunnel axis cause axial and curvature deformation along the longitudinal axis of the tunnel. The behaviour of the tunnel, formation of the axial and curvature deformation can be represented by an elastic beam under the effect of deformation or strain which are caused by the surrounding ground.

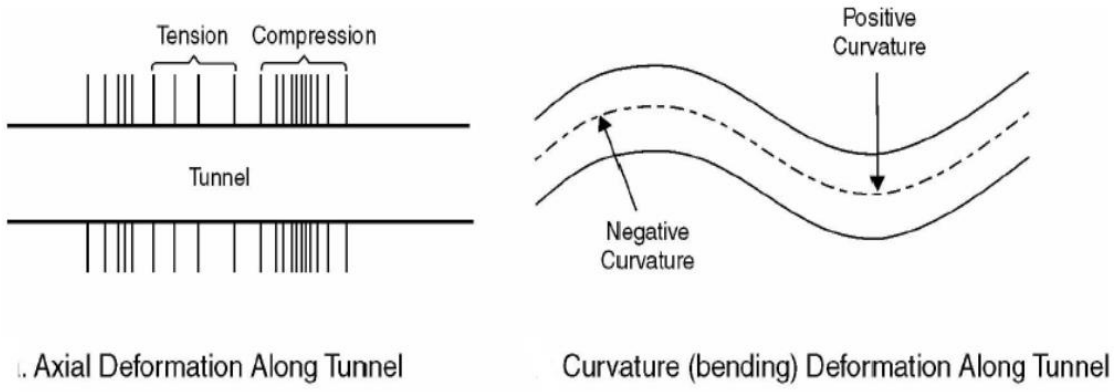

Figure 1.1 Idealized representations of axial and curvature deformations (US Department of Transportation Federal Highway Administration, 2009)

Ovaling and racking deformations are caused by horizontal seismic waves whose wave propogation is perpendicular or nearly perpendicular to the tunnel axis which results in distortion on the cross sectional shape of the tunnel lining (Wang, 1993). Therefore, the tunnel's cross section in transverse direction is most critical in seismic design. The approximate shape of the ovaling distortion and the racking deformation on rectangular shaped tunnels is shown in Figure 1.2. For rectangular cross sections, the differential deformation between the top and the bottom slab is defined as free field deformation (Δ_{ff}). In geotechnical engineering practice, free field is defined as the

ground surface, however in this study, terminology is a little bit different as shown in Figure 1.3.

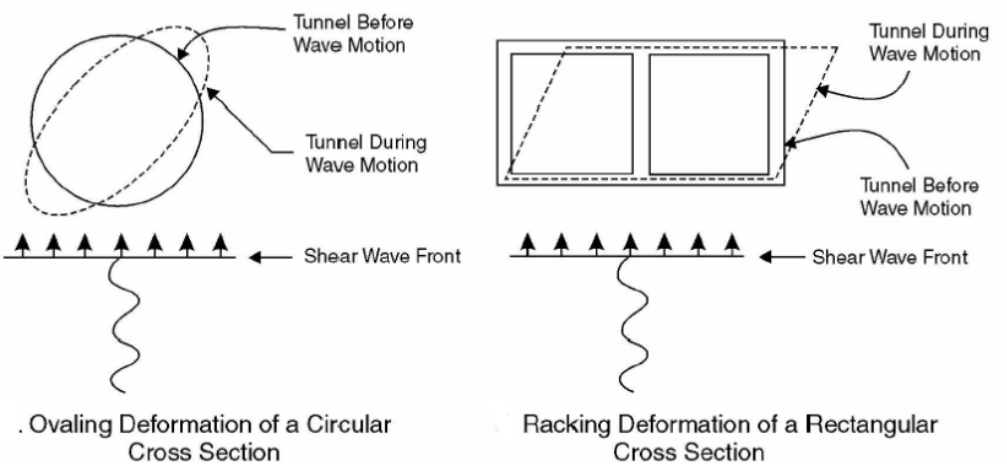

Figure 1.2 Ovaling deformation of circular cross section and Racking Deformation of rectangular cross section behaviour (US Department of Transportation Federal Highway Administration, 2009)

Newmark (1968) and Hendron (1985) proposed a simplified approach to estimate Δ_{ff} based on the assumption that the wave propagation occurs in a homogeneous, isotropic and elastic media. This approach can be used in the absence of detailed site response analysis since the estimates are reasonable for homogeneous soils and rocks (FHWA, 2009). However, change in the ground motion along the vertical soil profile is ignored; therefore, this approach provides conservative results for deeper structures. For a buried structure as shown in Figure 1.3, Δ_{ff} is calculated by using maximum free field shear strain (γ_{max}) and height of structure (h_1, h_2) as given in Equations 1.1 to 1.4.

$$\gamma_{max} = \frac{V_s}{C_{se}} \quad 1.1$$

$$C_{se} = \sqrt{\frac{G_m}{\rho}} \quad 1.2$$

$$\Delta_1 = h_1 \times \tan(\gamma) \quad 1.3$$

$$\Delta_2 = h_2 \times \tan(\gamma) \quad 1.4$$

In Equations 1.1 to 1.4, V_S is peak particle velocity, G_m is the strain-compatible effective shear modulus, ρ is mass density of the ground, C_{se} is effective shear wave propogation velocity, h_1, h_2 are height of demanded displacement levels from foundation, and Δ_1, Δ_2 are free field displacement values at demanded levels.

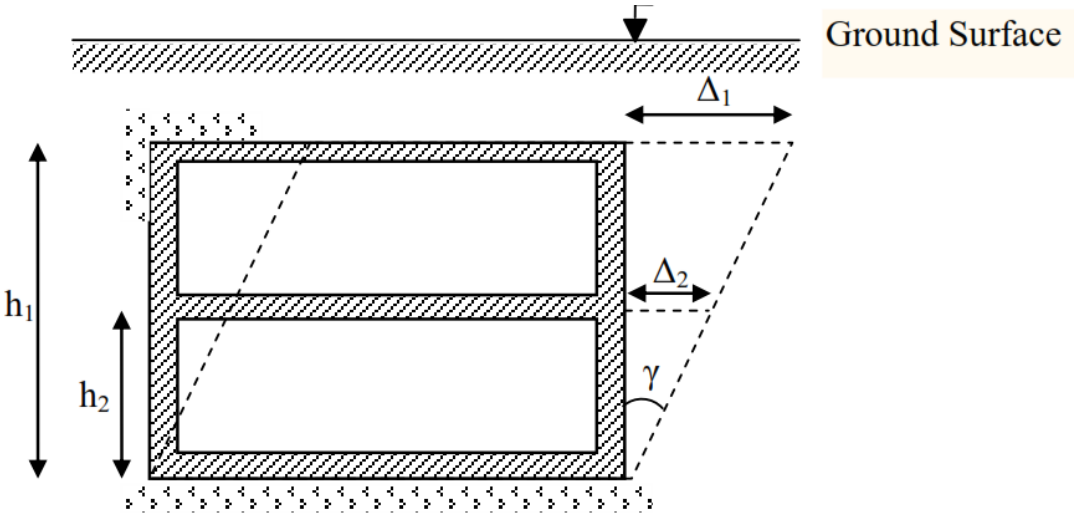

Figure 1.3 Deformation of elastic and buried structure (Güldağlı, 2004)

V_S is an important parameter in the estimation of rock and structural damage. In general, ground vibration is measured using a seismograph at a distance from the blast face to keep the instrument safe. Therefore, V_S is used interchangeably with the peak ground velocity (PGV) in general practice (Sykora et al., 1996). Value of PGV at the ground surface to be used in design can be estimated by ground motion prediction equations (GMPEs) or based on empirical factors depending on the peak ground acceleration (PGA) as in Equation 1.5. The empirical factor (b) depends on the earthquake magnitude, source to site distance and soil type as shown in Table 1.1.

$$V_S = PGA^* b \qquad 1.5$$

Table 1.1 Emprical factors used in converting PGA to V_S

Ratios of peak ground velocity to peak ground acceleration at surface in rock and soil (after Power et al., 1996)

Moment magnitude (M_w)	Ratio of peak ground velocity (cm/s) to peak ground acceleration (g)		
	Source-to-site distance (km)		
	0–20	20–50	50–100
Rock[a]			
6.5	66	76	86
7.5	97	109	97
8.5	127	140	152
Stiff soil[a]			
6.5	94	102	109
7.5	140	127	155
8.5	180	188	193
Soft soil[a]			
6.5	140	132	142
7.5	208	165	201
8.5	269	244	251

An alternative simplified method is suggested in FHWA Technical Manual for Design and Construction of Road Tunnels (2009) to estimate Δ_{ff}. This method is especially suitable for tunnels with shallow buried depths and concourse structures of metro stations. In this approach, Δ_{ff} is given by Equation 1.6.

$$\Delta_{ff} = \frac{\tau_{max}}{G_m} \text{ x } D = \frac{PGA \text{ x } \sigma_v \text{ x } r_d}{g \text{ x } G_m} \text{ x } D \qquad 1.6$$

where, r_d is the depth dependent stress reduction factor, τ_{max} is maximum earthquake-induced shear stress, σ_v is total vertical soil overburden pressure at invert elevation of tunnel, γ_t is total soil unit weight, H is soil cover thickness measured from the ground surface to the tunnel crown. In Equation 1.6, σ_v at the invert elevation is utilized for representing the stress at the foundation level of the structure. Therefore, height of the artifical fill (H) and height of the metro station (D) should be considered in calculating σ_v (Figure 1.4). In FHWA Technical Manual, the r_d factors proposed by Seed and Idriss (1971) is recommended. However, Çetin et al. (2004) proposed a new empirical r_d model as a function of depth (d), magnitude (M_w), PGA (a_{max}), and $V_{S,12m}$ (average

shear wave velocity at the first 12 meters on the profile) as given in Equations 1.7 and 1.8.

For d<20 m

$$r_d\,(d, M_w, a_{max}, V_{S,12m}) = \frac{1+\frac{-23.013 - 2.949*a_{max} + 0.999*M_w + 0.05252*V_{S,12m}}{16.258 + 0.201*e^{0.341(-d + 0.0785*V_{S12m} + 7.586)}}}{1+\frac{-23.013 - 2.949*a_{max} + 0.999*M_w + 0.0525*V_{S,12m}}{16.258 + 0.201*e^{0.341(0.0785*V_{S,12m} + 7.586)}}} \quad 1.7$$

For d>20 m

$$r_d\,(d, M_w, a_{max}, V_{S,12m}) = \frac{1+\frac{-23.013 - 2.949*a_{max} + 0.999*M_w + 0.05252*V_{S,12m}}{16.258 + 0.201*e^{0.341(-20 + 0.0785*V_{S,12m} + 7.586)}}}{1+\frac{-23.013 - 2.949*a_{max} + 0.999*M_w + 0.0525*V_{S,12m}}{16.258 + 0.201*e^{0.341(0.0785*V_{S,12m} + 7.586)}}} - 0.0046(d - 20) \pm \sigma_e \quad 1.8$$

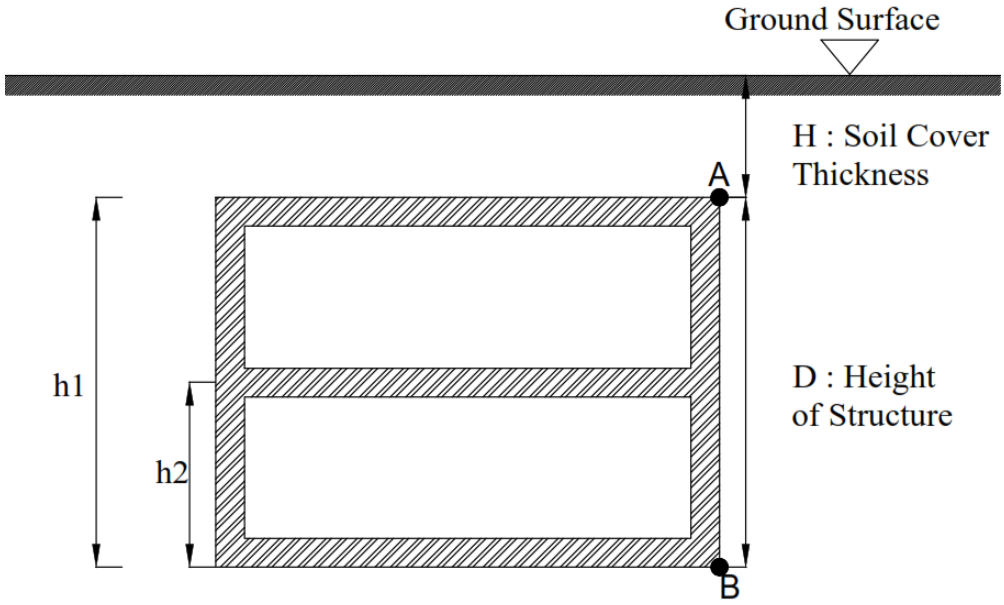

Figure 1.4 Geometrical parameters required to calculate the total stress

Özcebe (2009) recommended that a representative shear modulus should be estimated for multi-layered soil profiles instead of strain-compatible effective shear modulus to represent all soil layer properties in the simplified soil profile. The representative shear modulus can be calculated by Equation 1.9 .

$$G_{eq} = Vs_{eq}^2 \times \rho_{eq} \quad 1.9$$

In Equation 1.9, Vs_{eq} is determined by equivalent shear wave velocity concept (Özcebe, 2009) shown in Figure 1.5 and given in Equation 1.10. For soil density, similar to shear wave velocity, equivalent soil density is used (Equation 1.11).

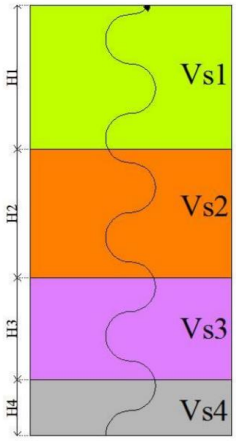

Figure 1.5 Equivalent Shear Wave Velocity Concept (Özcebe, 2009)

$$\frac{\Sigma H}{Vs_{eq}} = \frac{H_1}{V_{s1}} + \frac{H_2}{V_{s2}} + \frac{H_3}{V_{s3}} + \frac{H_4}{V_{s4}} \quad 1.10$$

$$\rho_{eq} = \frac{H_1*\rho_1+H_2*\rho_2+H_3*\rho_3+H_4*\rho_4}{H_1+H_2+H_3+H_4} \quad 1.11$$

Considering the above given equations and equivalent PGA is 65% of actual PGA, Equation 1.6 is modified into Equation 1.12.

$$\Delta_{ff} = 0.65 \text{ x } \frac{PGA \text{ x } \sigma_v \text{ x } r_d}{g \text{ x } G_{eq}} \text{ x } D \quad 1.12$$

Simplified approach given in Equation 1.12 is superior to the previous alternative (Equations 1.1-1.4) since the PGA given by the design code (eg. Turkish Seismic Hazard Map) can be directly implemented without conversion to PGV with emprical factors. Additionally, infrastructure's geometry and layered soil profile properties are effectively represented in Equation 1.12 by σ_v and G_{rep}. Therefore, Equation 1.12 is utilized in this study to represent Level 1 Methods.

1.2 Level 2 Method used in Earthquake Resisting Design of Metro Tunnels and Stations

Level 2 Method incorporates 1-D equivalent linear (EQL) site response analysis on estimating the Δ_{ff} for underground structures. EQL site response analysis is relatively easy to perform and widely preferred in engineering practice. On the other hand, EQL site response analysis does not incorporate soil non-linearity in the calculations. For high levels of ground shaking (where the soil is expected to behave nonlinearly), implementation of non-linear site response analysis is advised. However, significant expertise is needed to determine the additional input properties for incorporation of nonlinearity to the analysis. Therefore, especially for low levels of shaking, EQL approach seems to be sufficient to estimate Δ_{ff} (Hashash et al., 2010).

In Level 2 Method:

- The simplified site specific soil profile for the metro station shall be modelled in 1-D EQL analysis software (eg. Deepsoil). Simplified soil profiles are parameterized by the shear wave velocity profile, unit weight and thickness of soil layers.
- The dynamic soil properties of the soil layers (modulus degregation and damping curves) as a function of shear strain which is derived from laboratory test (Hashash et al., 2010) should be carefully selected. In the lack of laboratory test results, alternatives based on empirical correlations (eg. Drandeli, 2001; Vucetic and Dobry, 1991) can be used to determine modulus reduction and damping curves. According to Chiu et al. (2008) and Hashash et al. (2010), modulus reduction and damping curves based on emprical correlations should be checked for implied shear strength or friction angle.
- The input motion at the bedrock level can be determined from design codes and regulations at any specified hazard level. A suite of ground motions scaled to the input bedrock motion level needs to be incorporated into the 1-D EQL analysis software and propagated to the ground surface.

- The results of analysis provide the maximum horizontal displacement profiles at each run. The differences between the displacements at the demanded levels (eg. foundation and topslab) might be used to calculate Δ_{ff}. The average value and coefficient of variation for Δ_{ff} can be estimated based on the analysis results if multiple time histories are employed.

Level 2 Method allows the engineer to include the properties of the entire soil profile (e.g. unit weights, V_S profile, thickness of layers) in the calculations. Additionally, the input motion is represented by selected time histories instead of a single PGA value. Analysis might be performed for several time histories to estimate the body and the range of Δ_{ff} . On the other hand, these analyses are not fully probabilistic: The uncertainty in the V_S profile and soil properties can not be incorporated in most available softwares (eg. Deepsoil). Additionally, this method requires a significant effort in selecting and scaling the input ground motions which might be lacking in the majority of standard engineering applications. Despite the disadvantages discussed about Level 2 Method, it represents a significant step-forward compared to Level 1 Methods.

1.3 Level 3 Methods used in Earthquake Resisting Design of Metro Tunnels and Stations

1-D EQL analysis are not sufficient to predict the free field shear distortions especially for the cases with complex site stratigraphy (Hashash et al., 2001). For these cases, numerical methods can be utilized with different softwares (e.g. PLAXIS, FLAC) in the estimation of shear deformations. Additionally, the effect of soil-box interaction can be incorporated in the numerical analysis (Hashash et al., 2010). In these analysis, complex site geology is generally simplified into horizontally layered systems in 2-D or 3-D models and shear strain distortion on shear displacement can be determined by one dimensional wave propagation theory (Schnabel et al., 1972). Morever, by using

soil constitutive models, soil's nonlinear behaviour and hysteretic response at small strains can be incorporated (Hashash et al., 2010).

Özcebe (2009) conducted a study on seismic assessment of underground cut and cover structures using 2-D numerical analysis methods. By using multi-layered and randomly created soil profiles and limited number of emrprical ground motions in PLAXIS 9, Özcebe (2009) estimated the racking coefficient (R, as given in Equation 1.13). His study showed that the R values estimated in numerical analysis are comparable with the R values estimated by Level 1 Methods.

$$R = \frac{\Delta_{structure}}{\Delta_{ff}} \qquad 1.13$$

Similar to Özcebe (2009), Hashash (2010) compared the R-values estimated by site response analysis (EQL and Non-Linear) and by 2-D Racking (Pseudo-Static and Dynamic) analysis. In that study, distribution of R values from pseudo-static and dynamic racking analyses are evaluated for different flexibility ratios and compared with R values which are proposed by National Cooperative Highway Research NCHRP 611 (Anderson et al., 2008). The results also showed that the R values from the numerical analysis are consistent with R values from simplified closed-form solutions.

Modelling the soil profile in numerical analysis require expertise because more advanced testing is needed on the soil layers, to determine additional model parameters which incorporate nonlinearity and hysteresis of soil to the calculations. Moreover a large suite of ground motions have to be included in the analysis to properly model the uncertainty in the free field deformations. To propose a fully probabilistic framework for estimating Δ_{ff}, numerous analyses have to be performed; therefore, Level 3 Methods are not preferred in this study.

1.4 Research Statement

The objective of this study is to propose a fully probabilistic framework for estimating the free field deformations to be used in the seismic design of underground infrastructure, especially the metro stations. For this purpose, stations of two metro lines planned to be constructed in Istanbul: Kaynarca-Tuzla Tersane-Pendik (KPT) and Çekmeköy-Sancaktepe-Sultanbeyli (CSS) Metro Lines are used as case studies. In the first phase of study a new seismic source characterization model (SSC) is developed for the segments of North Anatolian Fault Zone (NAFZ) that are close the approximate locations of these metro stations. This SSC model is combined with current global and regionalized ground motion prediction models in PSHA framework to estimate the design ground motions for the metro stations at the bedrock level.

In the second phase of the study, simplified soil profiles of metro stations are developed and incorporated into 1-D EQL analysis (Level 2 Method). To model the uncertainty in the Δ_{ff} estimations, a large suite of empirical ground motions are utilized in the 1-D EQL site response analysis. Analysis results are found to be consistent with the Δ_{ff} estimations given by Level 1 Methods. Using analysis results, two prediction models for Δ_{ff} combining the parameters representing the site profile and input ground motion are developed. These prediction models can be used as probabilistic seismic demand models to estimate Δ_{ff} when detailed site specific analysis results are not available. Additionally, these models can be incorporated into the hazard integral in performance based earthquake engineering framework to provide annual rate of exceedence for specified Δ_{ff} levels.

In the third phase of the study, Δ_{ff} hazard curves are developed for approximate locations of metro stations of KPT and CSS Metro Lines and 475-year return period Δ_{ff} values are estimated for each station. These values are significantly different than the estimates of Level 1 Methods and median estimates of Level 2 Method showing that the return period of Δ_{ff} values estimated in Level 1 and Level 2 Methods are not equal to 475 years. Therefore, fully probabilistic approach proposed in this study

should be incorporated in earthquake resistant design to properly estimate the Δ_{ff} in the future.

1.5 Scope

The scope of this thesis can be summarized as:

In the first chapter, current methods for estimating free field deformations are presented and discussed. Research statement and the scope of the study are also given in this chapter.

In Chapter 2, details of the PSHA conducted for the approximate locations of KPT and CSS lines are provided. Proposed seimic source characterization models for Ganos-Saros, Central Marmara and Izmit segments of NAFZ are also presented in this Chapter.

In Chapter 3, free field displacements for each station estimated by Level 1 and Level 2 Methods are presented and compared. Two emprical prediction equations for free field displacements are proposed and discussed.

In the final chapter, two sets of hazard curves for proposed prediction models are developed in performance-based earthquake engineering framework. The differences between hazard curves and Level 1 and Level 2 methods are thoroughly discussed. Limitations of the proposed predictive models are explained and suggestions to improve the results in the future are presented.

CHAPTER 2

PROBABILISTIC SEISMIC HAZARD ASSESSMENT FOR METRO STATION LOCATIONS

This chapter provides an updated and properly documented fault-based seismic source characterization (SSC) model to be used in the PSHA studies in Istanbul. A significant portion of the tectonic database is acquired from the Updated Active Fault Maps of Turkey that was published by General Directorate of Mineral Research and Exploration (Emre et al., 2013). The 1/250.000 scale Çanakkale (NK 35-10b), Bandırma (NK 35-11b), Bursa (NK 35-12), Adapazarı (NK 36-13), Bolu (NK 36-14), and Istanbul (NK 35-9) sheets of Updated Active Fault Maps of Turkey were accessed and digitized by Gülerce and Kaymakçı (2017). The seismological database is taken from the Integrated and Homogeneous Turkish Earthquake Catalog published by Kandilli Observatory and Earthquake Research Institute (Kalafat et al., 2011). Seismotectonic information related to the active faults and the fault systems that are available in these databases and in the current scientific literature are used in combination with the segmentation models proposed by Gülerce and Ocak (2013) and Murru et al. (2016) to define the source model. The PSHA inputs (e.g. coordinates of the fault segments, logic tree branches and corresponding weights) are properly documented in Gülerce et al. (2017).

2.1 Fault Segmentation Models, Rupture Systems, and Partitioning of Slip Rates

The SSC model consists of one background source and four distinct (non-overlapping) rupture systems that are defined by considering the rupture zones of previous large magnitude earthquakes on the northern strand of North Anatolian Fault Zone (NAFZ). All sub-segments in the defined rupture systems except for North and South Çınarcık

Segments are assumed to be near vertical with right-lateral slip as suggested by geological, seismological, and GPS data.

2.1.1 Izmit and Düzce Rupture Systems

Location, geometry, and slip distribution of the rupture zones of 1999 Kocaeli and Düzce earthquakes have been studied extensively after these events (e.g. Barka et al., 2002; Langridge et al., 2002; Akyüz et al., 2002). The surface rupture of the 1999 Kocaeli earthquake extended for almost 165 km and 4 distinct segments were ruptured (Hersek Segment, Gölcük-Karamürsel-Izmit Segment, Sapanca-Akyazı Segment, and Karadere Segment as given in Barka et al., 2002). The co-seismic fault was terminated at the western end of the rupture, very near to the eastern side of the Marmara Sea (Ergintav et al., 2014). The northern strand of NAFZ that delimits the boundary between the Marmara Sea and Çınarcık Block did not rupture during 1999 Kocaeli Earthquake (Çınarcık Segment in Figure 2.1a). Mert et al. (2016) argued that the northern strand of NAFZ is observed as a single continuous fault strand along Izmit Bay and at its entrance to the sea southeast of Istanbul. North Çınarcık segment (Segment 3) is included in the Izmit rupture system because it is the western extension of the Hersek-Gölcük Segment that was developed in response to the bending of the main strand of the NAFZ towards NW. This bending results in a releasing bend and a slip re-distribution as dextral motion parallel to the main strand and normal motion perpendicular to the Çınarcık Segments (Gülerce and Kaymakçı, 2017). The dip of the North Çınarcık Segment is assumed to be 70°SW as suggested by Laigle et al. (2008) while the dip of South Çınarcık Segment is assumed to be 60°NW. The Izmit rupture system proposed here consists of five (Hersek-Gölcük, Izmit, Sapanca-Akyazı, Karadare and North Çınarcık) sub-segments. Düzce Earthquake produced 40-km-long surface rupture zone; however, there is a 4-km releasing step-over around Eften Lake (Akyüz et al. 2002). Therefore, a 2-segment model (Segments D1 and D2) is established for the rupture zone of the Düzce earthquake (Figure 2.1a). The segments and segment lengths for the Izmit and Düzce rupture systems are given in Table 2.1.

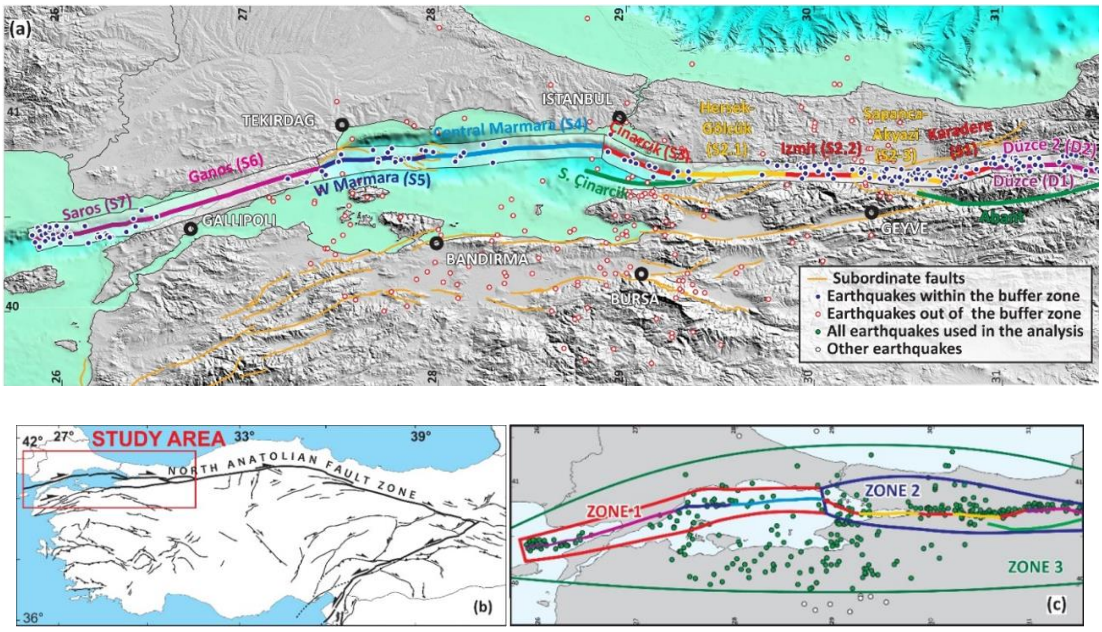

Figure 2.1 (a) Major branches of North Anatolian Fault Zone, defined rupture systems and the instrumental seismicity (M_w>4) in the study area. The buffer zones used for source-to-epicenter matching are shown around the rupture systems. (b) Simplified active tectonic scheme of Turkey (modified from Emre et al., 2013). Thick lines are North Anatolian and East Anatolian fault zones, thin lines are other active faults. (c) Distribution of the declustered seismicity used to calculate the b-values

2.1.2 Ganos/Saros Rupture System

The ENE-WSW trending Ganos Fault is the fault segment at the westernmost section of NAFZ that generated the August 9, 1912 Mürefte (Ganos) earthquake. Magnitude of this earthquake was estimated from historical catalogues and field observations as M_s = 7.3 ± 0.3 (by Ambraseys and Jackson, 2000) and M_w=7.4 (by Altunel et al., 2004), respectively (Aksoy et al., 2010). A second large event occured on the 13th of September, 1912 (M_s=6.8 ± 0.35 and the estimated seismic moment was 2.19 × 10^{19} Nm as given in Ambraseys and Jackson, 2000). Ambraseys and Jackson (2000) suggested a 37-km-long co-seismic rupture for this large second shock. Aksoy et al. (2010) used the duration of the recorded waveforms to estimate the rupture lengths of 1912 events: assuming the rupture width as 15-20 km, estimated values were 130 ± 15

km and 110 ± 30 km for August 9 and September 13 events, respectively. According to Aksoy et al. (2010), co-seismic surface ruptures were visible along the 45 km on-land section of this segment. Supporting the estimations based on waveforms by aerial photographs, satellite imagery, digital elevation models, bathymetry, and field measurements; Aksoy et al. (2010) proposed 120 ± 30 km-long fault rupture for the August 9, 1912 event. Murru et al. (2016) defined two segments covering the 120 ± 30 km long fault rupture of the 1912 Ganos Earthquake: a 74 km-long segment that includes the on-land section and a 46 km-long off-shore segment (Segments 6 and 7 in Figure 2.1a). The maximum seismogenic depth of these segments was assumed to be 15 km on the basis of the locking depth suggested by mechanical best fit modelling of GPS data (Flerit et al., 2003) and by the depth extent of instrumental seismicity (Gürbüz et al., 2000; Özalaybey et al., 2002; Örgülü and Aktar, 2001; Pınar et al., 2003). A similar segmentation model is adopted in this study by implementing minor changes in the sub-segment lengths as shown in Table 2.1.

Table 2.1 The fault segments and rupture systems included in the SSC model. References given in the last column are: 1) Flerit et al. (2004), 2) Murru et al. (2016), 3) Ergintav et al. (2014), 4) Ayhan et al. (2001), 5) Hergert et al. (2011). Weights associated with the mean, upper bound and lower bound are 0.5, 0.25, and 0.25, respectively

Rupture System	Segment No	Segment Name	Length (km)	Width (km)	Slip Rate and associated uncertainty (mm/yr)	Reference for the slip rate estimation
Izmit	3	North Çınarcık	34.6	18	17±2 (6±2 extension)	1, 2, 3
Izmit	2_1	Hersek- Gölcük	51.6	18	19±2	1, 2, 3
Izmit	2_2	İzmit	30.2	18	19±2	1, 2, 3
Izmit	2_3	Sapanca – Akyazı	39.1	18	19±2	1, 2, 3
Izmit	1	Karadere	24.7	18	10±2	1, 4
Düzce	D1	Düzce_1	10.5	25	10±2	1, 4
Düzce	D2	Düzce_2	41	25	10±2	1, 4
Ganos/Saros	6	Ganos	84	15	19±1	1, 3, 4, 5
Ganos/Saros	7	Saros	53	15	19±1	1, 3, 4, 5
Central Marmara	4	Central Marmara	80	15	19±2	1, 2
Central Marmara	5	West Marmara	49	15	19±2	1, 2
Çınarcık	8	South Çınarcık	39	18	(3±2 extension)	2

2.1.3 Central Marmara Rupture System

The northern strand of the NAFZ forms a major transtensional NW-SE right bend under the Sea of Marmara at the Çınarcık trough (Murru et al., 2016). The fault trace follows the northern margin of the Marmara Sea and connects the complex Central Marmara and Tekirdağ pull-apart basins, before merging into the NE-SW striking Ganos fault on land (Wong et al., 1995; Okay et al., 1999; Armijo et al. 2002; Le Pichon et al., 2001; Yaltirak, 2002; McNeill et al., 2004; Murru et al., 2016). Murru et al. (2016) noted that the segments under Marmara Sea are bounded by geometric fault complexities and discontinuities (e.g., jogs and fault bends) that can act as barriers to rupture propagation (Segall and Pollard, 1980; Barka and Kadinsky-Cade, 1988; Wesnousky, 1988; Lettis et al., 2002; An, 1997) and proposed two separate segments for Central Marmara Fault. The fault geometry and the segments proposed by Murru et al. (2016) were adopted to build the 2-segment Central Marmara rupture system (see Figure 2.1a for details).

2.1.4 Annual Slip Rates

Past studies based on GPS measurements (McClusky et al. 2000; Meade et al., 2002; Armijo et al., 2002; Reilinger et al., 2006; Hergert and Heidbach, 2010; Ergintav et al., 2014) suggest a 22 ± 3 mm/yr dextral motion along the major block-bounding structures of the NAFZ, with more than 80% being accommodated along the northern branch. On this branch, the segments that formed the west and central parts of Izmit rupture system (Segments 3, 2_1, 2_2 and 2_3 in Figure 2.1a) share the total slip rate with Geyve-Iznik Fault. The slip rate participation among the northern strand of NAFZ and Geyve-Iznik fault was given as 16 mm/yr and 9 mm/yr in Stein et al. (1997). However, Murru et al. (2016) have adopted the annual slip rate of 20±2 mm/yr for the northern strand based on the proposals of Flerit et al. (2003) and Ergintav et al. (2014). A better fit is achieved with the associated seismicity of Izmit rupture system by assigning 19±2 mm/yr annual slip rate to the northern strand of NAFZ. Similarly, the

total slip rate is distributed over the eastern segment of NAFZ Southern Strand (Segment 1 in Figure 2.1a) and the segments of Düzce Rupture System (D1 and D2). Ayhan et al. (2001) suggested that up to 10 mm/yr of the motion is accommodated on the Düzce-Karadere strand of the NAF. Same annual slip rate of 10±2 mm/yr is also utilized for Düzce_1, Düzce_2 and Karadere segments without any modifications (Table 2.1). The mean slip rates adopted for Central and West Marmara sub-segments (19 mm/yr) is consistent with the neighbouring sub-segments of the Izmit and Ganos/Saros rupture systems.

The slip rate given in the SSC model of Murru et al. (2016) is directly adopted for the Ganos sub-segment whereas; the slip rate partitioned in between the North Saros and South Saros sub-segments in Murru et al. (2016) is concentrated over the North Saros sub-segment (Table 2.1). The slip rate assigned to the Ganos and Saros sub-segments is consistent with the recent GPS velocity profiles given in Hergert and Heidbach (2010) and Ergintav et al. (2014). Table 2.1 summarizes the references for the utilized annual slip rates for each segment and the uncertainty related to the slip rate included in the logic tree.

2.2 Instrumental Earthquake Catalogue and Activity Rates of Earthquakes

The Integrated and Homogeneous Turkish Earthquake Catalog published by KOERI (Kalafat et al., 2011) including the events with M_w>4 that occurred between 1900 and 2010 is employed to represent the instrumental seismicity in the region. It is notable that areal source zones (or polygons) are not utilized in the SSC model to estimate the activity rates; therefore, the maximum magnitude estimates and the PSHA results are not solely dependent on the collected catalogue. The mainshock-aftershock classification of the catalog (de-clustering) is performed and the aftershocks are removed from the dataset using the Reasenberg (1985) methodology in the ZMAP software package (Wiemer, 2001).

Catalog completeness analysis for different magnitude ranges is performed in order to achieve the catalogue completeness levels used in calculating the magnitude recurrence parameters. Cumulative rates of earthquakes larger than specific magnitude levels are plotted vs. years to examine the completeness of catalog as shown in Figure 2.2. For different cut-off magnitudes, the breaking points for the linear trends in the cumulative rate of events are examined and a significant breaking point is observed to be at 52 years from the end of the catalogue for magnitudes smaller than 4.5 and 5.0. Therefore, the catalog was assumed to be complete for 52 years for $4.0 \leq M_w \leq 4.5$ and $4.5 \leq M_w \leq 5.0$ earthquakes, respectively. Although the larger magnitude plots in Figure 2.2 suffer from the lack of data due to the truncation of the catalog, the catalog is assumed to be complete for the greater magnitudes for the whole-time span (110 years).

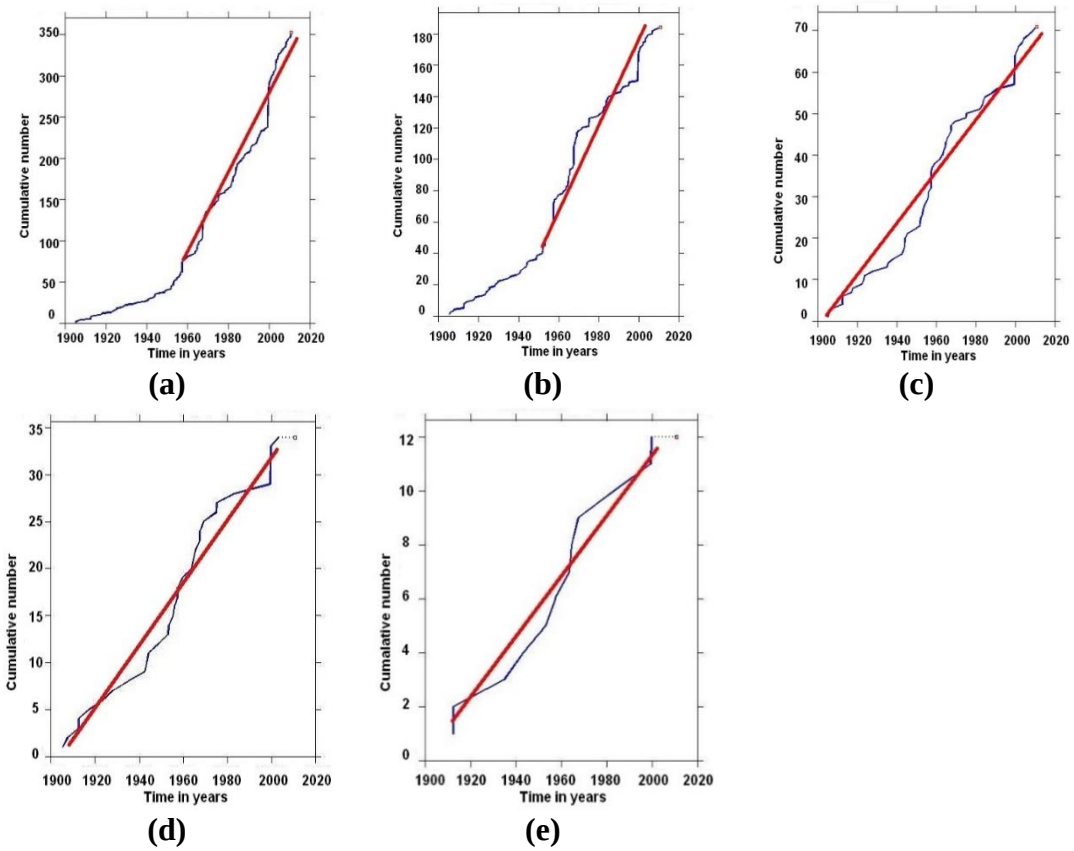

Figure 2.2 The catalogue completeness analysis for the instrumental earthquake catalogue showing the cumulative number of events for (a) $M_w \geq 4.0$, (b) $M_w \geq 4.5$, (c) $M_w \geq 5.0$, (d) $M_w \geq 5.5$, and (e) $M_w \geq 6.0$

Three different zones are delineated for estimating the b-value considering the temporal and spatial variability of this parameter as shown in Figure 2.1c. Zone 1 includes the Ganos/Saros and Central Marmara rupture systems, Zone 2 covers the Izmit and Düzce rupture systems, and Zone 3 is a larger area that includes both Zone 1 and 2. For each zone, the b-value is estimated using the maximum likelihood method provided in ZMAP software package. Figure 2.3 (a-c) shows the completeness magnitudes and the b-values for Zones 1, 2, and 3. Analysis results show that the b-value varies in between 0.68 and 0.74 for different rupture systems given in the previous section; whereas, the b-value for the large area covering whole system is equal to 0.76.

Additionally, the b-values for each zone are estimated using the modified maximum likelihood method (Weichert, 1980) that takes into account the completeness of the catalog for different magnitude bins. The b-values calculated by Weichert (1980) method is approximately 5% higher than the maximum likelihood estimations of ZMAP for Zones 1 and 2, but for the larger zone (Zone 3), estimated b-values are almost the same in both methods (Table 2.2). To acknowledge the uncertainty in the b-value estimations, 30% weight is assigned to the zone-specific b-value calculated by ZMAP and the zone-specific b-value calculated using Weichert (1980) method each, and 40% weight is given to the regional b-value since the number of data in this zone is larger and the estimated b-value is statistically more stable. Finally, the b-value for the background zone (limits shown in Figure 2.5) is calculated as 0.81 by removing the earthquakes within the buffer zones. Uncertainty in the b-value of background zone is determined using the method proposed by Shi and Bolt (1982) and included in the logic tree (Table 2.2).

2.3 Magnitude Recurrence Models – Seismic Moments

Seismic sources can generate varied sizes of earthquakes and magnitude distribution models describe the relative rate of these small, moderate and large earthquakes. The

basic and the most common magnitude frequency distribution (MFD) is the exponential model proposed by Gutenberg and Richter (1944) (G-R). Since there is a maximum magnitude (M_{max}) that the source can produce and a minimum magnitude (M_{min}) for engineering interest, the G-R distribution is usually truncated at both ends and renormalized so that it integrates to unity. The truncated exponential MFD (Cosentino et al., 1977) is given in Equation (2.1):

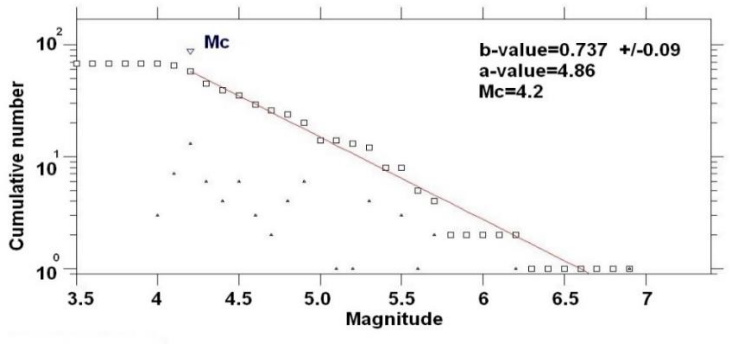

(a)

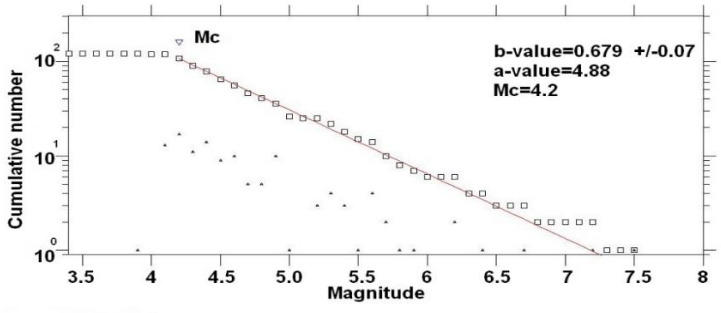

(b)

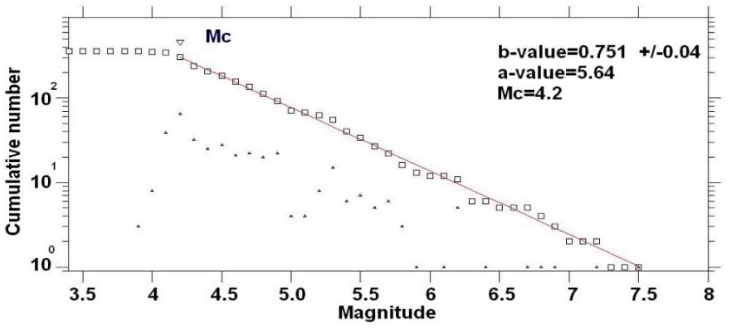

(c)

Figure 2.3 Estimated magnitude recurrence parameters for (a) Zone 1, (b) Zone 2, and (c) Zone 3.

Table 2.2 b-values estimated using different methods and corresponding weights in the logic tree.

Source Zone	Maximum likelihood estimation by ZMAP (Zone-specific)		Maximum likelihood estimation by Weichert (1980) (Zone-specific)		Regional Value	
	b-value	weight	b-value	weight	b-value	weight
Düzce Rupture System	0.68	0.3	0.72	0.3	0.76	0.4
Izmit Rupture System	0.68	0.3	0.72	0.3	0.76	0.4
Central Marmara Rupture System	0.74	0.3	0.78	0.3	0.76	0.4
Ganos/Saros Rupture System	0.74	0.3	0.78	0.3	0.76	0.4
	Maximum likelihood estimation by Weichert (1980) (Mean - 2σ)		Maximum likelihood estimation by Weichert (1980) (Mean)		Maximum likelihood estimation by Weichert (1980) (Mean + 2σ)	
	b-value	weight	b-value	weight	b-value	weight
Background Zone	0.714	0.20	0.81	0.60	0.906	0.20

$$f_m^{TE}(M) = \frac{\beta \exp(-\beta(M-M_{min}))}{1-\exp(-\beta(M_{max}-M_{min}))} \quad 2.1$$

where β = *Ln(10)×b-value*. Youngs and Coppersmith (1985) proposed that the truncated exponential distribution is suitable for large regions or regions with multiple faults but in most cases does not work well for individual faults. Instead, individual faults may tend to rupture at what have been termed as "*characteristic*" size events and the alternative magnitude distribution for this case is the characteristic model proposed by Schwartz and Coppersmith (1984). In characteristic MFD, once a fault begins to rupture in large earthquakes, it tends to rupture the entire fault segment and produce similar size earthquakes due to the geometry of the fault. It is notable that the characteristic model does not consider the small-to-moderate magnitude earthquakes on a fault. A third model was proposed by Youngs and Coppersmith in 1985 that

combines the truncated exponential and characteristic magnitude distributions as shown in Equation (2.2) and (2.3):

$$f_m^{YC}(M)=\begin{cases}\frac{1}{1+c_2}\times\frac{\beta\exp(-\beta(\bar{M}_{char}-M_{min}-1.25))}{1-\exp(-\beta(\bar{M}_{char}-M_{min}-0.25))} & \text{for } \bar{M}_{char}-0.25<M\leq\bar{M}_{char}+0.25\\ \frac{1}{1+c_2}\times\frac{\beta\exp(-\beta(M-M_{min}))}{1-\exp(-\beta(\bar{M}_{char}-M_{min}-0.25))} & \text{for } M_{min}<M\leq\bar{M}_{char}-0.25\end{cases} \quad 2.2$$

where,

$$c_2=\frac{0.5\beta\exp(-\beta(\bar{M}_{char}-M_{\min}-1.25))}{1-\exp(-\beta(M_{char}-M_{min}-0.25))} \quad 2.3$$

and M_{char} is the characteristic earthquake magnitude. The composite MFD proposed by Youngs and Coppersmith (1985) is utilized to represent the relative rates of small, moderate and large magnitude earthquakes generated by rupture sources defined in this study.

The rupture systems presented in Section 2.1 includes more than one sub-segment. The terminology of Working Group on California Earthquake Probabilities (2003) is adopted to define the rupture source as a fault sub-segment or a combination of multiple adjacent fault sub-segments that may rupture and produce an earthquake in the future. For Düzce, Central Marmara, and Ganos/Saros rupture systems with two sub-segments (as A and B), three different rupture sources can be defined; single segment sources (A and B) and a two-sub-segment source (A+B). Any possible combination of rupture sources that describes the complete rupture of the system is defined as the rupture scenario. Two rupture scenarios for these rupture systems are; (1) rupture of the two sub-segments individually and (2) rupture of the two sub-segments together. The rupture model includes the weighted combination of rupture scenarios of the rupture system. Five segments defined for Izmit rupture systems form a rupture model with 15 rupture sources and 16 rupture scenarios. For further explanations on rupture sources and scenarios of Izmit Rupture System, please refer to Gülerce et al. (2017). The minimum magnitude (M_{min}) is set to M_w=4.0 for all rupture sources considering the completeness magnitude. Mean characteristic magnitudes (M_{char}) for each rupture source are calculated using the relationships

proposed by Wells and Coppersmith (1994) and Hanks and Bakun (2014). The M_{char} values calculated using both equations are quite close to each other and the absolute value of the difference is smaller than 0.13 in magnitude units (Table 2.3). To grasp the epistemic uncertainty, average of the M_{char} value from both methods are utilized in the center of the logic tree with 50% weight and both the M_{char} -0.15 and M_{char} +0.15 values are included by assigning 25% weight. The upper bound for the magnitude PDF (M_{max}) is determined by adding 0.25 magnitude units to M_{char} for each source in each logic tree branch (Table 2.3).

MFD only represents the relative rate of different magnitude earthquakes. In order to calculate the absolute rate of events, the activity rate $N(M_{min})$ defined as the rate of earthquakes above the minimum magnitude should be used. For areal sources, $N(M_{min})$ may be calculated by using the seismicity within the defined area. For planar fault sources, the activity rate is defined by the balance between the accumulated and released seismic moments as shown in Equation 2.4. The accumulated seismic moment is a function of the annual slip rate (s) in cm/years, area of the fault (A in cm^2) and the shear modulus of the crust ($\mu = 30 \times 10^{12}$ dyne/cm^2, Brodsky et al., 2000; Field et al., 2009). The S for the rupture sources that includes more than one segment with different S values are calculated using the weighted average of annual slip rates (weighs are determined based on the area of the segment as shown in Equation 2.5).

$$N(M_{min}) = \frac{\mu A S}{\int_{M_{min}}^{M_{max}} f_m(M_w) 10^{1.5M_w+16.05} dM} \quad 2.4$$

$$S_{source} = \frac{\sum_{all\ segments\ for\ the\ source} S_{segment} \times A_{segment}}{\sum_{all\ segments\ for\ the\ source} A_{segment}} \quad 2.5$$

Ultimately the MFD and the activity rate are used to calculate the magnitude recurrence relation, N(M), as shown in Equation 2.6.

$$N(M) = N(M_{min}) \int_{M_{min}}^{M_{max}} f_m(M_w)\, dM \quad 2.6$$

Table 2.3 Logic tree representing epistemic uncertainty in maximum magnitudes. Weights for Mmax_1, Mmax_2, and Mmax_3 are 0.25, 0.5, and 0.25, respectively. (WC94: Wells and Coppersmith (1994) and HB14: Hanks and Bakun (2014) magnitude-rupture area relation)

Rupture System	Rupture Source	Source Width (km)	Source Length (km)	Characteristic Magnitude (WC94)	Characteristic Magnitude (HB14)	M_{max} 1	M_{max} 2	M_{max} 3
Düzce	D1	25	10.5	6.45	6.40	6.52	6.67	6.82
Düzce	D2	25	41	7.05	7.06	7.16	7.31	7.46
Düzce	D1+D2	25	51.5	7.15	7.19	7.27	7.42	7.57
Central Marmara	S4	15	80	7.12	7.15	7.23	7.38	7.53
Central Marmara	S5	15	49.2	6.91	6.89	7.00	7.15	7.30
Central Marmara	S4+S5	15	129.2	7.33	7.41	7.47	7.62	7.77
Ganos / Saros	S6	15	84	7.14	7.18	7.26	7.41	7.56
Ganos / Saros	S7	15	53	6.94	6.93	7.03	7.18	7.33
Ganos / Saros	S6+S7	15	137	7.36	7.44	7.50	7.65	7.80
Izmit	3	18	34.6	6.83	6.79	6.91	7.06	7.21
Izmit	2_1	18	51.6	7.01	7.01	7.11	7.26	7.41
Izmit	2_2	18	30.2	6.77	6.72	6.84	6.99	7.14
Izmit	2_3	18	39.1	6.88	6.86	6.97	7.12	7.27
Izmit	1	18	24.7	6.68	6.63	6.75	6.90	7.05
Izmit	3+2_1	18	86.2	7.23	7.29	7.36	7.51	7.66
Izmit	2_1+2_2	18	81.8	7.21	7.26	7.34	7.49	7.64
Izmit	2_2+2_3	18	69.3	7.14	7.17	7.25	7.40	7.55
Izmit	2_3+1	18	63.8	7.10	7.13	7.21	7.36	7.51
Izmit	3+2_1+2_2	18	116.4	7.37	7.45	7.51	7.66	7.81
Izmit	2_1+2_2+2_3	18	120.9	7.38	7.47	7.53	7.68	7.83
Izmit	2_2+2_3+1	18	94	7.27	7.34	7.40	7.55	7.70
Izmit	3+2_1+2_2+2_3	18	155.5	7.50	7.61	7.65	7.80	7.95
Izmit	2_1+2_2+2_3+1	18	145.6	7.47	7.57	7.62	7.77	7.92
Izmit	3+2_1+2_2+2_3+1	18	180.2	7.56	7.69	7.73	7.88	8.03
South Çınarcık	**South Çınarcık**	18	39	6.86	6.88	6.97	7.12	7.27
Background	-	18	-	-		6.5	6.80	7.1

The magnitude recurrence relation given in Equation 2.6 and the accuracy of the model parameters such as the b-value or M_{max} shall be tested by the relative frequency of the seismicity associated with the source in the moment-balanced PSHA procedure. Therefore, a weight is assigned to each rupture scenario and the cumulative rates of events attributed to that particular rupture system are plotted along with the weighted average of the rupture scenarios to calibrate the assigned weights and to evaluate the balance of the accumulated and released seismic moment. The "*moment-balancing*"

graphs for Izmit, Düzce, Central Marmara, and Ganos/Saros rupture systems are provided in Figure 2.4 and used to compare the modelled seismicity rate with the instrumental earthquake catalogue. In these plots, the black dots stand for the cumulative annual rates of earthquakes and the error bars represent the uncertainty introduced by unequal periods of observation for different magnitudes (Weichert, 1980). In Figure 2.4, the scenarios that are separated by plus signs in the legend are the scenarios with multiple rupture sources. When multiple segments rupture together, these scenarios are separated by a comma sign in the legend. For example, the "S4, S5" line in Figure 2.4c represents the scenario where S4 and S5 sub-segments are ruptured individually. This scenario brings in relatively higher rates for small-to-moderate earthquakes when compared to the S4+S5 scenario which represents the rupture of these two segments together to produce a larger event.

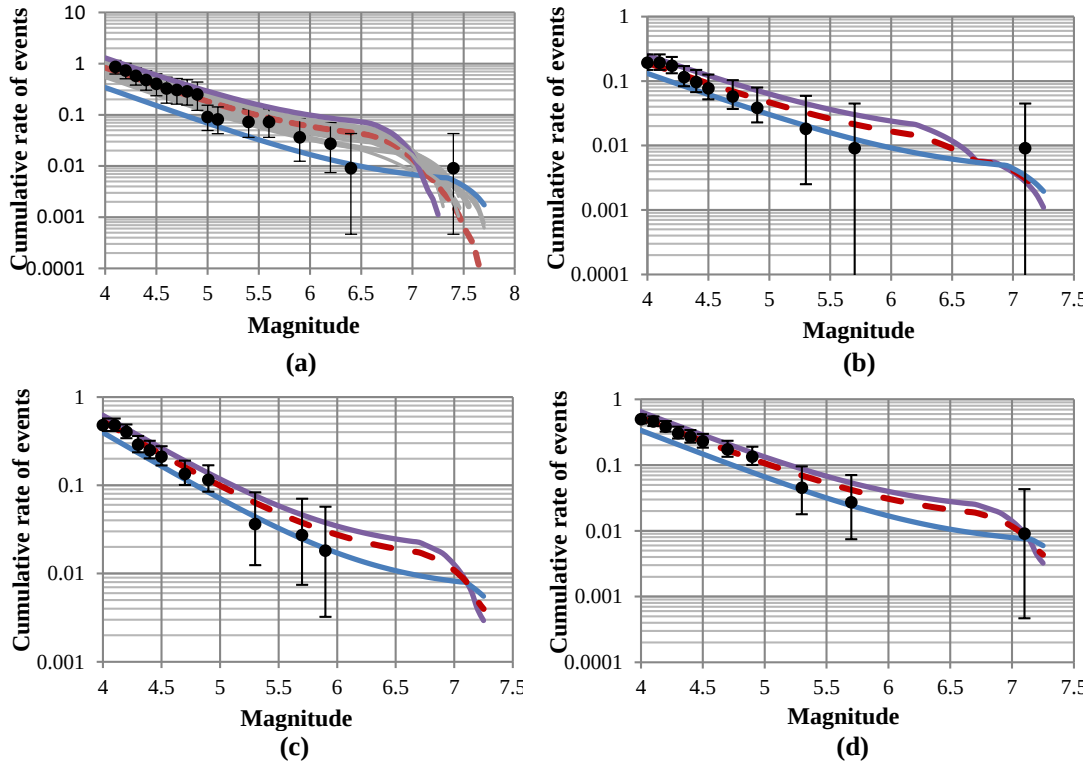

Figure 2.4 Cumulative rates of earthquakes for the magnitude recurrence model and associated events (moment balancing graphs) for (a) Izmit, (b) Düzce, (c) Central Marmara, and (d) Ganos/Saros rupture systems. Black points are the earthquakes associated with the rupture system, purple and blue lines show the single-segment and multi-segment ruptures, red broken line is the weighted average of the magnitude recurrence model. In these graphs, the median values of the slip rates and Mmax and zone-specific b-values are utilized

The good fit in the small magnitude range of Figure 2.4 shows that: i) the b-value calculated using the larger zone is compatible with the seismicity associated with the planar source, ii) utilized segmentation model is consistent with the relative rates of small-to-moderate and large events, and iii) annual slip rate is compatible with the seismicity over the fault. The large magnitude rates in Figure 2.4 are poorly constrained since the catalogue used herein only covers 110 years and that time span is obviously shorter than the recurrence rate for the large magnitude event. In each moment balancing plot, relatively higher weights are assigned to the rupture scenarios that combine the individual (single-segment) rupture sources based on the assumption (and modeller's preference) that single-segment ruptures are more likely than multiple-segment ruptures. The weights assigned to each rupture scenario are given in Table 2.4.

Table 2.4 Aleatory variability in the rupture scenario weights

Rupture System	Rupture type	Included sub-segment no	Weight
Düzce Rupture System	Single segment ruptures	D1, D2	0.5
	2-segment ruptures	D1+D2	0.5
Central Marmara Rupture System	Single segment ruptures	4,5	0.6
	2-segment ruptures	4+5	0.4
Ganos/Saros Rupture System	Single segment ruptures	6,7	0.6
	2-segment ruptures	6+7	0.4
Izmit Rupture System	Table 5 of Gülerce et al. (2017)		

2.4 Background Zone – Smoothed Seismicity

A background source zone of diffused seismicity is utilized to characterize the seismicity that is not associated with the rupture systems described in the previous sections. This additional background source zone represents the seismicity associated with the mapped active faults on the south of Marmara Sea (orange fault lines in Figure 2.1a) and the interpretation that even in areas where active faults or distinctive zones of seismicity clusters are not observed, earthquakes can still occur. Figure 2.1c shows that the spatial distribution of the earthquakes (outside the buffer zones around the rupture systems) is not homogeneous; density of the events increases significantly

around the Geyve-Iznik Fault Zone. Therefore, defining an areal source zone with homogeneous seismicity distribution would result in the overestimation of the seismic hazard in Istanbul. Instead, the background source is modelled as a source of gridded seismicity where the earthquakes are represented as point or planar fault sources at the centres of evenly spaced grid cells (0.05 degree spacing). The truncated exponential magnitude distribution (Equation 2.1) is selected to represent the relative frequency of the different magnitude events for this source. In the magnitude recurrence model, spatially uniform M_{max} and b-values and spatially variable a-values, or seismicity rates, are defined. The minimum magnitude (M_{min}) is again set to M_w=4.0 and the b-value is taken as 0.81. The a-value for each grid cell was calculated from the maximum likelihood method of Weichert (1980), based on events with magnitudes of 4.0 and larger. The gridded a-values were then smoothed by using an isotropic Gaussian kernel with a correlation distance of 10 km (Frankel, 1995). The smoothed-seismicity rates overlying the earthquakes outside the buffer zones are presented in Figure 2.5.

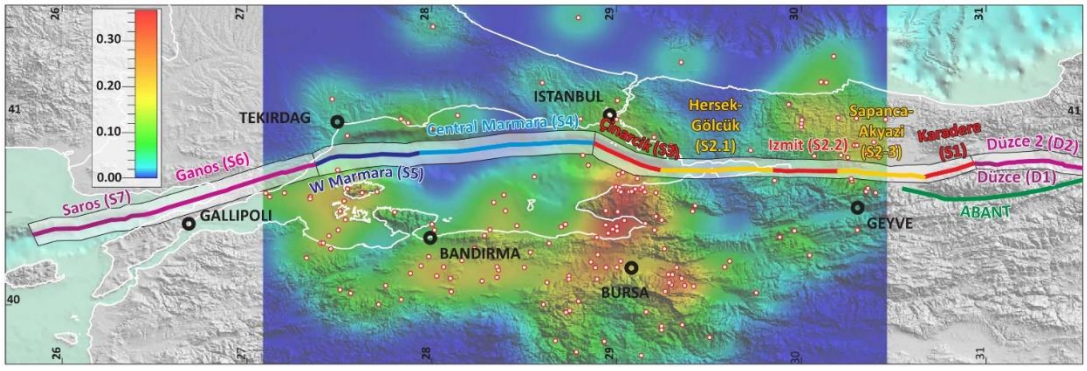

Figure 2.5 Spatial distribution of the activity rates in the smoothed seismicity source. Red circles are the earthquakes used in the analysis.

The logic tree for M_{max} (centered on M_w= 6.8) of the background zone is developed (Table 2.3). The focal mechanisms of the background source should reflect the tectonic style of the parent region; therefore, a weighted combination of strike-slip (SS, 75%), normal (N, 20%), and reverse (R, 5%), motion with weights that sum to 1 is assigned to this source. A uniform distribution of focal depths between the surface and 18 km depth is utilized (Emre et al., 2016).

2.5 PSHA for Metro Station Locations for Selected Metro Lines

Four metro stations along Kaynarca Merkez-Pendik-Tuzla Tersane (KPT) Metro Line and eight metro stations along Çekmeköy-Sancaktepe-Sultanbeyli (CSS) Merkez Metro Line (Figure 2.6) will be constructed in Istanbul (Yüksel Project – Geotechnical Site Survey Reports, 2015). Geotechnical site survey reports for each metro line show that the average shear wave velocities in the top 30 meters (V_{S30}) of the metro station locations are quite different than each other (details given in Chapter 3). The impact of these differences over the design ground motions and other seismic design parameters can be estimated by carrying out 1-D site specific ground response analysis. For performing site-specific response analysis, the response spectrum at the engineering bedrock level should be defined as the input for each station. Therefore, PSHA analysis are carried out by combining the SSC model presented here with a ground motion characterization logic tree for V_{S30}=1100 m/s, representing the engineering bedrock conditions. In the ground motion characterization logic tree, equal weights are given to global Next Generation Attenuation (NGA) West-2 prediction equations (NGA-West 2, Bozorgnia et al., 2014) and regionalized Turkey-adjusted NGA West-1 models (Gülerce et al., 2016). In the PSHA analysis, the HAZ43 software which is able to evaluate and combine all branches of the logic tree is used (PG&E, 2010). Seismic hazard curves for each station for peak ground acceleration (PGA) are presented in Figure 2.7 and Figure 2.8. The black dashed line in Figure 2.7 and Figure 2.8 represents the annual rate of exceedence for 2475-year return period, whereas the black solid line shows the annual rate of exceedence for 475-year return period.

The difference between hazard curves of the stations on the same metro line are small due to quite close locations of stations parallel to the shoreline. PGA values vary between 0.24g – 0.38g for 475-year return period, reaching up to 0.55g for 2475-year return period. The maximum PGA values for 475 and 2475-year return periods are observed at Tuzla Belediye Station (closest station to the fault) in the KPT Metro Line and the minimum PGA values for 475 and 2475-year return periods are observed at

Sarıgazi Station (most far away metro station to the fault zone) in CSS Metro Line. When the 475-year return period PGA values are compared with the Turkish Earthquake Code regulations (TEC, 2007), it is observed that the estimated PGA values along the KPT Metro Line are close (approximately 0.05g lower than 0.4g) to the code regulations for 475 years. Similarly, estimated 2475-year return period PGA values are generally 0.05g-0.1g lower than the code regulations. However, for CSS Metro Line, the PGA values for 475 and 2475-year return periods estimated from PSHA are nearly 0.15g and 0.25g lower than the code regulations. It is notable that the calculated values are representing the ground motions at the engineering bedrock level and significant amplification is expected at the ground surface. Therefore, these values should not be implemented in the design before the effect of site-specific soil response is estimated. Since the effect of site conditions are neglected in the PSHA analysis, locations of the metro stations are dominant factor that controls the estimated PGA values in PSHA.

Figure 2.6 (a) Fault system and approximate locations of analyzed metro stations (b) KPT Metro Line and (c) CSS Metro Line

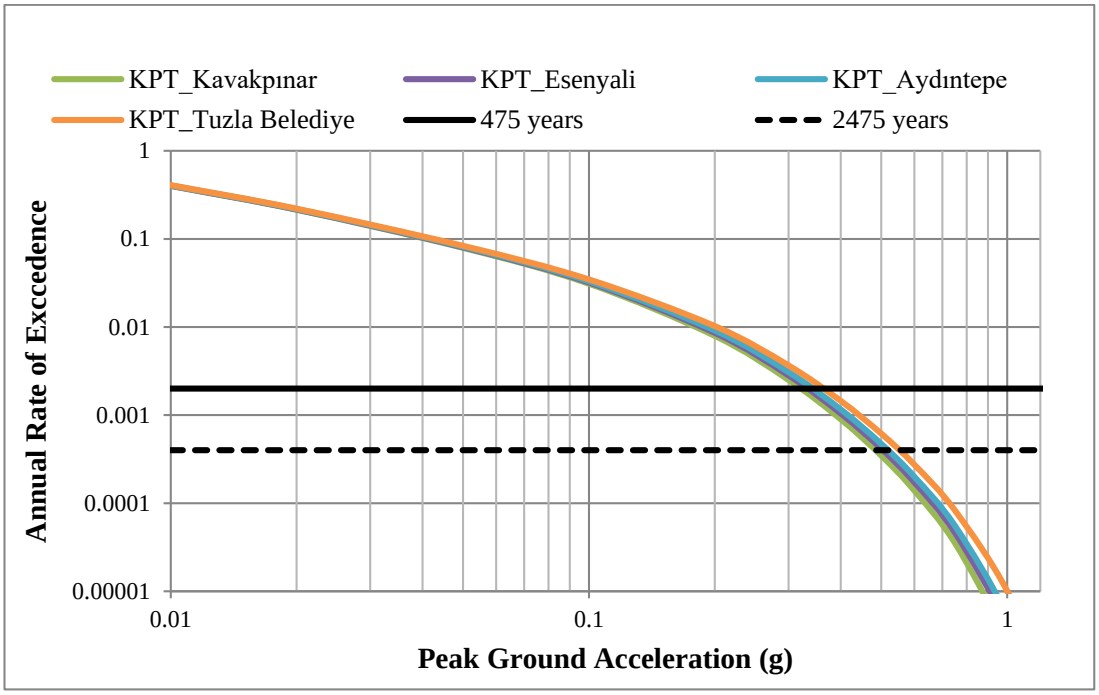

Figure 2.7 Hazard curves for PGA for the approximate locations of metro stations in KPT Line

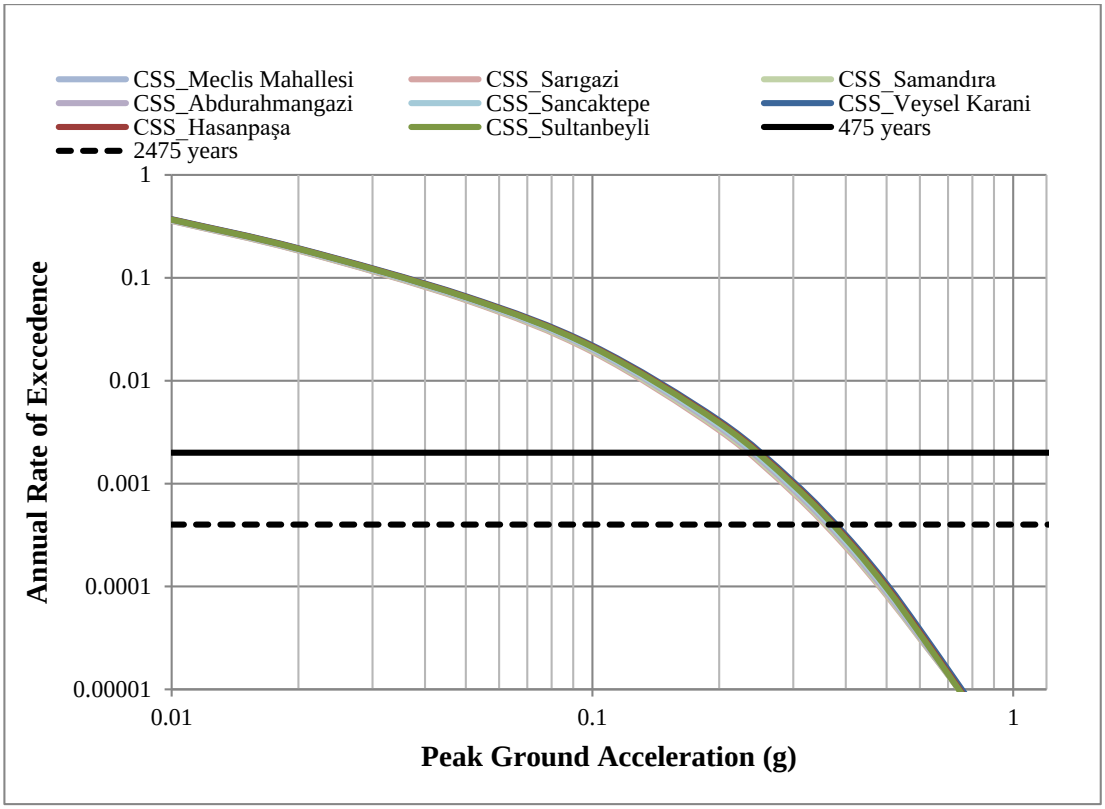

Figure 2.8 Hazard curves for PGA for the approximate locations of metro stations in CSS Line

Table 2.5 Estimated PGA values at different hazard levels for each station

Station #	Station Name	PGA (g) with 475-year return period	PGA (g) with 2475-year return period
1	Abdurrahmangazi	0.245	0.360
2	Aydıntepe	0.340	0.520
3	Esenyalı	0.330	0.500
4	Hasanpaşa	0.260	0.375
5	Kavakpınar	0.320	0.480
6	Meclis Mahallesi	0.240	0.360
7	Samandıra	0.240	0.370
8	Sancaktepe	0.250	0.370
9	Sarıgazi	0.235	0.360
10	Sultanbeyli	0.250	0.370
11	Tuzla Belediye	0.370	0.550
12	Veysel Karani	0.260	0.380

CHAPTER 3

EVALUATION OF FREE FIELD DISPLACEMENTS FOR METRO STATIONS USING LEVEL 1 AND LEVEL 2 METHODS

The PSHA for the stations of KPT and CSS metro lines given in Chapter 2 are performed for the generic engineering bedrock conditions (V_{S30}=1100 m/s). In this chapter, site-specific 1-D EQL ground response analysis are conducted for each station using simplified soil profiles and a suite of ground motions scaled to the PGA with 475-year return period at the bedrock level. Details of the simplified soil profiles and selected ground motions are provided in the first part of this chapter. Analysis results are used to determine the horizontal displacements at the top and the bottom slabs of the stations and to calculate the body and the range of Δ_{ff} values for each station. Calculated values are compared to Δ_{ff} values estimated by Level 1 Method for consistency, indicating that the median free-field displacements are in good agreement with Δ_{ff} values estimated by Level 1 Method for most of the stations and the analysis results can be used to develop a probabilistic model for estimating free-field displacements.

3.1 Simplified Soil Profiles of Metro Stations

All stations planned along the KPT and CSS Metro Lines have different structural dimensions (height, length etc.) and the thickness of the engineering fill varies from station to station according to environmental requirements and construction properties. Therefore, 12 individual simplified soil profiles are generated based on the information given in geological and geotechnical investigation reports for KPT and CSS Metro Lines prepared by Geological Services Group of Yuksel Project (YP) International Company for Istanbul Metropolitan Municipality (Yüksel Proje Int., 2016). Reports

cover the site investigation results including the Standard Penetration Test (SPT) logs, spatial distribution and lithologic properties of the soil layers, and geomechanical parameters of the lithological units. Additionally, seismic refraction and 2-D Remi measurements are avaliable along the KPT line. Based on these reports, Geological Services Group of YP formed idealized geological sections (example shown in Figure 3.1) to be used in static calculations for metro stations. Depending on the complexity of the soil layers and the size of the stations, two or more soil layers are included in each cross-section (e.g. Yd, Tso and Dpk layers in Figure 3.1). Optimized soil properties (e.g. unit weight (γ), cohesion (c'), drained angle of friction (φ'), Young's modulus (E) for each soil layer are also provided on the cross-sections. For simplified soil profiles prepared as input to the EQL analysis software DeepSoil (Hashash et al., 2016), parameters provided in these optimized soil profiles are used to determine the basic properties of soil layers (e.g. unit weight).

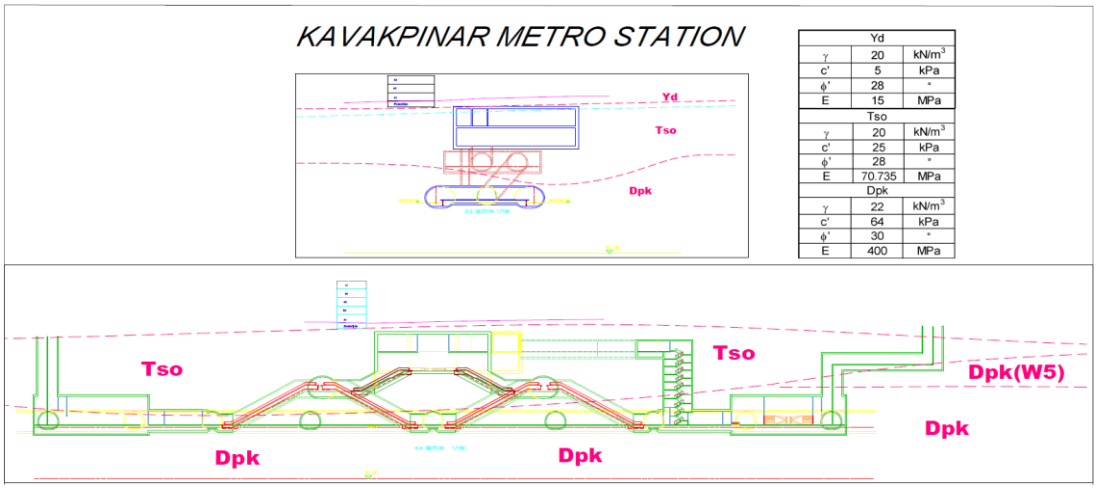

Figure 3.1 Example geologic cross-section for Kavakpınar Station (GIR, 2015)

The geotechnical report includes 31 and 21 SPT logs along CSS and KPT lines, respectively. For each station, the SPT log of the nearest borehole is used to determine the shear wave velocity profile (location of boreholes and stations are shown in Figure 3.2 and Figure 3.3). The raw SPT-N values provided in the borehole logs are used to determine the shear wave velocity (V_S) using Equation 3.1. The conversion equation given in Equation 3.1 was proposed by Hasançebi and Ulusay (2007) based on 97 data

pairs collected from north-western Turkey. Different empirical relationships for sands, clays, and for all soils types were proposed, but the latter one (applicable to all soils) is utilized in this study.

$$V_S = 90 \times N^{0.309} \quad 3.1$$

Tables 3.1 and 3.2 present the raw SPT-N values utilized in the conversion. It is notable that many SPT logs, especially along the KPT line, include R (refusal) instead of the SPT-N number (e.g. Aydıntepe Station and Tuzla Belediye Station in KPT Metro Line). For these cases, the shear wave velocity is defined as 360 m/s (the value representing the NHERP C/D boundary) if no other information is avaliable. On the other hand, the estimations of V_S profile for these stations are supported by the seismic refraction measurements taken along the KPT line. Figure 3.4 shows four velocity profiles measured along the KPT line and the optimized V_S pofile defined for this study (thick red line). The optimized V_S profile summarized in Table 3.3 is adopted as the upper limit for the stations with refusal throughout the borehole by modifiying it with the estimated V_S from SPT-N number when available. The shear wave velocity for the engineering bedrock is set to 1100 m/sec for consistency with PSHA results.

Simplified soil profiles (an example given in Figure 3.5) are implemented in Deepsoil software considering following critical points:

- The metro stations will be constructed by the cut and cover technique; therefore, the ground surface will be excavated up to the level of foundation and then an artificial fill will be placed between the top slab and ground surface. For each station, an artificial fill layer at the top (at least 2-3 m-thick) is modelled using the soil properties given in the geotechnical report.
- The thickness of the defined soil layers does not exceed 3 meters, except for special case in Sarıgazi Metro Station (a fault layer with 9 m thickness and unknown soil properties was defined in the borehole log).
- The thickness of the soil layers are arranged to be able to measure the horizontal dispalecements at the top and the bottom slabs (Figure 3.5).

- Minimum 5 meters of soil is defined between the foundation and the engineering bedrock to eliminate possible boundary effects.

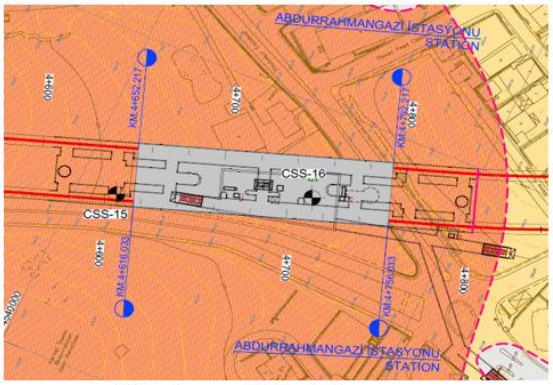

Abdurrahmangazi Metro Station

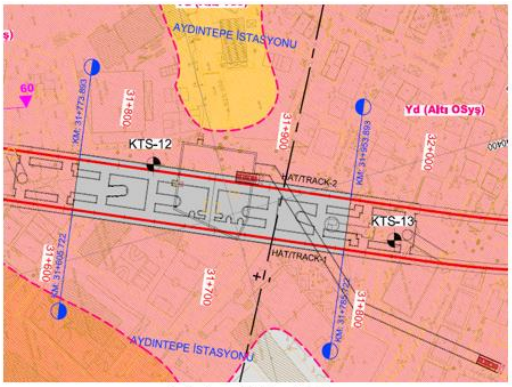

Aydıntepe Metro Station

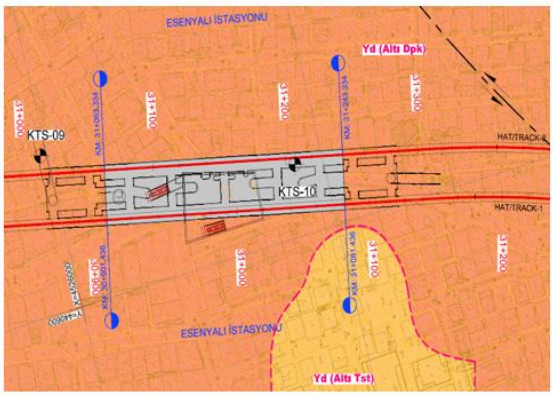

Esenyalı Metro Station

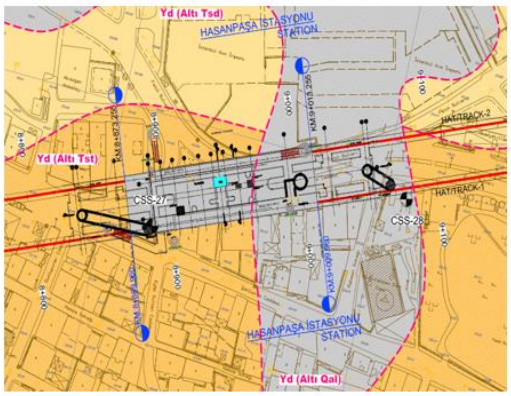

Hasanpaşa Metro Station

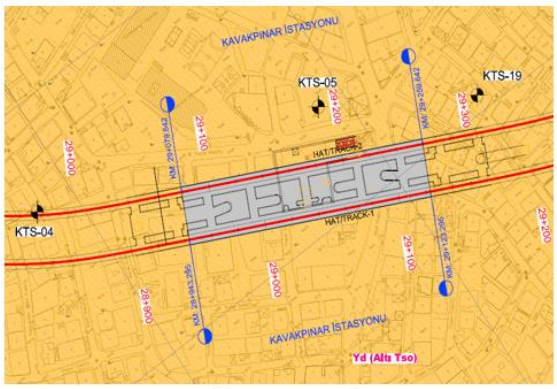

Kavakpınar Metro Station

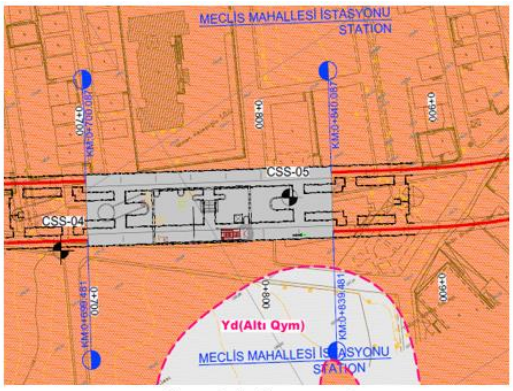

Meclis Mahallesi Metro Station

Figure 3.2 Layout of borehole logs in metro station area (1/2)

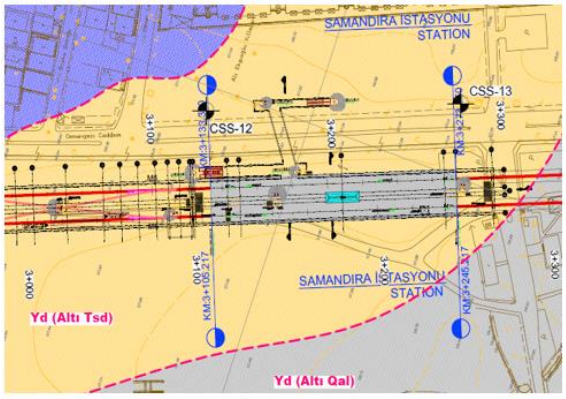

Samandıra Metro Station

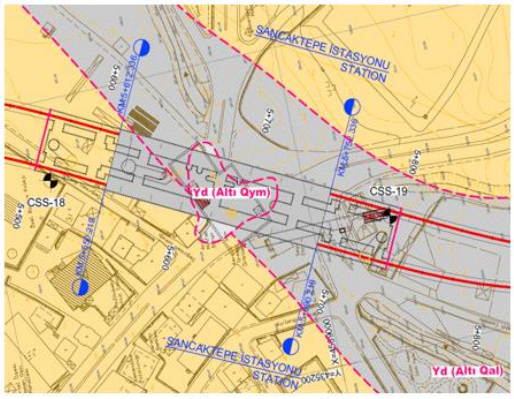

Sancaktepe Metro Station

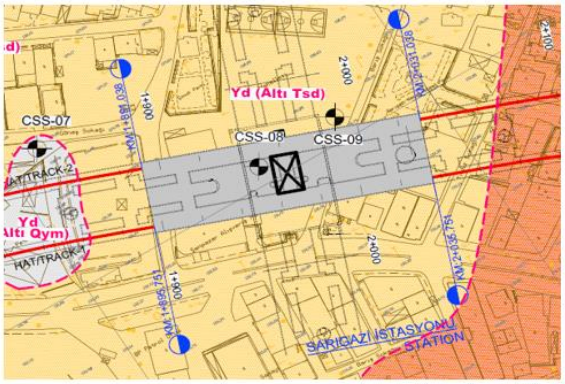

Sarıgazi Metro Station

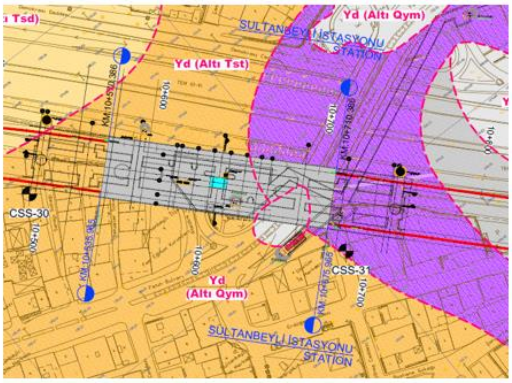

Sultanbeyli Metro Station

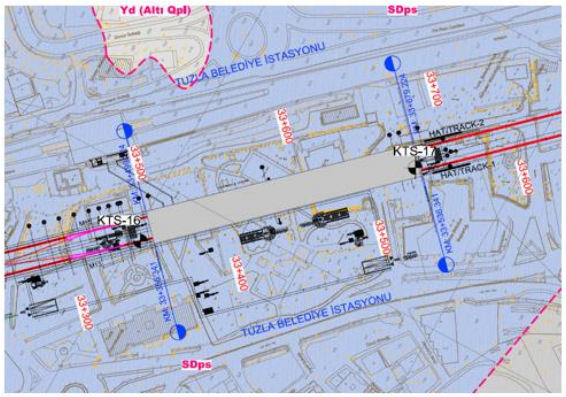

Tuzla Belediye Metro Station

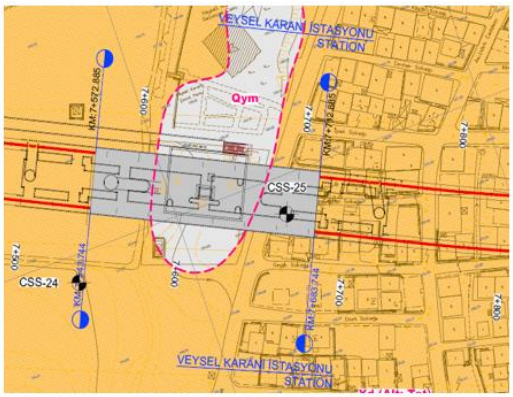

Veysel Karani Metro Station

Figure 3.3 Layout of borehole logs in metro station area (2/2)

Table 3.1 Selected borehole datas for conversion of SPT-N to V_S in CSS

#	Meclis Mahallesi Station	Sarıgazi Station	Samandıra Station	Abdurrahmangazi Station	Sancaktepe Station	Veysel Karani Station	Hasanpaşa Station	Sultanbeyli Station
Depth (m)	***CSS-05***	***CSS-08***	***CSS-13***	***CSS-16***	***CSS-19***	***CSS-25***	***CSS-27***	***CSS-31***
1.5	25	6	10	76	22	34	11	-
3	65	32	24	34	35	24	17	75
3.35	-	-	-	-	-	-	-	-
4.5	R	21	25	R	44	17	45	73
4.71	-	-	-	-	-	-	-	-
5	-	-	-	-	-	-	-	-
6	-	30	67	R	19	56	24	74
6.2	-	-	-	-	-	-	-	-
6.4	-	-	-	-	-	-	-	-
7	-	-	-	-	-	-	-	-
7.5	-	14	54		23	28	34	R
8	-	-	-	-	-	-	-	-
9	-	R	43	R	24	26	20	-
9.45	-	-	-	-	-	-	-	-
10.5	-	-	51	-	21	26	43	71
12	-	-	52	-	18	27	52	R
12.4	-	-	-	-	-	-	-	-
12.5	-	-		-	-	-	-	-
13.5	-	-	49	-	38	20	R	71
14	-	-	-	-	-	-	-	-
15	-	-	30	-	44	28		65
15.3	-	-	-	-	-	-	-	-
15.45	-	-	-	-	-	-	-	-
16	-	-	-	-	-	-	-	-
16.5	-	-	R	-	73	27	-	R
17	-	-	-	-	-	-	-	-
18	-	-	-	-	80	R	-	71
18.3	-	-	-	-	-	-	-	-
19.5	-	-	-	-	72	29	-	R
21	-	-	-	-	R	35	-	R
21.5	-	-	-	-	-	-	-	-
22.5	-	-	-	-	80	40	-	R
23.40-23.50	-	-	14	-	-	-	-	-
24	-	-	-	-	82	81	-	R
25.5	-	-	26	-	R	64	-	R
27	-	-	-	-	-	73	-	R
27.5	-	-	-	-	-	-	-	-
28.5	-	-	18	-	-	R	-	R
30	-	-	-	-	-		-	-
31.5	-	-	-	-	-	37	-	-
33	-	-	-	-	-	25	-	-
34.5	-	-	-	-	-	33	-	-
36	-	-	-	-	-	54	-	-
37.5	-	-	-	-	-	R	-	-

Table 3.2 Selected borehole datas for conversion of SPT-N to V_S in KPT

#	Kaynarca Merkez Station	Kavakpınar Station	Esenyalı Station	Aydıntepe Station	Tuzla Belediye Station
Depth	***PKS08***	***KTS05***	***KTS10***	***KTS12***	***KTS17***
1.5	11	53	13	60	R
3	43	R	16	R	-
3.35	-	-	-	-	-
4.5	30	R	82		40
4.71	-	-	-	-	-
5	-	-	-	-	-
6	12	R	-	-	-
6.2	-	-	-	-	-
6.4	-	-	-	-	-
7	-	-	-	-	-
7.5	25	R	-	-	-
8	-	-	-	-	-
9	R	51	-	-	-
9.45	-	-	-	-	-
10.5	-	55	R	-	R
12	-	38	-	-	-
12.4	-	-	-	-	-
12.5	-	-	-	-	-
13.5	-	40	-	-	-
14	-	-	-	-	-
15	-	70	-	-	-
15.3	-	-	-	-	-
15.45	-	-	-	-	-
16	-	-	-	-	-
16.5	-	58	-	-	-
17	-	-	-	-	-
18	-	53	-	-	-
18.3	-	-	-	-	-
19.5	-	33	-	-	-
21	-	52	-	-	-
21.5	-	-	-	-	-
22.5	-	38	-	-	-
23.50	-	-	-	-	-
24	-	47	-	-	-
25.5	-	92	-	-	-
27	-	51	-	-	-
27.5	-	-	-	-	-
28.5	-	59	-	-	-
30	-	R	-	-	-

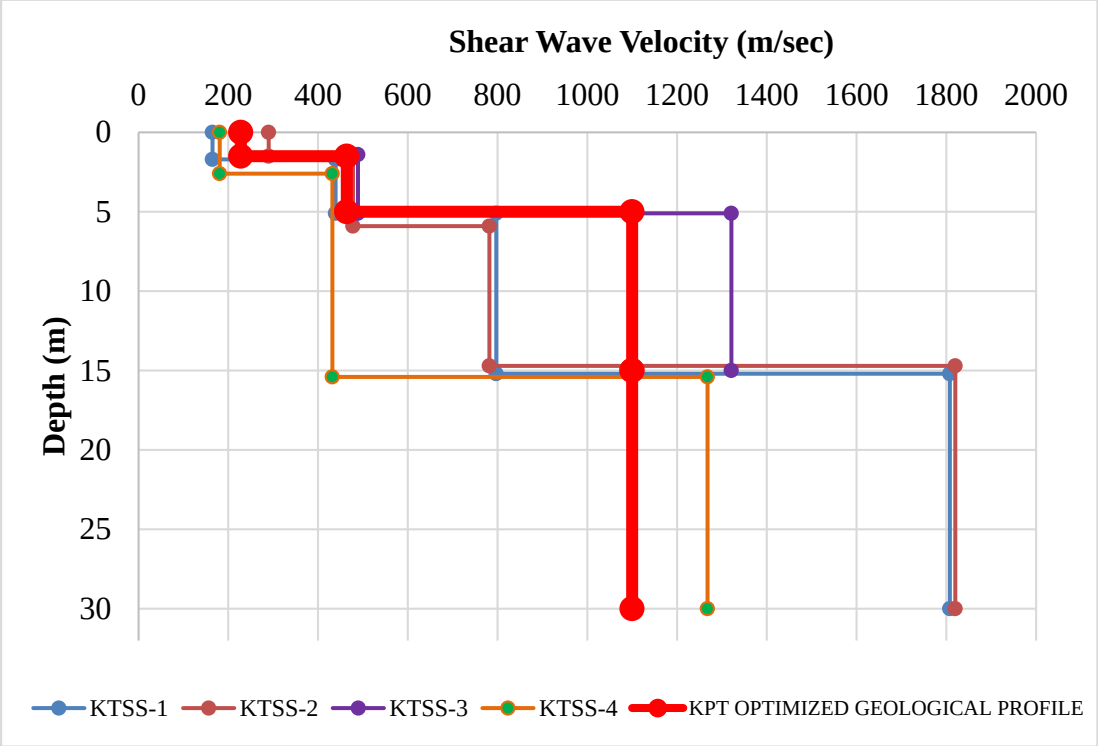

Figure 3.4 Optimized geological profile in terms of V_S in KPT vs depth graph

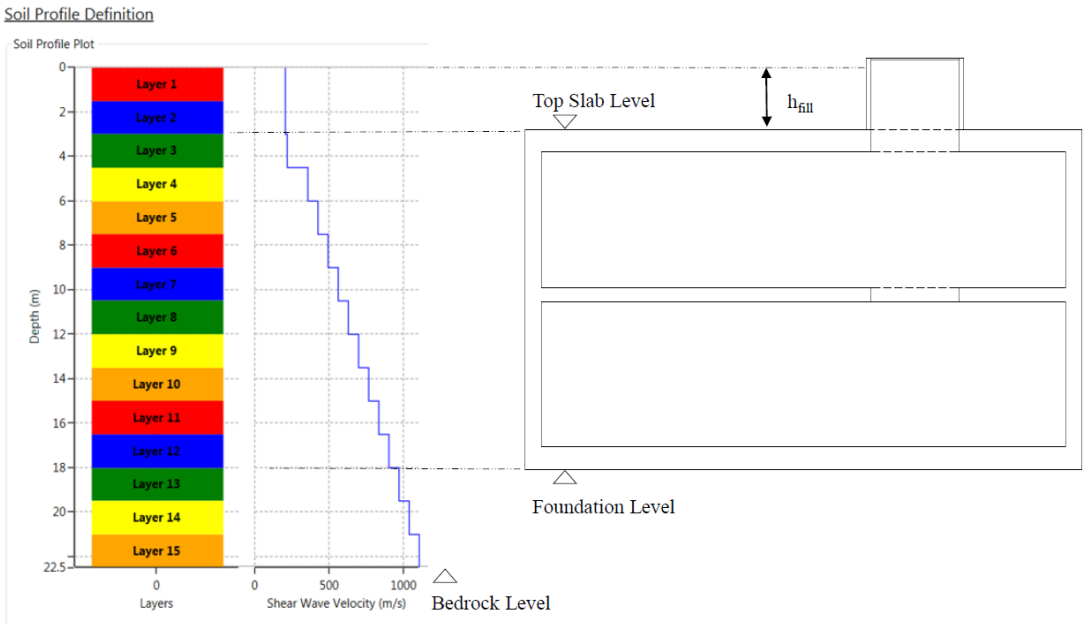

Figure 3.5 Deepsoil model of Esenyalı Station

Table 3.3 Optimized geological profile in terms of V_S in KPT

KPT Optimized Geological Profile	
Depth (m)	**V_S (m/sec)**
0-1.5,2	165-290
5	439-489
15	1100
Bedrock	

Four G/G_{max} and damping ratio curves (given in Figure 3.6 and 3.7, respectively) are assigned to the soil layers of the simplified profiles in DeepSoil software based on the soil properties such as plasticity index, gathered from the GIR. Table 3.4 exemplifies one of the simplified soil profiles utilized in the analysis; whereas, the other simplified profiles are provided in Appendix.

Table 3.4 Simplified soil profile of Esenyalı Station implemented in Deepsoil

Layer Number	Layer Name	Thickness (m)	Unit Weight (kN/m^3)	Shear Wave Velocity (m/s)	Soil Type
1	Artifical Fill	1.5	20	199	Vucetic and Dobry (1991) Clay PI:30
2	Artifical Fill	1.5	20	199	Vucetic and Dobry (1991) Clay PI:30
3	Artifical Fill	1.5	20	212	Vucetic and Dobry (1991) Clay PI:30
4	Silt Stone Clay Stone	1.5	22	351	Vucetic and Dobry (1991) Clay PI:30
5	Silt Stone Clay Stone	1.5	22	419	Vucetic and Dobry (1991) Clay PI:30
6	Silt Stone Clay Stone	1.5	22	487	Vucetic and Dobry (1991) Clay PI:30
7	Silt Stone Clay Stone	1.5	22	555	Vucetic and Dobry (1991) Clay PI:30
8	Silt Stone Clay Stone	1.5	22	623	Vucetic and Dobry (1991) Clay PI:30
9	Silt Stone Clay Stone	1.5	22	692	Vucetic and Dobry (1991) Clay PI:30
10	Silt Stone Clay Stone	1.5	22	760	Vucetic and Dobry (1991) Clay PI:30
11	Silt Stone Clay Stone	1.5	22	828	Vucetic and Dobry (1991) Clay PI:30
12	Silt Stone Clay Stone	1.5	22	896	Vucetic and Dobry (1991) Clay PI:30
13	Silt Stone Clay Stone	1.5	22	964	Vucetic and Dobry (1991) Clay PI:30
14	Silt Stone Clay Stone	1.5	22	1032	Vucetic and Dobry (1991) Clay PI:30
15	Silt Stone Clay Stone	1.5	22	1100	Vucetic and Dobry (1991) Clay PI:30
Bedrock			25	1100	Damping Ratio % 5

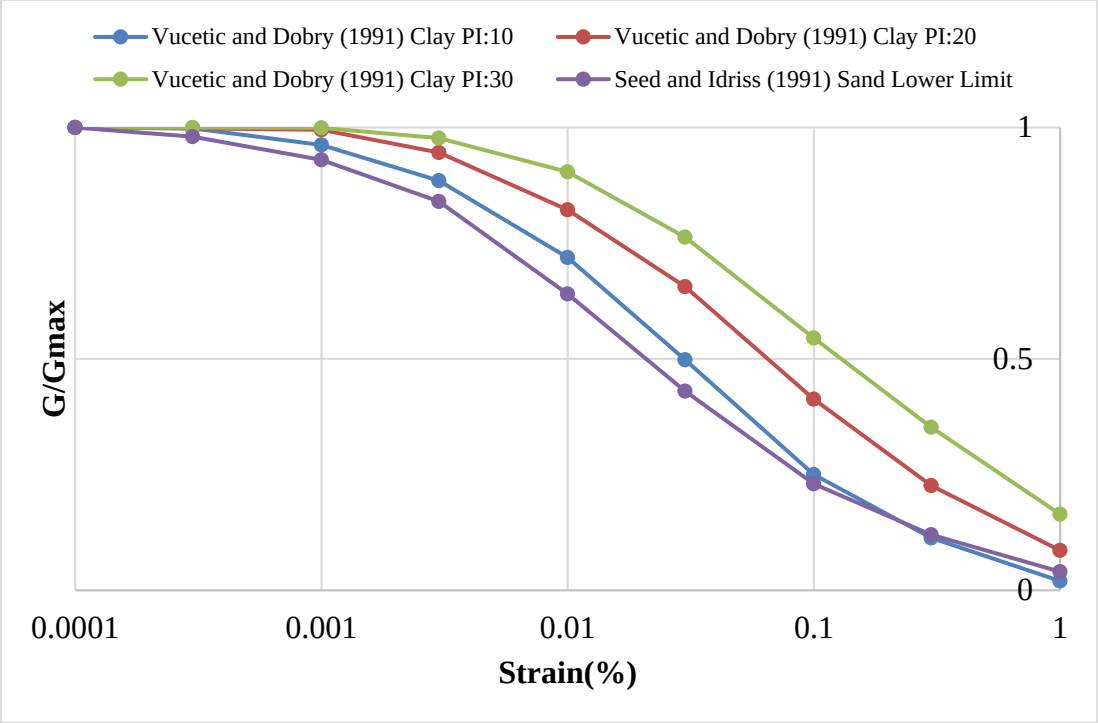

Figure 3.6 G/Gmax vs Strain (%) Graph for selected Deepsoil soil types

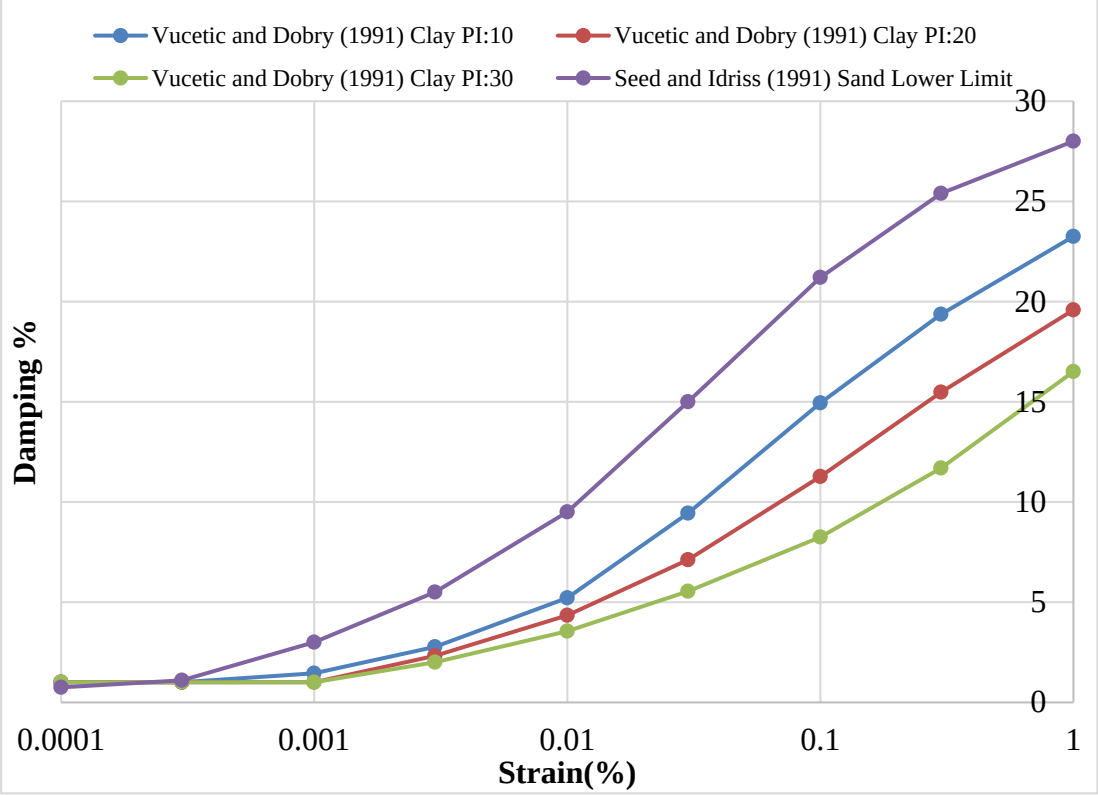

Figure 3.7 Damping vs Strain (%) Graph for selected Deepsoil soil types

3.2 Selected Time Series

To eliminate any possible site effects on the recorded ground motions, recordings from stations located on hard rock sites are preferred for the 1-D EQL site response analysis. 51 ground motions from the recording stations with V_{S30}>800 m/s are selected from the Pacific Earthquake Engineering Research Center (PEER) Ground Motion Database (https://ngawest2.berkeley.edu, last accessed on January, 2016) without considering the magnitude and distance values of the recordings. For each recording, the largest horizontal component is utilized in the analysis. Response spectra for the selected ground motions, mean and mean ± σ of the response spectra are given in Figure 3.8. Selected ground motions are scaled to the 475-year return period PGA at the bedrock level for each station using Eq. 3.2. The scale factors of each ground motion for each station are presented in Table 3.5 and Table 3.6. Scaled ground motions for an example station are given in Figure 3.9.

$$\text{PGA Scale Factor} = \frac{\text{475 Years Metro Station Expected PGA Value}}{\text{Selected Earthquake Critical Horizontal Acceleration Value}} \qquad 3.2$$

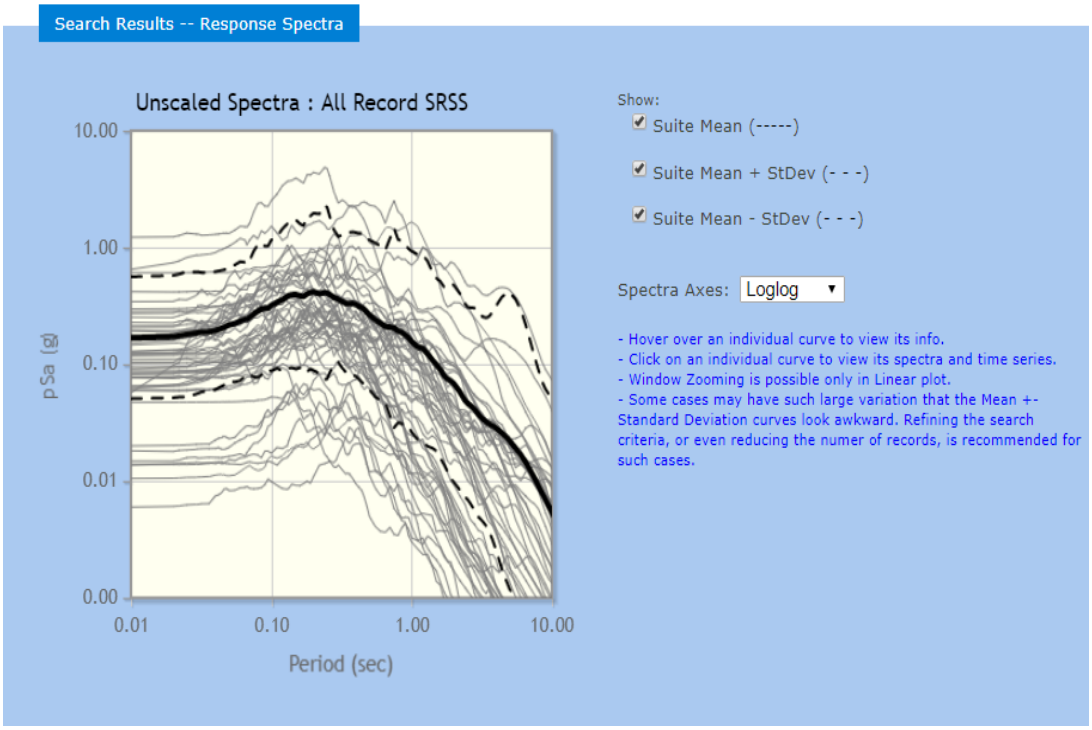

Figure 3.8 Unscaled horizontal spectrum acceleration values of all selected earthquakes

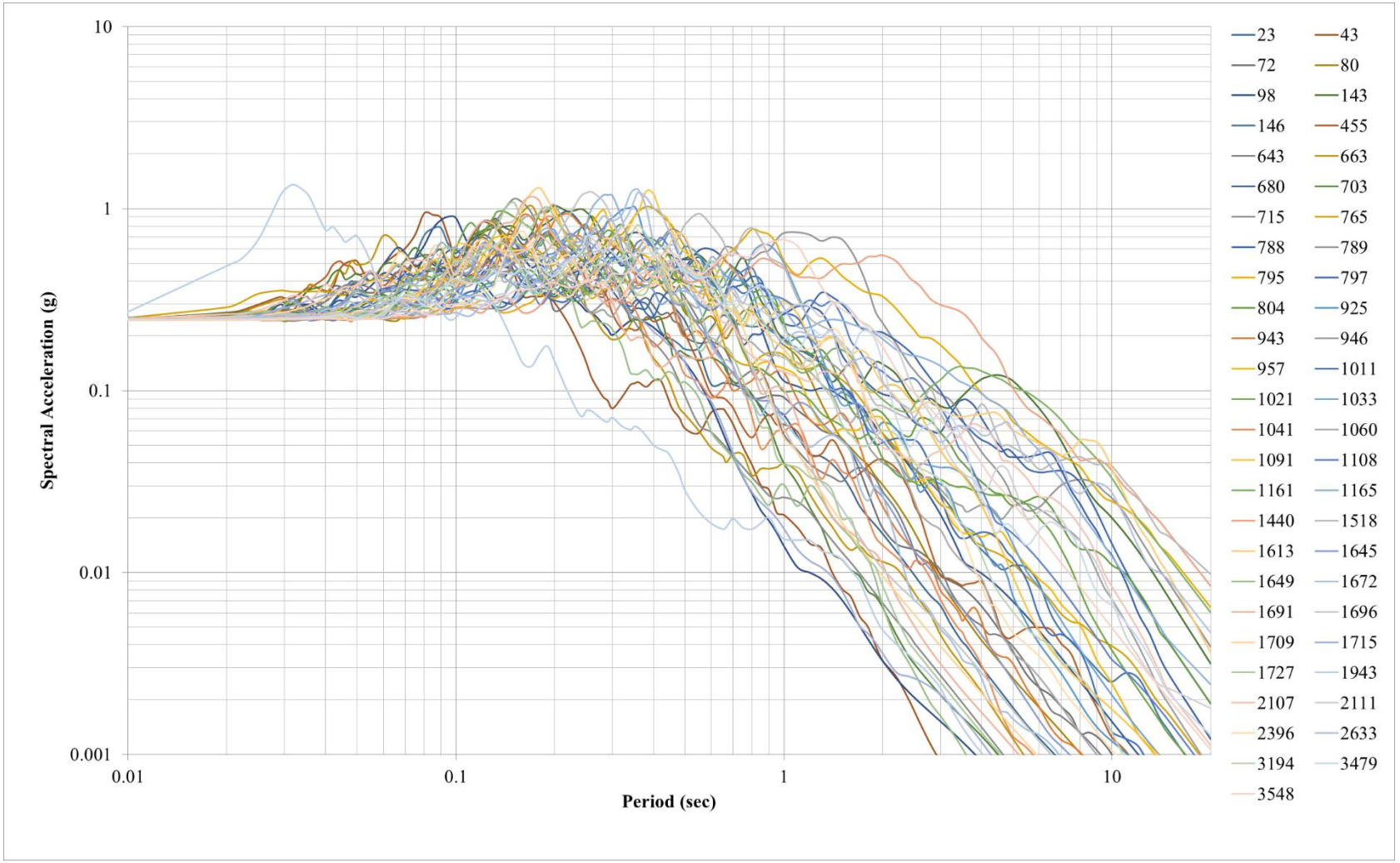

Figure 3.9 Scaled horizontal spectrum acceleration values of all selected earthquakes

Table 3.5 Properties of selected earthquakes and calculated scale factors (1/2)

						Scale Factors of Metro Stations											
RSN	**Earthquake**	**$V_{S,30}$ (m/s)**	**Mw**	**Rupture Distance (km)**	**Critical Horizontal Acceleration**	**St.1 S.R**	**St.2 S.R**	**St.3 S.R**	**St.4 S.R**	**St.5 S.R**	**St.6 S.R**	**St.7 S.R**	**St.8 S.R**	**St.9 S.R**	**St.10 S.R**	**St.11 S.R**	**St.12 S.R**
23	San Francisco-USA	874	5.3	11.02	0.095	2.570	3.567	3.462	2.728	3.357	2.518	2.518	2.623	2.465	2.623	3.882	2.728
43	Lytle Creek-USA	813	5.3	19.35	0.046	5.298	7.353	7.137	5.623	6.920	5.190	5.190	5.407	5.082	5.407	8.002	5.623
72	San Fernando-USA	822	6.6	25.07	0.198	1.239	1.719	1.669	1.315	1.618	1.214	1.214	1.264	1.188	1.264	1.871	1.315
80	San Fernando-USA	969	6.6	21.5	0.205	1.196	1.659	1.611	1.269	1.562	1.171	1.171	1.220	1.147	1.220	1.806	1.269
98	Hollister-USA-03	1428	5.1	10.46	0.141	1.744	2.420	2.348	1.850	2.277	1.708	1.708	1.779	1.672	1.779	2.633	1.850
143	Tabas, Iran	767	7.4	2.05	0.862	0.284	0.395	0.383	0.302	0.371	0.278	0.278	0.290	0.273	0.290	0.429	0.302
146	Coyote Lake-USA	1428	5.7	10.67	0.117	2.101	2.915	2.829	2.229	2.744	2.058	2.058	2.144	2.015	2.144	3.172	2.229
455	Morgan Hill-USA	1428	6.2	14.91	0.099	2.479	3.441	3.339	2.631	3.238	2.429	2.429	2.530	2.378	2.530	3.744	2.631
643	Whittier Narrows-USA-01	1223	6	27.64	0.049	5.040	6.994	6.789	5.349	6.583	4.937	4.937	5.143	4.834	5.143	7.612	5.349
663	Whittier Narrows-USA-01	822	6	22.73	0.180	1.363	1.891	1.836	1.446	1.780	1.335	1.335	1.391	1.307	1.391	2.058	1.446
680	Whittier Narrows-USA-01	969	6	18.12	0.112	2.192	3.042	2.952	2.326	2.863	2.147	2.147	2.237	2.103	2.237	3.310	2.326
703	Whittier Narrows-USA-01	996	6	50.39	0.066	3.721	5.163	5.011	3.948	4.860	3.645	3.645	3.797	3.569	3.797	5.619	3.948
715	Whittier Narrows-USA-02	822	5.3	19.78	0.155	1.579	2.191	2.126	1.675	2.062	1.546	1.546	1.611	1.514	1.611	2.384	1.675
765	Loma Prieta-USAa	1428	6.9	9.64	0.485	0.506	0.702	0.681	0.537	0.660	0.495	0.495	0.516	0.485	0.516	0.763	0.537
788	Loma Prieta-USA	895	6.9	73	0.084	2.924	4.058	3.939	3.103	3.820	2.865	2.865	2.984	2.805	2.984	4.416	3.103
789	Loma Prieta-USA	1316	6.9	83.45	0.074	3.331	4.623	4.487	3.535	4.351	3.263	3.263	3.399	3.195	3.399	5.031	3.535
795	Loma Prieta-USA	1250	6.9	76.05	0.062	3.953	5.486	5.324	4.195	5.163	3.872	3.872	4.034	3.792	4.034	5.970	4.195
797	Loma Prieta-USA	873	6.9	74.14	0.093	2.638	3.660	3.553	2.799	3.445	2.584	2.584	2.691	2.530	2.691	3.983	2.799
804	Loma Prieta-USA	1021	6.9	63.15	0.105	2.329	3.232	3.137	2.472	3.042	2.282	2.282	2.377	2.234	2.377	3.517	2.472
925	Big Bear-USA-01	822	6.5	59.87	0.051	4.767	6.616	6.421	5.059	6.227	4.670	4.670	4.865	4.573	4.865	7.200	5.059
943	Northridge-USA-01	822	6.7	68.93	0.067	3.642	5.054	4.906	3.865	4.757	3.568	3.568	3.716	3.493	3.716	5.500	3.865
946	Northridge-USA-01	822	6.7	46.91	0.068	3.582	4.971	4.825	3.801	4.678	3.509	3.509	3.655	3.436	3.655	5.409	3.801
957	Northridge-USA-01	822	6.7	16.88	0.159	1.540	2.138	2.075	1.635	2.012	1.509	1.509	1.572	1.478	1.572	2.326	1.635
1011	Northridge-USA-01	1223	6.7	20.29	0.159	1.541	2.138	2.076	1.635	2.013	1.510	1.510	1.572	1.478	1.572	2.327	1.635
1021	Northridge-USA-01	822	6.7	31.66	0.084	2.914	4.043	3.924	3.092	3.805	2.854	2.854	2.973	2.795	2.973	4.400	3.092

Table 3.6 Properties of selected earthquakes and calculated scale factors (2/2)

						Scale Factors of Metro Stations											
RSN	**Earthquake**	**$V_{S,30}$ (m/s)**	**Mw**	**Rupture Distance (km)**	**Critical Horizontal Acceleration**	**St.1 S.R**	**St.2 S.R**	**St.3 S.R**	**St.4 S.R**	**St.5 S.R**	**St.6 S.R**	**St.7 S.R**	**St.8 S.R**	**St.9 S.R**	**St.10 S.R**	**St.11 S.R**	**St.12 S.R**
1033	Northridge-USA-01	822	6.7	46.58	0.072	3.402	4.721	4.582	3.610	4.443	3.332	3.332	3.471	3.263	3.471	5.137	3.610
1041	Northridge-USA-01	822	6.7	35.88	0.234	1.048	1.454	1.411	1.112	1.368	1.026	1.026	1.069	1.005	1.069	1.582	1.112
1060	Northridge-USA-01	822	6.7	79.99	0.071	3.427	4.756	4.616	3.637	4.476	3.357	3.357	3.497	3.287	3.497	5.176	3.637
1091	Northridge-USA-01	996	6.7	23.64	0.151	1.622	2.252	2.185	1.722	2.119	1.589	1.589	1.656	1.556	1.656	2.450	1.722
1108	Kobe, Japan	1043	6.9	0.92	0.312	0.786	1.090	1.058	0.834	1.026	0.770	0.770	0.802	0.754	0.802	1.187	0.834
1161	Kocaeli, Turkey	792	7.5	10.92	0.261	0.940	1.304	1.266	0.997	1.227	0.920	0.920	0.959	0.901	0.959	1.419	0.997
1165	Kocaeli, Turkey	811	7.5	7.21	0.230	1.064	1.477	1.434	1.130	1.390	1.043	1.043	1.086	1.021	1.086	1.608	1.130
1440	Chi-Chi, Taiwan	1023	7.6	122.48	0.038	6.382	8.856	8.596	6.773	8.336	6.252	6.252	6.512	6.121	6.512	9.638	6.773
1518	Chi-Chi, Taiwan	1000	7.6	58.09	0.063	3.862	5.359	5.202	4.098	5.044	3.783	3.783	3.941	3.704	3.941	5.832	4.098
1613	Duzce, Turkey	782	7.1	25.88	0.053	4.617	6.408	6.219	4.900	6.031	4.523	4.523	4.712	4.429	4.712	6.973	4.900
1645	Sierra Madre-USA	822	5.6	10.36	0.276	0.888	1.232	1.196	0.942	1.160	0.870	0.870	0.906	0.852	0.906	1.341	0.942
1649	Sierra Madre-USA	996	5.6	39.81	0.125	1.955	2.714	2.634	2.075	2.554	1.916	1.916	1.995	1.876	1.995	2.953	2.075
1672	Northridge-USA-03	822	5.2	44.6	0.011	22.940	31.835	30.899	24.345	29.963	22.472	22.472	23.408	22.004	23.408	34.644	24.345
1691	Northridge-USA-06	822	5.3	82.63	0.013	18.575	25.777	25.019	19.712	24.261	18.196	18.196	18.954	17.817	18.954	28.052	19.712
1696	Northridge-USA-06	822	5.3	19.31	0.063	3.920	5.440	5.280	4.160	5.120	3.840	3.840	4.000	3.760	4.000	5.920	4.160
1709	Northridge-USA-06	1016	5.3	21.69	0.056	4.380	6.078	5.899	4.648	5.720	4.290	4.290	4.469	4.201	4.469	6.614	4.648
1715	Northridge-USA-06	1223	5.3	17.14	0.055	4.486	6.226	6.043	4.761	5.860	4.395	4.395	4.578	4.303	4.578	6.775	4.761
1727	Northridge-USA-06	822	5.3	81.67	0.013	18.256	25.335	24.590	19.374	23.845	17.884	17.884	18.629	17.511	18.629	27.571	19.374
1943	Anza-USA-02	845	4.9	32.12	0.041	6.015	8.348	8.102	6.384	7.857	5.892	5.892	6.138	5.770	6.138	9.084	6.384
2107	Denali, Alaska	964	7.9	50.94	0.095	2.568	3.564	3.459	2.725	3.354	2.516	2.516	2.621	2.463	2.621	3.878	2.725
2111	Denali, Alaska	964	7.9	43	0.109	2.253	3.127	3.035	2.391	2.943	2.207	2.207	2.299	2.161	2.299	3.403	2.391
2396	Chi-Chi, Taiwan-02	1000	5.9	78.38	0.010	23.740	32.946	31.977	25.194	31.008	23.256	23.256	24.225	22.771	24.225	35.853	25.194
2633	Chi-Chi, Taiwan-03	1000	6.2	103.56	0.005	46.402	64.394	62.500	49.242	60.606	45.455	45.455	47.348	44.508	47.348	70.076	49.242
3194	Chi-Chi, Taiwan-05	1000	6.2	91.83	0.016	15.806	21.935	21.290	16.774	20.645	15.484	15.484	16.129	15.161	16.129	23.871	16.774
3479	Chi-Chi, Taiwan-06	1000	6.3	83.43	0.007	32.754	45.455	44.118	34.759	42.781	32.086	32.086	33.422	31.417	33.422	49.465	34.759
3548	Loma Prieta-USA	1070	6.9	5.02	0.443	0.553	0.768	0.745	0.587	0.723	0.542	0.542	0.565	0.531	0.565	0.836	0.587

3.3 Horizontal Displacement Profiles

Simplified soil profiles are analyzed by utilizing the selected and scaled strong ground motions in the frequency domain using total stress analysis. The maximum horizontal displacement along the soil profile is estimated in each analysis as shown in Figure 3.10 for Sancaktepe station. Distribution of the displacement profiles indicate that the estimated values have a strong dependence on the selected ground motion even if the ground motions are scaled to the same shaking level. As a result, the coefficient of variation (COV) for the top slab displacement is 61.88% for this example and varies between 61.88% and 348.46% for each station. It is observed that the COV of horizontal displacement is significantly high in soil profiles which have shear velocity reversals (velocity reversals are layers within the soil/rock profile that have a velocity lower than that of the overlying strata as defined by Yagoda-Biran et al., 2017) and at stations with higher structural sizes (e.g. Samandıra station with 24.5m height). In each station, approximately 3-6 outlying analysis results are eliminated to properly model the uncertainity (eliminated recordings are listed in Table 3.7). After the elimination, Δ_{ff} values of each station are calculated using Eq. 3.3 for each recording then, the average horizontal displacement profile for each station are estimated as shown in Figure 3.10 by using average value of Δ_{ff}.

$$\Delta_{ff} = \Delta_{topslab} - \Delta_{foundation} \quad (3.3)$$

Table 3.7 Eliminated recordings for each station

Station	Outlier Recordings (RSN) – Not included in probabilistic model	Disgarded Recordings (RSN) - Due to Negative Differential Displacement
Abdurrahmangazi	946,1021,1108,1645	-
Aydıntepe	946,1108,1645	1161,2633
Esenyalı	946,1108,1645	-
Hasanpaşa	946,1108,1645	-
Kavakpınar	1943,1645	-
Meclis Mahallesi	946,1108,1645	-
Samandıra	946,1645,1943	-
Sancaktepe	946,1108,1645	943
Sarıgazi	946,1108,1645,1943	-
Sultanbeyli	946,1108,1645	-
Tuzla Belediye	946,1108,1645,1943	1161
Veysel Karani	1943,1645	23,943,1649,946

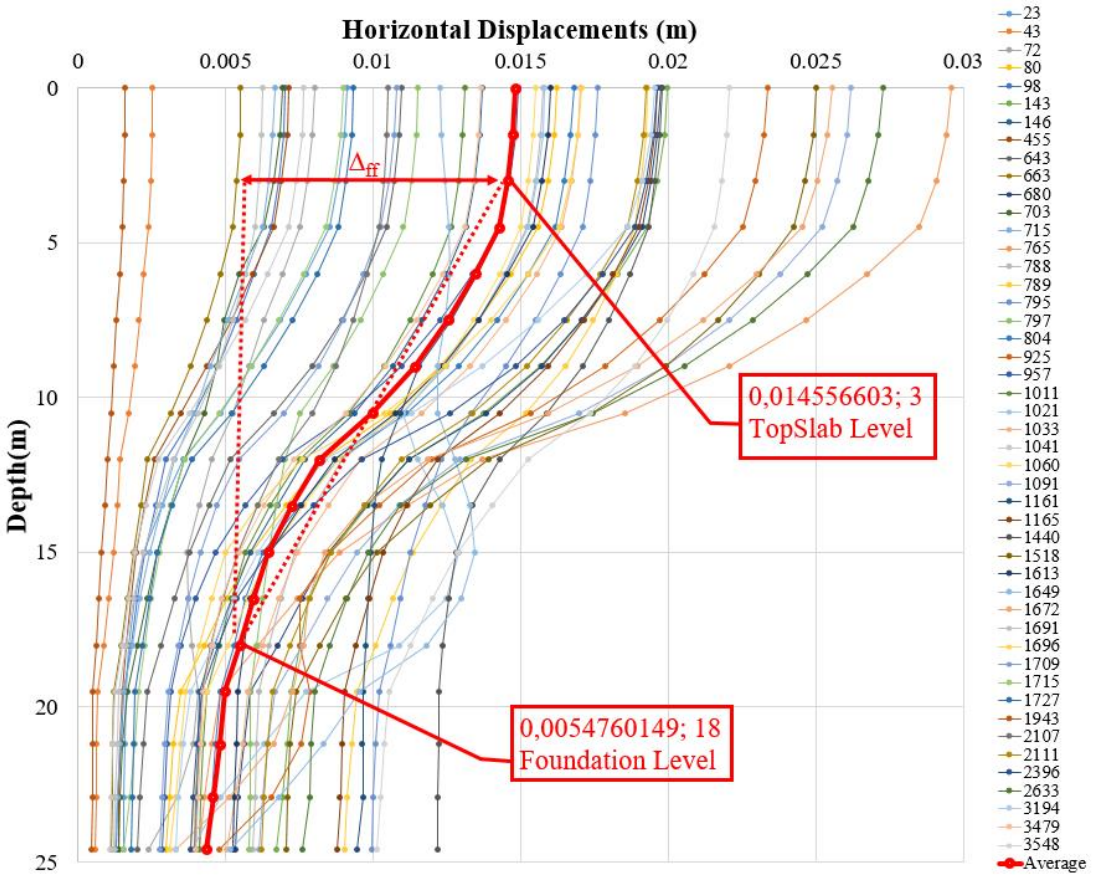

Figure 3.10 Horizontal displacement profile of Sancaktepe Station under scaled ground motions

Average free field displacement values estimated from the 1-D EQL analysis are compared to the Δ_{ff} values calculated by Equation 1.12 (Level 1 Method) in Table 3.8 and in Figure 3.11. Comparison of the results show that the average Δ_{ff} values estimated in 1-D EQL analysis are mostly in good agreement with the Δ_{ff} values found by Level 1 Method. The variation around the average value is significantly high for Samandıra station due to the height of the structure and shear velocity reversal in the soil profile. Additonally, high variation is valid for Veysel Karani station which has the maximum number of shear wave velocity reversals along the soil profile.

3.4 Emprical Prediction Equations for Free Field Displacement

Two empirical prediction equations for Δ_{ff} are developed based on the 1-D EQL analysis results using the functional form given in Equation 3.4. Model 1 only utilizes the average Δ_{ff} values for each station. Model 2 uses all analysis results for each station (approximately 50 data points per station) to model the uncertainty in record selection procedure. Model coefficients (a_1, a_2, a_3) are estimated by nonlinear regression analysis in SPSS software (Version 22, IBM Corp, 2013). Regression results for both models are provided in Tables 3.9 and 3.10, respectively.

$$\text{Ln (Displacement)} = a_1 + a_2 * \text{Ln (PGA)} + a_3 * \text{Ln (} Vs_{eq} \text{)} \pm \sigma \qquad 3.4$$

Vs_{eq} is defined in Equation 1.10 (From the top slab level up to bedrock level).

Table 3.8 Comparision of Δ_{ff} from 1-D EQL analysis average and Level 1 Method

Station	Δ_{ff} from 1-D EQL Analysis Average (cm)	Δ_{ff} from Level 1 Method (from Eq. 1.12, cm)
Abdurrahmangazi	0.098159	0.13214477
Aydıntepe	0.149486	0.18922926
Esenyalı	0.210621	0.28555032
Hasanpaşa	0.564831	0.25160332
Kavakpınar	0.918791	0.47903622
Meclis Mahallesi	0.144744	0.18407783
Samandıra	2.058843	1.01008289
Sancaktepe	0.908059	0.37954582
Sarıgazi	1.081462	1.01301854
Sultanbeyli	0.126067	0.17983308
Tuzla Belediye	0.239204	0.44459149
Veysel Karani	1.076280	0.39152041

Table 3.9 : Coefficients and standard deviations of Model 1

Model		Unstandardized Coefficients		Standardized Coeff.	t	Sig.
		B	Std. Error	Beta		
1	(Constant)	25.067	3.395	0.000	7.383	4.18×10^{-5}
	Ln (Vs_{eq})	-3.962	0.462	-1.048	-8.583	1.256×10^{-5}
	Ln (PGA)	1.692	0.791	0.261	2.139	0.061

**R square of equation is 0.898, Standard deviation of equation is 0.370.*

Table 3.10 : Coefficients and standard deviations of Model 2

Model		Unstandardized Coefficients		Standardized Coeff.	t	Sig.
		B	Std. Error	Beta		
1	(Constant)	29.984	1.368	0.000	21.912	2.343×10^{-77}
	Ln (Vs_{eq})	-4.784	0.187	-0.822	-25.619	1.944×10^{-96}
	Ln (PGA)	2.031	0.318	0.205	6.384	3.613×10^{-10}

**R square of equation is 0.556, Standard deviation of equation is 1.026.*

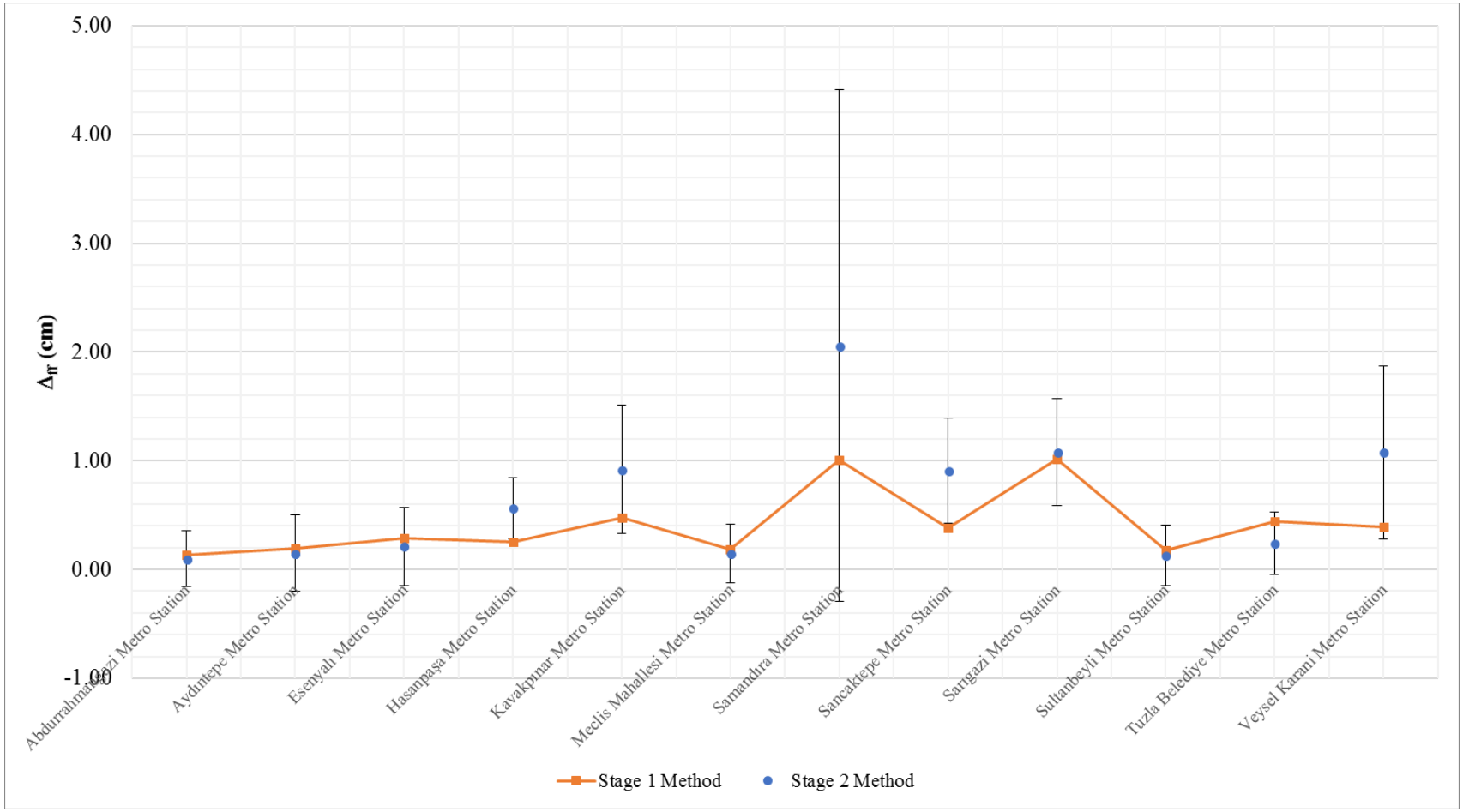

Figure 3.11 Comparision of Δ_{ff} from Level 1 Method And Level 2 Method

$$\text{Ln (Displacement)} = 25.067 + 1.692 * \text{Ln (PGA)} - 3.962 * \text{Ln (} Vs_{eq} \text{)} \quad 3.5$$

$$\text{Ln (Displacement)} = 29.984 + 2.031 * \text{Ln (PGA)} - 4.784 * \text{Ln (} Vs_{eq} \text{)} \quad 3.6$$

The median predictions for both models are compared to the average Δ_{ff} values from 1-D EQL analysis results in Table 3.11. Table 3.11 shows that the model predictions are quite close to the actual values for Model 1; whereas, the median model predictions are generally lower than the actual average Δ_{ff} values for Model 2. Standard deviation of both models are also significantly different; Model 2 has a sigma value of almost 3 times higher than that of Model 1 as expected (in ln units). The standard deviation of the mean is ignored in Model 1.

Table 3.11 : Comparision of actual displacements and median displacements of prediction models

Station Name	Actual (cm)	Median Model 1 (cm)	Median Model 2 (cm)
Abdurrahmangazi	0.098159	0.102431	0.048941
Aydıntepe	0.149486	0.160832	0.084025
Esenyalı	0.210621	0.368336	0.228625
Hasanpaşa	0.564831	0.474983	0.311765
Kavakpınar	0.918791	1.004451	0.768047
Meclis Mahallesi	0.144744	0.167633	0.088738
Samandıra	2.058843	1.340695	1.092556
Sancaktepe	0.908059	1.040255	0.803817
Sarıgazi	1.081462	0.746505	0.538889
Sultanbeyli	0.126067	0.158519	0.082901
Tuzla Belediye	0.239204	0.130201	0.065033
Veysel Karani	1.076280	1.460801	1.210548

Prediction models are evaluated by analyzing the distribution of residuals (difference of actual values from the model predictions in ln units) with model parameters, PGA and Vs_{eq} in Figures 3.12 for Model 1 and Model 2, respectively. Residuals for prediction model 1 are equally distributed along the zero line, indicating no significant trends with PGA. Similarly, no significant trends are observed for soft to hard soil sites with smaller Vs_{eq} values (<400 m/sn). However for higher Vs_{eq} values for stiff soil to

soft rock sites, residuals are negative, indicating that the model overestimates the actual Δ_{ff} values. Distribution of the residuals with PGA for prediction model 2 is not different than prediction model 1. On the other hand, both positive and negative residuals are present for high Vs_{eq} values in prediction model 2. Figure 3.12 shows a significant under estimation for Tuzla Belediye station with PGA_{rock} = 0.37g however data points above 0.35g is very limited to understand if a modification in the model for high ground shaking values are necessary.

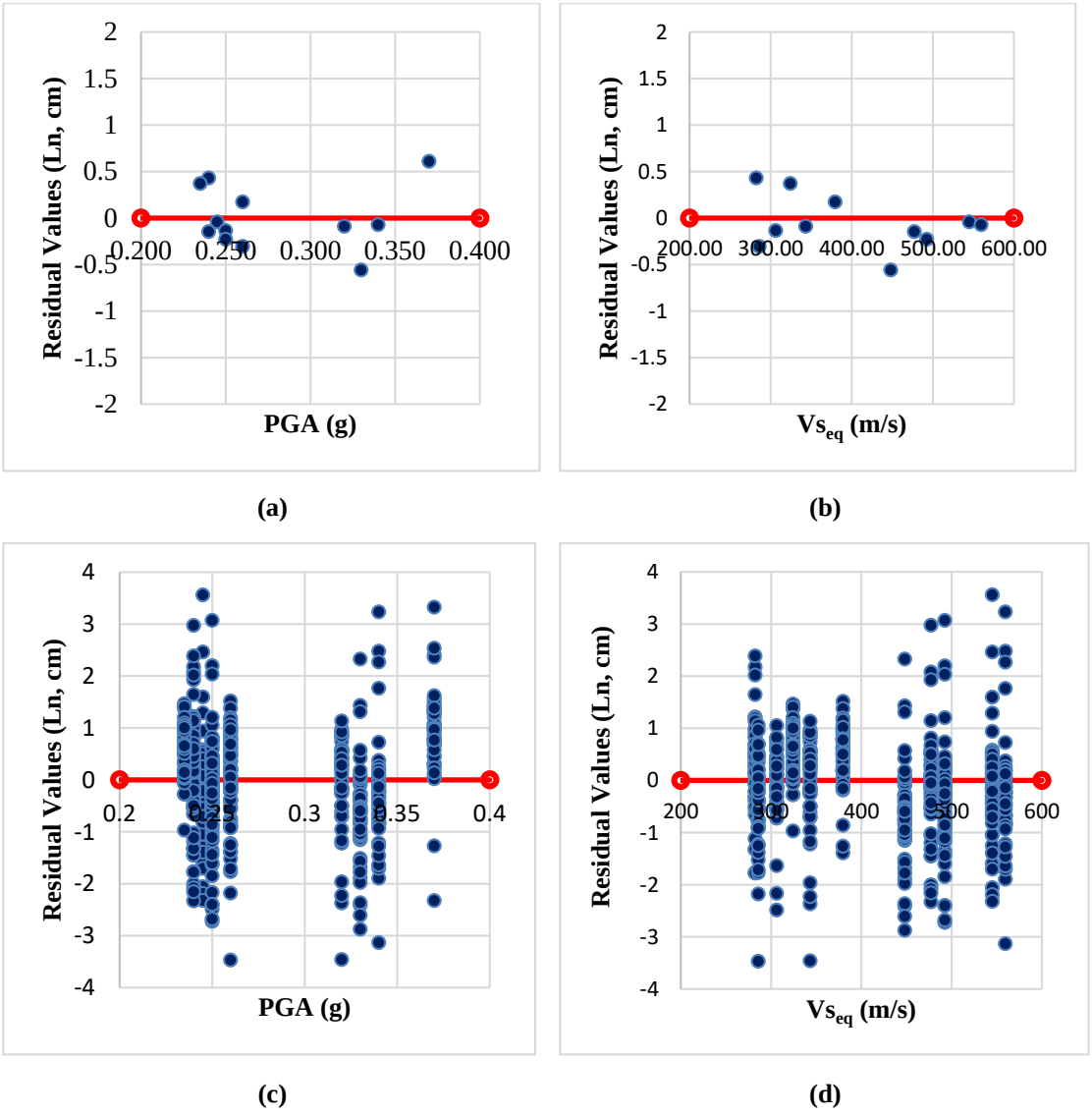

Figure 3.12 Distribution residuals with PGA (a), Vs_{eq} (b) for Prediction Model 1, with PGA (c) and Vs_{eq} (d) for Prediction Model 2.

CHAPTER 4

HAZARD CURVES FOR FREE FIELD DISPLACEMENT AND CONCLUSIONS

In Chapter 3, two prediction models (Equation 3.4 and Equation 3.5) are proposed for estimating free field displacement based on PGA and Vs_{eq} of the soil profile. In this chapter, proposed prediction equations are integrated into the PSHA integral to built free field displacement hazard curves within the Performance Based Earthquake Engineering (PBEE) framework. These hazard curves are used to estimate 475-year return period Δ_{ff} values. Estimated Δ_{ff} values are compared to Δ_{ff} values calculated by Level 1 and Level 2 Methods and median estimations from the proposed prediction equations. Differences in these values are thoroughly discussed within this chapter to evaluate the return period of Δ_{ff} values estimated by Level 1 and Level 2 Methods.

4.1 Performance Based Earthquake Engineering

Performance-based seismic evaluation calls for the assessment of structural performance under seismic loads by measurable and meaningful terms for decision makers. In other words, performance-based earthquake engineering aims to estimate the seismic risk due to earthquakes which will occur in the future. PEER developed the performance-based earthquake engineering (PBEE) framework by connecting the earthquake scenarios, design ground motions, structural demand, and performance variables (Stewart et al., 2002). According to Stewart et al. (2002), PBEE includes the assessment of four fundamental variables; i) assessment of the probability of exceeding ground motion intensity measures (IM), ii) distribution of engineering demand parameters (EDPs), iii) distribution of damage measures (DMs); iv) assessment of the probability of exceeding decision variables (DV). The relation

between the key variables in PEER-PBEE framework are presented in Figure 4.1. Connecting these variables with the total probability theorem results in the PBEE integral given in Equation 4.1.

$$v(DV) = \int\int\int G(DV \mid DM) \times dG(DM \mid EDP) \times dG(EDP \mid IM) \times v(IM) \qquad 4.1$$

where, G(DV | DM) is the probability of exceeding DV given DM, dG (DM | EDP) is the probability of exceeding DM given EDP, dG (EDP | IM) is the probability of exceeding EDP given IM, v(IM) is the annual rate of exceeding the IM. In this study, elements of first part (e.g. seismic sources, seismic source characterization, earthquake scenarios) shown in Figure 4.1 are presented in Chapter 2 with details. The ground motion IM utilized in this study is PGA and v(IM) values are provided by the hazard curves for each station (Figure 2.7 and 2.8).

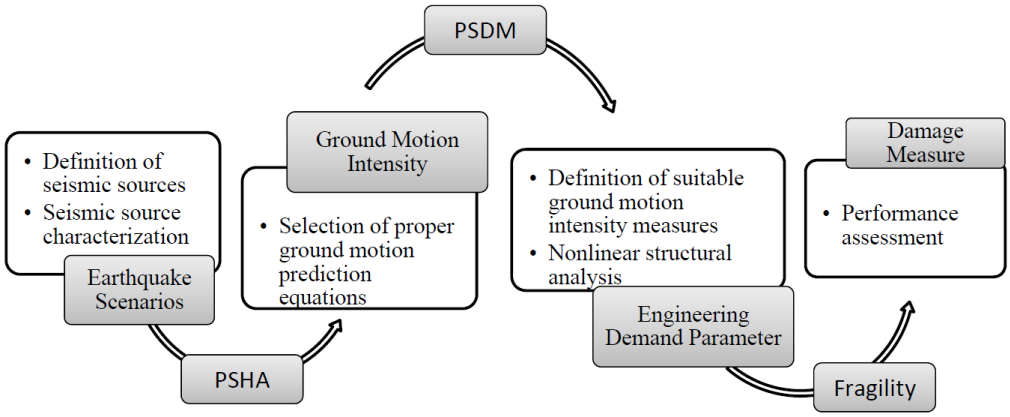

Figure 4.1 PEER PBEE framework scheme (from Gülerce, 2013, p. 538)

Cornell and co-workers (Baker and Cornell, 2003; Tothong and Cornell, 2006) proposed the probabilistic seismic demand model (PSDM) approach where the results of dynamic analyses for a specific structures are used to model the behaviour of important EDPs in terms of different IMs. A similar approach can be implemented in geotechnical earthquake engineering: for the case of underground structures, Δ_{ff} is a representative engineering demand parameter. Selection procedure of an efficient, sufficient and feasible IM was thoroughly discussed by Luco and Cornell (2007). For

this study, PGA is selected as the IM since Level 1 Method directly show the relationship between Δ_{ff} and PGA.

According to Luco (2002), formulation of the relationship between EDPs and IMs is an important step for developing a PSDM. Cornell et al. (2012) found out that the PSDMs for steel moment frame buildings are lognormally distributed. Therefore, the relationship between EDPs and IMs can be interpreted with a linear dependence in log-log space as shown in Equation 4.2 (Gülerce, 2013):

$$\ln(EDP) = c_1 \times \ln(IM) + c_2 \pm \sigma_{PSDM} \quad 4.2$$

In this study, functional form given in Equation 4.2 is used to develop the prediction models given in the Chapter 3 with an additional parameter (Vs_{eq}) representing the site stiffness.

The traditional form of the hazard integral is given in Equation 4.3 where N_{min} is the annual rate of earthquakes, M is moment magnitude, R is the distance, $f_m(M)$ and $f_R(M,R)$ are the probability density functions for the magnitude and distance, $f_\varepsilon(\varepsilon)$ is the probability density function for the epsilon, and $P(IM > z \mid M, R, \varepsilon)$ is the probability that IM exceed z.

$$v(IM > z) = N_{min} * \int_M \int_R \int_\varepsilon f_M(M)\, f_R(M,R)\, f_\varepsilon(\varepsilon)\, P\left(IM > z \mid M, R, \varepsilon\right) \times dM \times dR \times d\varepsilon \quad 4.3$$

If this form of hazard integral is slightly modified as shown in Equation 4.4, then the second part of the PEER-PBEE framework presented in Figure 4.1 and the PSDMs can be directly included in the hazard calculations. Gülerce and Abrahamson (2010) showed that a scalar PSDM can be incorporated to the hazard integral to determine the annual probability of exceeding a certain EDP as shown below:

$$v(EDP>y) = N_{min} * \int_M \int_R \int_\varepsilon f_M(M)\, f_R(M,R)\, f_\varepsilon(\varepsilon)\, P\left(\widehat{EDP} > y \mid EP\left[IM(M,R,\varepsilon)\right], \sigma_{\ln EDP}\right) dM \times dR \times d\varepsilon \quad 4.4$$

where $\widehat{EDP}(IM(M,R,\varepsilon))$ is the median EDP, σ_{InEDP} is standard deviation of In(EDP). The output of Equation 4.4 will be the hazard curves for the selected EDP.

To develop a full PBEE framework, the damage measures for Δ_{ff} should be determined and decision variables should be defined. Typically the DM values or the damage states are defined by codes and regulations (Miranda and Aslani, 2003); however DM values or fragility curves for Δ_{ff} are not available in TEC (2007) or in the updated earthquake code of Turkey. Therefore, a full PBEE framework is not developed within in the contents of this study.

4.2 Hazard Curves For The Displacement

The modified form of hazard integral (Equation 4.4) is used to develop the hazard curves for Δ_{ff} for the approximate locations of metro stations along KPT and CSS Metro Line. Hazard curves based on Prediction Model 1 and Prediction Model 2 are presented in Figure 4.2 and 4.3, respectively. Figure 4.2 and 4.3 are significantly different than each other because of the differences in implemented prediction models. It should be underlined that the median predictions of Model 1 and Model 2 are pretty similar; however, the standard deviations of the models are significantly different. Therefore, the differences between the hazard curves are related to the differences in the standard deviations of prediction models. Still, the maximum 475- year return period Δ_{ff} value and the minimum 475-year return period Δ_{ff} value are observed at the same metro stations for different prediction models.

The Δ_{ff} values calculated by Level 1 and Level 2 Methods are compared with the 475-year return period Δ_{ff} values in Table 4.1. Estimated Δ_{ff} values for 475-year return period vary between 0.12-1.60 cm and 0.092-2.20 cm for Prediction Model 1 and Model 2, respectively. The highest 475-year return period Δ_{ff} values are estimated for Samandıra and Veysel Karani stations with smallest Vs_{eq} values. The minimum 475-year return period Δ_{ff} value is estimated for Abdurrahmangazi station; even if it is not the station with highest Vs_{eq} value, the Δ_{ff} value is small because the 475-year return period PGA value is low for this station. It is clear that the hazard curves based on Prediction Model 1 suffers from the small standard deviation value of the prediction

model; therefore, hazard curves given in Figure 4.3 more accurately represent the possible uncertainties involved in Level 2 Method. When the uncertainties in the input soil parameters, such as V_S profile, unit weight, equilavent linear soil properties etc. are included, the uncertainty range will be wider and 475- year return period Δ_{ff} estimations will be higher.

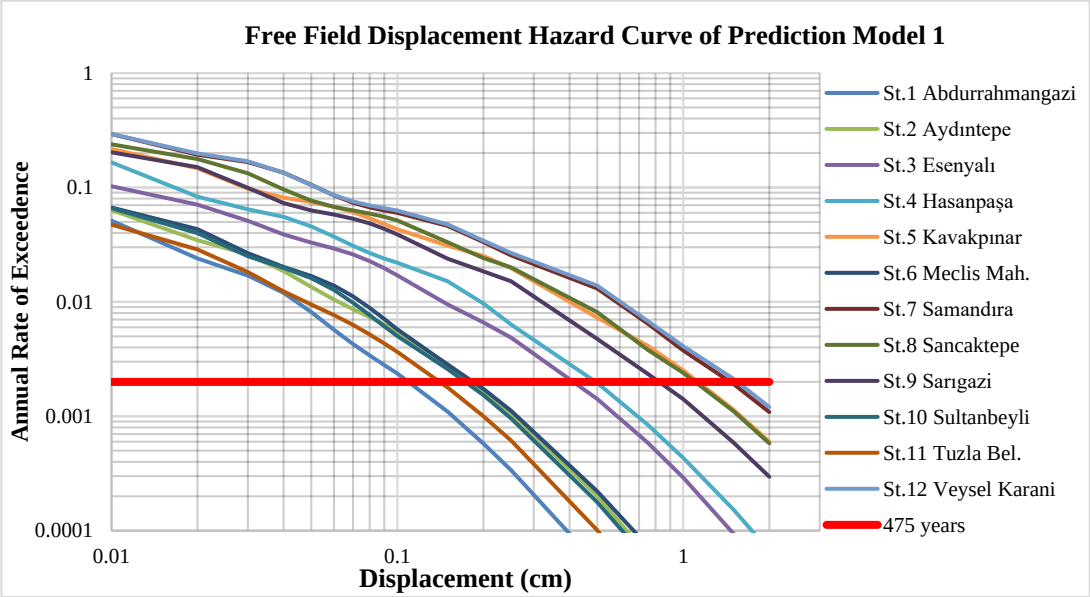

Figure 4.2 Hazard Curve based on Prediction Model 1

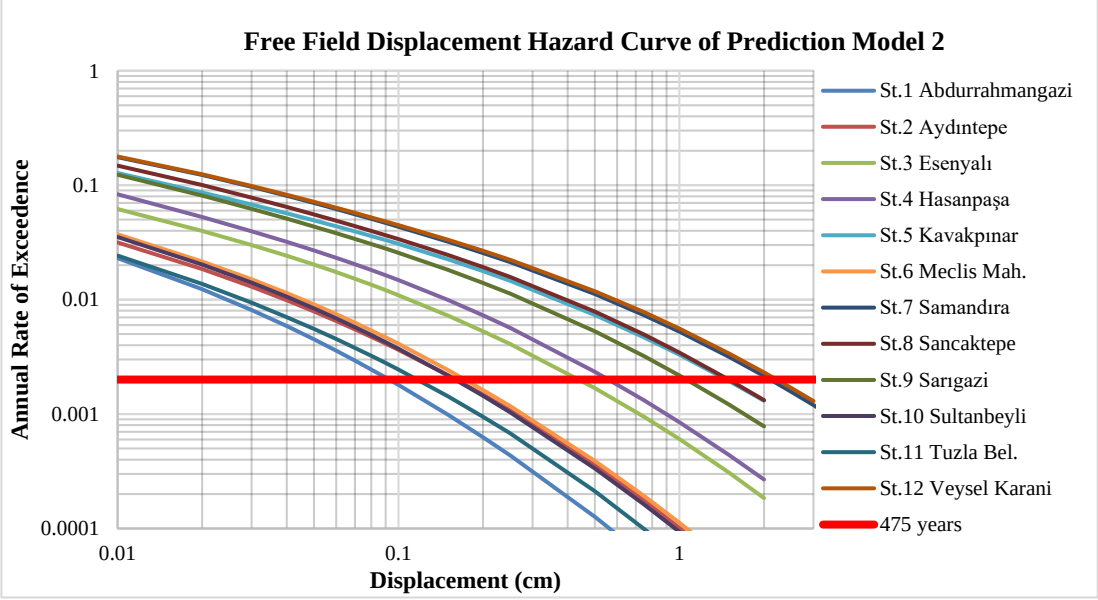

Figure 4.3 Hazard Curve based on Prediction Model 2

Table 4.1 Comparison of Δ_{ff} outputs from Level 1 Methods, Level 2 Method, 475-year return period Δ_{ff} from prediction models

Station Name	Level 1 Method Δ_{ff} (cm)	Level 2 Method Δ_{ff} (cm)	475 years Prediction Model 1 Displacement (cm)	475 years Prediction Model 2 Displacement (cm)	Prediction Model 1 Displacement (cm)	Prediction Model 2 Displacement (cm)
Abdurrahmangazi	0.132	0.0982	0.120	0.092	0.102	0.049
Aydıntepe	0.189	0.150	0.180	0.160	0.161	0.084
Esenyalı	0.286	0.211	0.420	0.430	0.368	0.229
Hasanpaşa	0.252	0.565	0.480	0.560	0.475	0.312
Kavakpınar	0.479	0.919	1.200	1.500	1.004	0.768
Meclis Mahallesi	0.184	0.145	0.180	0.170	0.168	0.089
Samandıra	1.010	2.059	1.500	2.050	1.341	1.093
Sancaktepe	0.380	0.908	1.200	1.500	1.040	0.804
Sarıgazi	1.013	1.082	0.800	1.100	0.747	0.539
Sultanbeyli	0.180	0.126	0.180	0.160	0.159	0.083
Tuzla Belediye	0.445	0.239	0.150	0.120	0.130	0.065
Veysel Karani	0.392	1.076	1.600	2.200	1.461	1.211

Based on Table 4.1, following observations can be made;

- For Abdurrahmangazi, Aydıntepe, Meclis Mahallesi, and Sultanbeyli stations, calculated Δ_{ff} values by Level 1 Method (column 1), median predictions of Model 1 (column 5) and 475-year return period Δ_{ff} values from hazard curves based on Prediction Model 1 (column 3) are quite close to each other.
- For Abdurrahmangazi, Aydıntepe, Meclis Mahallesi, Samandıra, Sarıgazi stations, calculated Δ_{ff} values by Level 2 Method (column 2) and 475-year return period Δ_{ff} values from hazard curves based on Prediction Model 2 (column 4) are similar to each other. It should be noted that for Prediction Model 2, median predictions (column 6) are not similar to 475-year return period Δ_{ff} values estimated from the hazard curves (column 4) because of the high standard deviation of the prediction model.

- The 6 metro stations discussed above, Abdurrahmangazi, Aydıntepe, Esenyalı, Meclis Mahallesi, Sultanbeyli and Tuzla Belediye, do not have shear wave velocity reversals in the soil profile. For these stations, ratio of Δ_{ff} from Level 1 Method (column 1) to Level 2 Method (column 2) are between 1.27-1.86. The highest ratio, 1.86 is seen in Tuzla Belediye Metro Station which has a significantly high structure (25.5 meters) compared to other stations, indicating the importance of structural dimensions on the Δ_{ff} estimations.
- For other 6 metro stations that have shear velocity reversals in the soil profile, the observations are completely opposite. Level 2 Method (column 2) gives relatively high Δ_{ff} values compared to Level 1 Method (column 1). For these stations, ratio of Δ_{ff} from Level 2 Method to Level 1 Method varies between 1.068-2.749. The highest ratio is observed in Veysel Karani Metro Station which includes maximum number of shear wave velocity reversals along the soil profile.
- These observations clarify that Δ_{ff} should be determined by Level 2 Method especially for metro stations which have shear velocity reversals in the soil profile. In the Level 1 Method, soil profile's strength is represented by a single parameter (Vs_{eq}); therefore, effect of shear velocity revelsal is not represented in the estimations.
- Median estimates of Prediction Model 1 (column 5) are generally higher than median estimates of Prediction Model 2 (column 6). The ratio of estimated Δ_{ff} from Model 1 to Model 2 is between 1.21-2.09.
- Estimated 475-year return period Δ_{ff} values based on both prediction models are different that Δ_{ff} values calculated by Level 1 and Level 2 Methods. This observation proves that the Δ_{ff} values calculated by Level 1 and Level 2 Methods have a different return period than 475 years even if the 475-year return period PGA is implemented in the calculations.
- In order to properly model the effect of shear wave velocity reversal in the soil profile on the Δ_{ff} estimations, Prediction Model 2 that incorporates the

variability related to the ground motion is preferable. When a fully probabilistic framework that includes the variability in the soil parameters is utilized, effect of shear wave velocity reversal on the results may be better understood.

4.3 Summary and Conclusion

This study makes the first attempt to propose a fully probabilistic framework for estimating the free field deformations to be used in the seismic design of underground infrastructure, especially the metro stations. For this purpose, stations of two metro lines planned to be constructed in Istanbul: KPT and CSS Metro Lines are used as case studies. A new planar seismic source characterization model is developed which includes the segments of NAFZ that are close to approximate locations of metro stations and used in the estimation of PGA values with 475-year return period. In the first phase of the study, Δ_{ff} values are estimated by using current and deterministic methods (Level 1 and Level 2 Methods) however a large suite of ground motions are incorporated to the Level 2 analysis to properly model the uncertainty related to ground motion selection. Based on the analysis results, two preditions models are proposed and incorporated to the hazard integral to estimate Δ_{ff} values in a probabilistic PBEE framework. At the final phase of the study, Δ_{ff} values calculated by Level 1 and Level 2 Methods and estimated from Δ_{ff} hazard curves are compared, showing that these values are significantly different especially when shear velocity reversals exist in the soil profile. A detailed discussion related to return period of Δ_{ff} values from Level 1 and Level 2 Methods is provided in Section 4.2.

The limitations of study and suggestions on the future works are elaborated below:

- The SPT-N values given in borehole logs show that the profiles generally consist of stiff soils (SPT-N>20). Therefore, Δ_{ff} values calculated here only represent temporary deformations due to seismic events. Possible permanent deformations related to soil liquefaction are disregarded in the calculations, however, these deformations may be more critical for the sites that include softer soil layers.

- In the 1-D EQL analysis (Level 2 Method), the total stress analysis in frequency domain is applied. In Level 2 and Level 3 Methods, it is possible to include the effect of pore water pressure increase during the seismic exitation and soil's nonlinearity in calculations. However, time domain analysis in EQL approach requires additional soil properties to be implemented in the analysis and the dynamic numerical analysis are time consuming especially when a large suite of ground motions are included in the analysis scheme. Therefore, these methods are not implemented in this study but might be used in the future studies.
- Equivalent shear wave velocity of metro stations used in the study varies between 282.35 m/sec and 611.98 m/sec, representing NEHRP C and NEHRP D type of soils. It is notable that the Vs_{eq} range of the analyzed soil profiles is relatively narrow. Additionally, the 475-year return period PGA values changes between 0.245g and 0.37g for metro stations. Therefore, the proposed prediction models are only valid for these intervals and based on a limited number of cases. If these models will be used for estimating Δ_{ff} in future studies, applicability of the models out of these ranges should be validated with additional analysis. In the future, proposed model's applicability range may be extended to include softer soil sites and wider PGA range.
- For constructing Δ_{ff} hazard curves, second prediction model is preferable since the standard deviation of the model includes the uncertainty in ground motions selection. When the uncertainty in the soil properties is included, the standard deviation of the prediction model is expected to increase and the 475-year return period Δ_{ff} values will also increase.
- Proposed approach requires the user to calculate the probability of exceeding the Δ_{ff} value based on probability of exceeding the PGA value (in other words conditional probabilities need to be used in the calculations). Therefore, knowing the 475-year return period PGA value will not be sufficient and the whole hazard curve should be included in the calculations.

REFERENCES

Aksoy, M. E., Meghraoui, M., Vallée, M., and Çakır, Z. (2010). Rupture Characteristics of the AD 1912 Mürefte (Ganos) Earthquake Segment of the North Anatolian Fault (Western Turkey). Geology, 38.11, 991-994, doi:10.1130/G31447.1.

Akyüz, S., Hartleb, R.D., Barka, A.A, Altunel, E., Sunal, G., Meyer, B., Armijo, R. (2002). Surface rupture and slip distribution of the 12 November 1999 Düzce earthquake (M7.1), North Anatolian Fault, Bolu, Turkey, Bull. Seismological Society of America 92(1), 61–66.

Altunel, E., Meghraoui, M., Akyüz, H. S., and Dikbas, A. (2004). Characteristics of the 1912 Co-Seismic Rupture Along the North Anatolian Fault Zone (Turkey): Implications for the Expected Marmara Earthquake. Terra Nova, 16(4), 198-204, doi: 10.1111/j.1365-3121.2004.00552.x.

Ambraseys, N. N., and Jackson, J. A. (2000). Seismicity of the Sea of Marmara (Turkey) since 1500. Geophysical Journal International, 141(3), F1-F6, doi:10.1046/j.1365-246x.2000.00137.x.

An, L. Y. (1997). Maximum link distance between strike-slip faults: Observations and constraints. Pure Appl. Geophys., 150, 19-36.

Anderson, D. G. (2008). Seismic analysis and design of retaining walls, buried structures, slopes, and embankments (Vol. 611). Transportation Research Board.

Armijo, R., Meyer, B., Navarro, S., King, G., and Barka, A. (2002). Asymmetric slip partitioning in the Sea of Marmara pull-apart: a clue to propagation processes of the North Anatolian Fault?. Terra Nova, 14, 80-86.

Arango, I. (2008). Theme Paper: Earthquake Engineering for Tunnels and Underground Structures. A Case History. In Geotechnical Earthquake Engineering and Soil Dynamics IV (pp. 1-34).

Ayhan, M. E., Bürgmann, R., McClusky, S., Lenk, O., Aktug, B., Herece, E., and Reilinger, R. E. (2001). Kinematics of the Mw=7.2, 12 November 1999, Düzce, Turkey Earthquake. Geophysical Res. Lett., 28 (2): 367-370.

Baker, J. W., & Cornell, C. A. (2003). Uncertainty specification and propagation for loss estimation using FOSM method (p. 100). Pacific Earthquake Engineering Research Center, College of Engineering, University of California.

Barka, A. A. and Kadinsky-Cade, K. (1988). Strike-Slip Fault Geometry in Turkey and Its Influence on Earthquake Activity. Tectonics, 7(3), 663-684.

Barka, A., Akyüz, H. S., Altunel, E., Sunal, G., Cakir, Z., Dikbas, A., Yerli, B., Armijo, R., Meyer, B., De Chabalier, J. B. and Rockwell, T. (2002). The surface rupture and slip distribution of the August 17, 1999 Izmit earthquake (M 7.4). North Anatolian Fault, Bull. Seism. Soc. Am. 92(1): 43–60.

Bozorgnia, Y., Abrahamson, N. A., Atik, L. A., Ancheta, T. D., Atkinson, G. M., Baker, J. W., ... & Darragh, R. (2014). NGA-West2 research project. Earthquake Spectra, 30(3), 973-987.

Brodsky, E.E., Karakostas, V. and Kanamori, H. (2000). A new observation of dynamically triggered regional seismicity: Earthquakes in Greece following the August 1999 Izmit, Turkey earthquake. Geophy. Res. Let., 27(17): 2741-2744.

Cetin, K. O., Seed, R. B., Der Kiureghian, A., Tokimatsu, K., Harder Jr, L. F., Kayen, R. E., & Moss, R. E. (2004). Standard penetration test-based probabilistic and deterministic assessment of seismic soil liquefaction potential. Journal of geotechnical and geoenvironmental engineering, 130(12), 1314-1340.

Chiu, P., Pradel, D. E., Kwok, A. O. L., & Stewart, J. P. (2008). Seismic response analyses for the silicon valley rapid transit project. In Geotechnical Earthquake Engineering and Soil Dynamics IV (pp. 1-10).

Cosentino, P., Ficarra, V. and Luzio, D. (1977). Truncated exponential frequency-magnitude relationship in earthquake statistics. Bulletin of the Seismological Society of America, 67(6): 1615-1623.

Emergency Management Authority. (2018). Turkey's New Earthquake Hazard Map is Published - News - AFAD Republic of Turkey Prime Ministry Disaster and Emergency Management Authority. Retrieved from https://www.afad.gov.tr/en/26735/Turkeys-New-Earthquake-Hazard-Map-is-Published.

Emre, Ö., Duman, T. Y., Özalp, S., Elmacı, H., Olgun, Ş. and Şaroğlu, F. (2013). Active Fault Map of Turkey, Special Publication, Series 30. General Directorate of Mineral Research and Exploration (MTA), Ankara.

Emre, Ö., Duman, T.Y., Özalp, S., Şaroğlu, F., Olgun, Ş., Elmacı, H. and Çan, T. (2016). Active fault database of Turkey. Bulletin of Earthquake Engineering,1-47.

Ergintav, S., Reilinger, R.E., Çakmak, R., Floyd, M., Cakir, Z., Doğan, U., King, R.W., McClusky, S. and Özener, H. (2014). Istanbul's Earthquake Hot Spots: Geodetic Constraints on Strain Accumulation Along Faults in the Marmara Seismic Gap. Geophysical Research Letters, doi:10.1002/2014GL060985.

Field, E.H., Dawson, T.E., Felzer, K.R., Frankel, A.D., Gupta, V., Jordan, T.H., Parsons, T., Petersen, M.D., Stein, R.S., Weldon, R.J. and Wills, C.J. (2009). Uniform California earthquake rupture forecast, version 2 (UCERF 2). Bulletin of the Seismological Society of America, 99(4): 2053-2107.

Flerit, F., Armijo, R., King, G. C. P., Meyer, B., Barka, A. (2003). Slip Partitioning in the Sea of Marmara Pull-Apart Determined from GPS Velocity Vectors. Geophysical Journal International, 154(1), 1-7,doi:10.1046/j.1365-246X.2003.01899.x.

Flerit, F., Armijo, R., King, G. and Meyer, B. (2004). The mechanical interaction between the propagating North Anatolian Fault and the back-arc extension in the Aegean. Earth and Planetary Science Letters, 224(3), 347-362.

Frankel, A. (1995). Mapping Seismic Hazard in the Central and Eastern United States. Seismological Research Letters, 66 (4) 8-21, doi:10.1785/gssrl.66.4.8.

Gurbuz, C., Aktar, M., Eyidogan, H., Cisternas, A., Haessler, H., Barka, A., Ergin, M., Türkelli, N., Polat, O., Üçer, S.B. and Kuleli, S. (2000). The Seismotectonics of the Marmara Region (Turkey): Results from a Microseismic Experiment. Tectonophysics, 316(1), 1-17.

Gutenberg, B., & Richter, C. F. (1944). Frequency of earthquakes in California. Bulletin of the Seismological Society of America, 34(4), 185-188.

Gutenberg, B., and Richter, C. F. (1956). Earthquake magnitude, intensity, energy, and acceleration. Bulletin of the Seismological Society of America, 46(2), 105-145.

Güldağlı, O. (2004). Yeraltı Yapılarının Tasarımı Ve Sismik Analizi (Doctoral dissertation, Fen Bilimleri Enstitüsü).

Gülerce, Z. (2013). Using a performance-based earthquake engineering (PBEE) approach to estimate structural performance targets for bridges. In Handbook of Seismic Risk Analysis and Management of Civil Infrastructure Systems (pp. 536-560).

Gülerce, Z. and Ocak, S. (2013). Probabilistic Seismic Hazard Assessment of Eastern Marmara Region. Bulletin of Earthquake Engineering, 11(5), 1259-1277, doi:10.1007/S10518-013-9443-6.

Gülerce, Z., Kargoığlu, B., & Abrahamson, N. A. (2016). Turkey-adjusted NGA-W1 horizontal ground motion prediction models. Earthquake Spectra, 32(1), 75-100.

Gülerce, Z., Soyman, K. B., Güner, B., & Kaymakci, N. (2017). Planar seismic source characterization models developed for probabilistic seismic hazard assessment of Istanbul. Natural Hazards and Earth System Sciences, 17(12), 2365.

Gülerce, Z. and Kaymakçı, N. (2017). Probabilistic Seismic Hazard Assessment - Design Ground Motions For ÇNAEM TR-2 Research Reactor Building. Report submitted to Turkish Atomic Energy Agency (TAEK).

Hanks, T.C. and Bakun, W.H. (2014). M–logA Models and Other Curiosities. Bulletin of the Seismological Society of America, 104(5): 2604-2610.

Hasancebi, N., & Ulusay, R. (2007). Empirical correlations between shear wave velocity and penetration resistance for ground shaking assessments. Bulletin of Engineering Geology and the Environment, 66(2), 203-213.

Hashash, Y., Hook, J., Schmidt, B. and I-Chiang Yao, J. (2001). Seismic design and analysis of underground structures. Tunnelling and Underground Space Technology, 16(4), pp.247-293.

Hashash, Y. M. A., Karina, K., Koutsoftas, D., & O'Riordan, N. (2010). Seismic design considerations for underground box structures. In Earth Retention Conference 3 (pp. 620-637).

Hashash, Y.M.A., Musgrove, M.I., Harmon, J.A., Groholski, D.R., Phillips, C.A., and Park, D. (2016) "DEEPSOIL 6.1, User Manual". Urbana, IL, Board of Trustees of University of Illinois at Urbana-Champaign.

Hergert, T., and Heidbach, O. (2010). Slip-Rate Variability and Distributed Deformation in the Marmara Sea Fault System. Nature Geoscience, 3(2), 132, doi:10.1038/NGEO739.

Hergert, T., Heidbach, O., Bécel, A., & Laigle, M. (2011). Geomechanical model of the Marmara Sea region—I. 3-D contemporary kinematics. Geophysical Journal International, 185(3), 1073-1089.

Hung, C. J., Monsees, J., Munfah, N., & Wisniewski, J. (2009). Technical manual for design and construction of road tunnels–civil elements. US Department of Transportation, Federal Highway Administration, National Highway Institute, New York.

Iida, H., Hiroto, T., Yoshida, N., & Iwafuji, M. (1996). Damage to Daikai subway station. Soils and foundations, 36(Special), 283-300.

Kahraman, S. (Yuksel Proje International Company) (2015). Final Project Geological – Geotechnical Investigation Report (GIR) for Çekmeköy – Sultanbeyli and Çekmeköy (Hastane) – Taşdelen Lines, Ankara, Turkey.

Kahraman, S. (Yüksel Proje International Company) (2015). Final Project Geological – Geotechnical Investigation Report (GIR) for Kaynarca Merkez – Tuzla and Pendik – Kaynarca Merkez Lines, Ankara, Turkey.

Kalafat, D., Güneş, Y., Kekovali, K., Kara, M., Deniz, P., Yılmazer, M. (2011). Bütünleştirilmiş Homojen Türkiye Deprem Kataloğu (1900-2010); M≥4.0). Boğaziçi Üniversitesi, Kandilli Rasathanesi ve Deprem Araştırma Enstitüsü, İstanbul, Yayın No: 1049, 640 s, Istanbul.

Laigle, M., Becel, A., de Voogd, B., Hirn, A., Taymaz, T. and Ozalaybey, S. (2008). A first deep seismic survey in the Sea of Marmara: Deep basins and whole crust architecture and evolution. Earth and Planetary Science Let., 270(3): 168-179.

Langridge, R. M., Stenner, H. D., Fumal, T. E., Christofferson, S. A., Rockwell, T. K., Hartleb, R. D., ... and Barka, A. A. (2002). Geometry, slip distribution, and kinematics of surface rupture on the Sakarya fault segment during the 17 August 1999 Izmit, Turkey. Bull. Seism. Soc. Am. 92(1): 107–125.

Le Pichon, X, A.M.C. Sengör, E. Demirbag, C. Rangin, C. Imren, R. Armijo, N. Görür, N. Çagatay, B. Mercier de Lepinay, B. Meyer, R. Saatçilar and B. Tok (2001). The Active Main Marmara Fault, Earth and Plan. Science Letters, 192(4), 595-616.

Lettis, W., Bachhuber, J., Witter, R., Brankman, C., Randolph, C. E., Barka, A., ... & Kaya, A. (2002). Influence of releasing step-overs on surface fault rupture and fault segmentation: Examples from the 17 August 1999 Izmit earthquake on the North Anatolian fault, Turkey. Bulletin of the Seismological Society of America, 92(1), 19-42.

Luco, N., Mai, P. M., Cornell, C. A., & Beroza, G. C. (2002). Probabilistic seismic demand analysis, SMRF connection fractures, and near-source effects.

McClusky, S., Balassanian, S., Barka, A., Demir, C., Ergintav, S. Georgiev, I., Gurkan, O., Hamburger, M., Hurst, K., et al. (2000). Global Positioning System Constraints On Plate Kinematics and Dynamics in The Mediterranean and Caucasus. Journal of Geophysical Research, 105, 5685-5719, doi:10.1029/1999JB900351.

McNeill, L. C., Mille, A., Minshull, T. A., Bull, J. M., Kenyon, N. H., and Ivanov, M. (2004). Extension of the North Anatolian Fault into the North Aegean Trough: Evidence for Transtension, Strain Partitioning, and Analogues for Sea of Marmara Basin Models. Tectonics, 23(2), doi:10.1029/2002TC001490.

Meade, B. J., B. H. Hager, S. C. McClusky, R. E. Reilinger, S. Ergintav, O. Lenk, A. Barka, and H. Ozener (2002). Estimates of seismic potential in the Marmara Sea region from block models of secular deformation constrained by Global Positioning System measurements. Bull. Seismol. Soc. Am., 92, 208–215, doi:10.1785/0120000837.

Mert, A., Fahjan, Y.M., Hutchings, L.J. and Pınar, A. (2016). Physically based probabilistic seismic hazard analysis using broadband ground motion simulation: a case study for the Prince Islands Fault, Marmara Sea. Earth. Planets and Space, 68(1): 146.

Miranda, E., & Aslani, H. (2003). Probabilistic response assessment for building-specific loss estimation. Pacific Earthquake Engineering Research Center.

Murru, M., Akinci, A., Falcone, G., Pucci, S., Console, R., and Parsons, T. (2016). M≥ 7 earthquake rupture forecast and time-dependent probability for the Sea of Marmara region, Turkey. Journal of Geophysical Research: Solid Earth, 121(4), 2679-2707, doi:10.1002/2015JB012595.

Okay, A. I., E. Demirbağ, H. Kurt, N. Okay, and I. Kuşçu (1999). An active, deep marine strike-slip basin along the North Anatolian fault in Turkey. Tectonics, 18, 129–147.

Owen, G. N., & Scholl, R. E. (1981). Earthquake engineering of large underground structures. NASA STI/Recon Technical Report N, 82.

Örgülü, G., and M. Aktar (2001). Regional moment tensor inversion for strong aftershocks of the August 17, 1999 Izmit earthquake (Mw =7.4). Geophys. Res. Lett., 28(2), 371–374, doi:10.1029/2000GL011991.

Özalaybey, S., Ergin, M., Aktar, C., Tapırdamaz, Biçmen, F., and Yörük, A. (2002). The 1999 İzmit earthquake sequence in Turkey: Seismological and tectonic aspects. Bull. Seismol. Soc. Am., 92, 376–386.

Özcebe, A. G. (2009). A comparative assessment of available methods for seismic performance evaluation of buried structures (Doctoral dissertation, Dissertation submitted in partial fulfillment of the requirements for the degree of Master of Science in Civil Engineering, Middle East Technical University, Ankara, Turkey).

Parra-Montesinos, G. J., Bobet, A., & Ramirez, J. A. (2006). Evaluation of soil-structure interaction and structural collapse in Daikai subway station during Kobe earthquake. ACI structural journal, 103(1), 113.

Parsons, T. (2004). Recalculated probability of M > 7 earthquakes beneath the Sea of Marmara, Turkey. J. Geophys. Res., 109, B05304, doi:10.1029/2003JB002667.

Pınar, A., Kuge, K., and Honkura, Y. (2003). Moment Tensor Inversion of Recent Small to Moderate Sized Earthquakes: Implications for Seismic Hazard and Active Tectonics Beneath the Sea of Marmara. Geophysical Journal International, 133-145, doi:10.1046/j.1365-246X.2003.01897.x.

Rohde, M. (2018). World Metro Database. Retrieved from mic-ro.com/metro/table.html.

Schnabel, P. B. (1972). SHAKE a computer program for earthquake response analysis of horizontally layered sites. EERC Report, Univ. of California, Berkeley.

Schwartz, D. P., and K. J. Coppersmith: Fault behaviour and characteristic earthquakes (1984). Examples from the Wasatch and San Andreas Fault Zones. J. Geophys. Res., 89(B7), 5681–5698.

Seed, H. B., & Idriss, I. M. (1971). Simplified procedure for evaluating soil liquefaction potential. Journal of Soil Mechanics & Foundations Div.

Segall, P., and D. D. Pollard (1980). Mechanics of discontinuous faults. J. Geophys. Res., 85, 4337–4350.

Shi, Y., and Bolt, B.A. (1982). The standard error of the magnitude-frequency b-value. Bull. Seis. Soc. Am., 72, 1677-1687.

SPSS (IBM Corp. Released 2013. IBM SPSS Statistics for Windows, Version 22.0. Armonk, NY: IBM Corp.).

Stein, R.S., Barka, A.A., Dieterich, J.H. (1997). Progressive failure on the North Anatolian fault since 1939 by earthquake stress triggering. Geophys. Journal Int. 128: 594-604.

Stewart, J. P., Chiou, S. J., Bray, J. D., Graves, R. W., Somerville, P. G., & Abrahamson, N. A. (2002). Ground motion evaluation procedures for performance-based design. Soil dynamics and earthquake engineering, 22(9-12), 765-772.

Sykora, D. W., Moriwaki, Y., Barneich, J. A., & Abrahamson, N. A. (1996). Measured variation of peak acceleration and peak particle velocity with depth at soil sites. In Proc., Eleventh World Conf., Earthquake Engineering, Paper (No. 1573).

Tothong, P., and Cornell, C. A. (2006). Probabilistic seismic demand analysis using advanced ground motion intensity measures, attenuation relationships, and near-fault effects. Pacific Earthquake Engineering Research Center, University of California, Berkeley. PEER Report 2006-11.

Turkish Ministry of Public Works and Settlement 2007, Specification for Structures to be Built in Disaster Areas, TEC-07, Ankara, Turkey.

Wang, J.N. (1993). Seismic Design of Tunnels. A State-of-the-Art Approach, Monograph 7. New York, NY: Parsons Brinckerhoff Quade & Douglas, Inc. Wu, C.

Weichert, D. (1980). Estimation of the earthquake recurrence parameters for unequal observation periods for different magnitudes. Bull. Seismo. Soc. Am., 70(4), 1337-1346.

Wells, D. L. and Coppersmith, K. J. (1994). New Empirical Relationships Among Magnitude, Rupture Length, Width, Area and Surface Displacement. Bull. Seism. Soc. Am., 84(4), 974-1002.

Wesnousky, S. G. (1988). Seismological and structural evolution of strike-slip faults. Nature, 335, 340–343, doi: doi:10.1038/335340a0.

Wiemer, S. (2001). A software package to analyse seismicity: ZMAP. S. Res. Let., 72, 373-382, doi: 10.1785/gssrl.72.3.373.

Wong, H. K., T. Lüdmann, A. Ulug, and N. Görür (1995). The Sea of Marmara: A plate boundary sea in an escape tectonic regime. Tectonophysics, 244, 231–250, doi:10.1016/0040-1951(94)00245-5.

Working Group on California Earthquake Probabilities (WGCEP-2003) (2003). Earthquake probabilities in the San Francisco Bay Region: 2002–2031. U.S. Geol. Soc., Open-File Rept., 03-214.

Wu, C. L., & Penzien, J. (1994, July). Seismic design of MUNI metro turnback project. In Fifth US National Conference on Earthquake Engineering (pp. 799-808).

Yagoda-Biran, G., Kerpel, B., & Kamai, R. (2017). Never Fear Velocity ReversalsShort Note. Bulletin of the Seismological Society of America, 107(4), 1969-1974.

Yaltirak, C. (2002). Tectonic evaluation of Marmara Sea and its surroundings, Mar. Geol., 190, 439–529, doi:10.1016/S0025-3227(02)00360-2.

Yoshida, N. (1999). Underground and buried structure. In Seco e Pinto (ed.) Earthquake geotechnical engineering. Rotterdam: Balkema.

Youngs, R. R. and Coppersmith, K. J. (1985). Implications of Fault Slip Rates and Earthquake Recurrence Models to Probabilistic Seismic Hazard Estimates. Bull. Seism. Soc. Am., 75(4), 939-964.

APPENDICES

A. SITE SPECIFIC SOIL PROFILES

Table A.1 Site Specific Soil Profile of Abdurrahmangazi Station (H=15.00 m)

Layer Number	Layer Name	Thickness (m)	Unit Weight (kN/m^3)	Shear Wave Velocity (m/s)	Soil Type
1	Artifical Fill	1.5	20	343	Vucetic and Dobry (1991) Clay PI:20
2	Artifical Fill	1.5	22	268	Vucetic and Dobry (1991) Clay PI:20
3	Silt Stone Dpk	1.5	23	337	Vucetic and Dobry (1991) Clay PI:30
4	Silt Stone Dpk	1.5	23	407	Vucetic and Dobry (1991) Clay PI:30
5	Silt Stone Dpk	1.5	23	476	Vucetic and Dobry (1991) Clay PI:30
6	Silt Stone Dpk	1.5	23	545	Vucetic and Dobry (1991) Clay PI:30
7	Silt Stone Dpk	1.5	23	615	Vucetic and Dobry (1991) Clay PI:30
8	Silt Stone Dpk	1.5	23	684	Vucetic and Dobry (1991) Clay PI:30
9	Silt Stone Dpk	1.5	23	753	Vucetic and Dobry (1991) Clay PI:30
10	Silt Stone Dpk	1.5	23	823	Vucetic and Dobry (1991) Clay PI:30
11	Silt Stone Dpk	1.5	23	892	Vucetic and Dobry (1991) Clay PI:30
12	Silt Stone Dpk	1.5	23	961	Vucetic and Dobry (1991) Clay PI:30
13	Silt Stone Dpk	1.5	23	1031	Vucetic and Dobry (1991) Clay PI:30
14	Silt Stone Dpk	1.5	23	1100	Vucetic and Dobry (1991) Clay PI:30
Bedrock			25	1100	Damping Ratio % 5

**Depth of top slab is 1.50 m, depth of foundation is 16.50 m.*

Table A.2 Site Specific Soil Profile of Aydıntepe Station (H=15.00 m)

Layer Number	Layer Name	Thickness (m)	Unit Weight (kN/m³)	Shear Wave Velocity (m/s)	Soil Type
1	Artifical Fill	3	20	223	Vucetic and Dobry (1991) Clay PI:30
2	Sandstone Osys	1.5	25	464	Seed and Idriss (1991) Sand Lower Limit
3	Sandstone Osys	1.5	25	517	Seed and Idriss (1991) Sand Lower Limit
4	Sandstone Osys	1.5	25	570	Seed and Idriss (1991) Sand Lower Limit
5	Sandstone Osys	1.5	25	623	Seed and Idriss (1991) Sand Lower Limit
6	Sandstone Osys	1.5	25	676	Seed and Idriss (1991) Sand Lower Limit
7	Sandstone Osys	1.5	25	729	Seed and Idriss (1991) Sand Lower Limit
8	Sandstone Osys	1.5	25	782	Seed and Idriss (1991) Sand Lower Limit
9	Sandstone Osys	1.5	25	835	Seed and Idriss (1991) Sand Lower Limit
10	Sandstone Osys	1.5	25	888	Seed and Idriss (1991) Sand Lower Limit
11	Sandstone Osys	1.5	25	941	Seed and Idriss (1991) Sand Lower Limit
12	Sandstone Osys	1.5	25	994	Seed and Idriss (1991) Sand Lower Limit
13	Sandstone Osys	1.5	25	1047	Seed and Idriss (1991) Sand Lower Limit
14	Sandstone Osys	1.5	25	1100	Seed and Idriss (1991) Sand Lower Limit
Bedrock			25	1100	Damping Ratio % 5

**Depth of top slab is 3.00 m, depth of foundation is 18.00 m.*

Table A.3 Site Specific Soil Profile of Esenyalı Station (H=15.00 m)

Layer Number	Layer Name	Thickness (m)	Unit Weight (kN/m^3)	Shear Wave Velocity (m/s)	Soil Type
1	Artifical Fill	1.5	20	199	Vucetic and Dobry (1991) Clay PI:30
2	Artifical Fill	1.5	20	199	Vucetic and Dobry (1991) Clay PI:30
3	Artifical Fill	1.5	20	212	Vucetic and Dobry (1991) Clay PI:30
4	Silt Stone Clay Stone	1.5	22	351	Vucetic and Dobry (1991) Clay PI:30
5	Silt Stone Clay Stone	1.5	22	419	Vucetic and Dobry (1991) Clay PI:30
6	Silt Stone Clay Stone	1.5	22	487	Vucetic and Dobry (1991) Clay PI:30
7	Silt Stone Clay Stone	1.5	22	555	Vucetic and Dobry (1991) Clay PI:30
8	Silt Stone Clay Stone	1.5	22	623	Vucetic and Dobry (1991) Clay PI:30
9	Silt Stone Clay Stone	1.5	22	692	Vucetic and Dobry (1991) Clay PI:30
10	Silt Stone Clay Stone	1.5	22	760	Vucetic and Dobry (1991) Clay PI:30
11	Silt Stone Clay Stone	1.5	22	828	Vucetic and Dobry (1991) Clay PI:30
12	Silt Stone Clay Stone	1.5	22	896	Vucetic and Dobry (1991) Clay PI:30
13	Silt Stone Clay Stone	1.5	22	964	Vucetic and Dobry (1991) Clay PI:30
14	Silt Stone Clay Stone	1.5	22	1032	Vucetic and Dobry (1991) Clay PI:30
15	Silt Stone Clay Stone	1.5	22	1100	Vucetic and Dobry (1991) Clay PI:30
Bedrock			25	1100	Damping Ratio % 5

**Depth of top slab is 3.00 m, depth of foundation is 18.00 m.*

Table A.4 Site Specific Soil Profile of Hasanpaşa Station (H=15.00 m)

Layer Number	Layer Name	Thickness (m)	Unit Weight (kN/m³)	Shear Wave Velocity (m/s)	Soil Type
1	Artifical Fill	1.5	20	189	Vucetic and Dobry (1991) Clay PI:20
2	Gravelly Sand Clay	1.5	20	216	Vucetic and Dobry (1991) Clay PI:20
3	Gravelly Sand Clay	1.5	20	292	Vucetic and Dobry (1991) Clay PI:20
4	Gravelly Sand Clay	1.5	20	240	Vucetic and Dobry (1991) Clay PI:20
5	Gravelly Sand Clay	1.5	20	268	Vucetic and Dobry (1991) Clay PI:20
6	Gravelly Sand Clay	1.5	20	227	Vucetic and Dobry (1991) Clay PI:20
7	Gravelly Sand Clay	1.5	20	288	Vucetic and Dobry (1991) Clay PI:20
8	Limestone	1.5	25	305	Seed and Idriss (1991) Sand Lower Limit
9	Limestone	1.5	25	385	Seed and Idriss (1991) Sand Lower Limit
10	Limestone	1.5	25	464	Seed and Idriss (1991) Sand Lower Limit
11	Limestone	1.5	25	544	Seed and Idriss (1991) Sand Lower Limit
12	Limestone	1.5	25	623	Seed and Idriss (1991) Sand Lower Limit
13	Limestone	1.5	25	703	Seed and Idriss (1991) Sand Lower Limit
14	Limestone	1.5	25	782	Seed and Idriss (1991) Sand Lower Limit
15	Limestone	1.5	25	862	Seed and Idriss (1991) Sand Lower Limit
16	Limestone	1.5	25	941	Seed and Idriss (1991) Sand Lower Limit
17	Limestone	1.5	25	1021	Seed and Idriss (1991) Sand Lower Limit
18	Limestone	1.5	25	1100	Seed and Idriss (1991) Sand Lower Limit
Bedrock			25	1100	Damping Ratio % 5

**Depth of top slab is 3.00 m, depth of foundation is 18.00 m.*

Table A.5 Site Specific Soil Profile of Kavakpınar Station (H=15.00 m)

Layer Number	Layer Name	Thickness (m)	Unit Weight (kN/m³)	Shear Wave Velocity (m/s)	Soil Type
1	Gravelly Silt Clay	1.5	20	307	Vucetic and Dobry (1991) Clay PI:30
2	Gravelly Silt Clay	2.2	20	300	Vucetic and Dobry (1991) Clay PI:30
3	Gravelly Silt Clay	1.8	20	300	Vucetic and Dobry (1991) Clay PI:20
4	Gravelly Silt Clay	2	20	300	Vucetic and Dobry (1991) Clay PI:20
5	Gravelly Sand Clay	1.5	20	303	Vucetic and Dobry (1991) Clay PI:20
6	Gravelly Sand Clay	1.5	20	310	Vucetic and Dobry (1991) Clay PI:20
7	Gravelly Sand Clay	1.5	20	277	Vucetic and Dobry (1991) Clay PI:20
8	Gravelly Sand Clay	1.5	20	281	Vucetic and Dobry (1991) Clay PI:20
9	Gravelly Sand Clay	1.5	20	334	Vucetic and Dobry (1991) Clay PI:20
10	Gravelly Sand Clay	1.5	20	316	Vucetic and Dobry (1991) Clay PI:20
11	Gravelly Sand Clay	1.5	20	307	Vucetic and Dobry (1991) Clay PI:20
12	Gravelly Sand Clay	0.7	20	265	Vucetic and Dobry (1991) Clay PI:20
13	Gravelly Sand Clay	0.8	20	265	Vucetic and Dobry (1991) Clay PI:20
14	Gravelly Sand Clay	1.5	20	305	Vucetic and Dobry (1991) Clay PI:20
15	Gravelly Sand Clay	1.5	20	277	Vucetic and Dobry (1991) Clay PI:20
16	Gravelly Sand Clay	1.5	20	296	Vucetic and Dobry (1991) Clay PI:20
17	Gravelly Sand Clay	1.5	20	364	Vucetic and Dobry (1991) Clay PI:20
18	Gravelly Sand Clay	1.5	20	303	Vucetic and Dobry (1991) Clay PI:20
19	Gravelly Sand Clay	1.5	20	317	Vucetic and Dobry (1991) Clay PI:20
20	Claystone	1.5	20	474	Seed and Idriss (1991) Sand Lower Limit
21	Claystone	1.5	20	630	Seed and Idriss (1991) Sand Lower Limit
22	Claystone	1.5	20	787	Seed and Idriss (1991) Sand Lower Limit
23	Claystone	1.5	20	943	Seed and Idriss (1991) Sand Lower Limit
24	Claystone	1.5	20	1100	Seed and Idriss (1991) Sand Lower Limit
Bedrock			25	1100	Damping Ratio % 5

**Depth of top slab is 3.70 m, depth of foundation is 18.70 m.*

Table A.6 Site Specific Soil Profile of Meclis Mahallesi Station (H=15.00 m)

Layer Number	Layer Name	Thickness (m)	Unit Weight (kN/m³)	Shear Wave Velocity (m/s)	Soil Type
1	Artifical Fill	1.5	20	243	Vucetic and Dobry (1991) Clay PI:20
2	Artifical Fill	1.5	20	243	Vucetic and Dobry (1991) Clay PI:20
3	Artifical Fill	1.5	20	243	Vucetic and Dobry (1991) Clay PI:20
4	Claystone	1.5	22	327	Vucetic and Dobry (1991) Clay PI:30
5	Claystone	1.5	22	404	Vucetic and Dobry (1991) Clay PI:30
6	Claystone	1.5	22	480	Vucetic and Dobry (1991) Clay PI:30
7	Claystone	1.5	22	549	Vucetic and Dobry (1991) Clay PI:30
8	Claystone	1.5	22	618	Vucetic and Dobry (1991) Clay PI:30
9	Claystone	1.5	22	687	Vucetic and Dobry (1991) Clay PI:30
10	Claystone	1.5	22	756	Vucetic and Dobry (1991) Clay PI:30
11	Claystone	1.5	22	825	Vucetic and Dobry (1991) Clay PI:30
12	Claystone	1.5	22	893	Vucetic and Dobry (1991) Clay PI:30
13	Claystone	1.5	22	962	Vucetic and Dobry (1991) Clay PI:30
14	Claystone	1.5	22	1031	Vucetic and Dobry (1991) Clay PI:30
15	Claystone	1.5	22	1100	Vucetic and Dobry (1991) Clay PI:30
Bedrock			25	1100	Damping Ratio % 5

**Depth of top slab is 3.00 m, depth of foundation is 18.00 m.*

Table A.7 Site Specific Soil Profile of Samandıra Station (H=24.50 m)

Layer Number	Layer Name	Thickness (m)	Unit Weight (kN/m^3)	Shear Wave Velocity (m/s)	Soil Type
1	Artifical Fill	1.5	20	183	Vucetic and Dobry (1991) Clay PI:20
2	Artifical Fill	0.5	20	240	Vucetic and Dobry (1991) Clay PI:20
3	Artifical Fill	1	20	240	Vucetic and Dobry (1991) Clay PI:20
4	Gravelly Sandy Clay	1.5	20	243	Vucetic and Dobry (1991) Clay PI:30
5	Gravelly Sandy Clay	1.5	20	330	Vucetic and Dobry (1991) Clay PI:30
6	Gravelly Sandy Clay	1.5	20	309	Vucetic and Dobry (1991) Clay PI:30
7	Gravelly Sandy Clay	1.5	20	288	Vucetic and Dobry (1991) Clay PI:30
8	Gravelly Sandy Clay	1.5	20	303	Vucetic and Dobry (1991) Clay PI:30
9	Gravelly Sandy Clay	1.5	20	305	Vucetic and Dobry (1991) Clay PI:30
10	Gravelly Sandy Clay	1.5	20	300	Vucetic and Dobry (1991) Clay PI:30
11	Gravelly Sandy Clay	1.5	20	257	Vucetic and Dobry (1991) Clay PI:30
12	Gravelly Sandy Clay	1.5	20	360	Vucetic and Dobry (1991) Clay PI:30
13	Gravelly Sandy Clay	3	20	203	Vucetic and Dobry (1991) Clay PI:30
14	Gravelly Sandy Clay	2	20	203	Vucetic and Dobry (1991) Clay PI:30
15	Gravelly Sandy Clay	2	20	203	Vucetic and Dobry (1991) Clay PI:30
16	Limestone	1.5	26	246	Seed and Idriss (1991) Sand Lower Limit
17	Limestone	1.5	26	220	Seed and Idriss (1991) Sand Lower Limit
18	Limestone	1.5	26	220	Seed and Idriss (1991) Sand Lower Limit
19	Limestone	1.5	26	396	Seed and Idriss (1991) Sand Lower Limit
20	Limestone	1.5	26	572	Seed and Idriss (1991) Sand Lower Limit
21	Limestone	1.5	26	748	Seed and Idriss (1991) Sand Lower Limit
22	Limestone	1.5	26	924	Seed and Idriss (1991) Sand Lower Limit
23	Limestone	1.5	26	1100	Seed and Idriss (1991) Sand Lower Limit
Bedrock			25	1100	Damping Ratio % 5

**Depth of top slab is 2.00 m, depth of foundation is 26.50 m.*

Table A.8 Site Specific Soil Profile of Sancaktepe Station (H=15.00 m)

Layer Number	Layer Name	Thickness (m)	Unit Weight (kN/m³)	Shear Wave Velocity (m/s)	Soil Type
1	Artifical Fill	1.5	20	234	Vucetic and Dobry (1991) Clay PI:30
2	Artifical Fill	1.5	20	270	Vucetic and Dobry (1991) Clay PI:30
3	Artifical Fill	1.5	20	290	Vucetic and Dobry (1991) Clay PI:30
4	Gravelly Sandy Clay	1.5	20	224	Vucetic and Dobry (1991) Clay PI:30
5	Gravelly Sandy Clay	1.5	20	237	Vucetic and Dobry (1991) Clay PI:30
6	Gravelly Sandy Clay	1.5	20	240	Vucetic and Dobry (1991) Clay PI:30
7	Gravelly Sandy Clay	1.5	20	231	Vucetic and Dobry (1991) Clay PI:30
8	Gravelly Sandy Clay	1.5	20	220	Vucetic and Dobry (1991) Clay PI:30
9	Gravelly Sandy Clay	1.5	20	277	Vucetic and Dobry (1991) Clay PI:30
10	Gravelly Sandy Clay	1.5	20	290	Vucetic and Dobry (1991) Clay PI:30
11	Gravelly Sandy Clay	1.5	20	339	Vucetic and Dobry (1991) Clay PI:30
12	Gravelly Sandy Clay	1.5	20	349	Vucetic and Dobry (1991) Clay PI:30
13	Gravelly Sandy Clay	1.5	20	337	Vucetic and Dobry (1991) Clay PI:30
14	Gravelly Sandy Clay	1.7	20	550	Vucetic and Dobry (1991) Clay PI:30
15	Gravelly Sandy Clay	1.7	20	550	Vucetic and Dobry (1991) Clay PI:30
16	Gravelly Sandy Clay	1.7	20	550	Vucetic and Dobry (1991) Clay PI:30
17	Gravelly Sandy Clay	1.7	20	550	Vucetic and Dobry (1991) Clay PI:30
Bedrock			25	1100	Damping Ratio % 5

**Depth of top slab is 3.00 m, depth of foundation is 18.00 m.*

Table A.9 Site Specific Soil Profile of Sarıgazi Station (H=29.50 m)

Layer Number	Layer Name	Thickness (m)	Unit Weight (kN/m³)	Shear Wave Velocity (m/s)	Soil Type
1	Artifical Fill	1.5	20	157	Vucetic and Dobry (1991) Clay PI:20
2	Clay	1.5	20	263	Vucetic and Dobry (1991) Clay PI:30
3	Clayey Sand	1.5	20	231	Seed and Idriss (1991) Sand Lower Limit
4	Sandy Silt Clay	1.5	20	257	Vucetic and Dobry (1991) Clay PI:30
5	Sandy Silt Clay	1.5	20	203	Vucetic and Dobry (1991) Clay PI:30
6	Fault Zone	3	20	360	Vucetic and Dobry (1991) Clay PI:20
7	Fault Zone	3	20	360	Vucetic and Dobry (1991) Clay PI:20
8	Fault Zone	3	20	360	Vucetic and Dobry (1991) Clay PI:20
9	Fault Zone	3	20	360	Vucetic and Dobry (1991) Clay PI:20
10	Fault Zone	3	20	360	Vucetic and Dobry (1991) Clay PI:20
11	Fault Zone	4	20	360	Vucetic and Dobry (1991) Clay PI:20
12	Clayey Limestone	1.5	25	483	Vucetic and Dobry (1991) Clay PI:20
13	Clayey Limestone	1.5	25	607	Vucetic and Dobry (1991) Clay PI:20
14	Clayey Limestone	1.5	25	730	Vucetic and Dobry (1991) Clay PI:20
15	Clayey Limestone	1.5	25	792	Vucetic and Dobry (1991) Clay PI:20
16	Clayey Limestone	1.5	25	977	Vucetic and Dobry (1991) Clay PI:20
17	Clayey Limestone	1.5	25	1100	Vucetic and Dobry (1991) Clay PI:20
Bedrock			25	1100	Damping Ratio % 5

**Depth of top slab is 1.50 m, depth of foundation is 31.00 m.*

Table A.10 Site Specific Soil Profile of Sultanbeyli Station (H=15.00 m)

Layer Number	Layer Name	Thickness (m)	Unit Weight (kN/m³)	Shear Wave Velocity (m/s)	Soil Type
1	Artifical Fill	1.5	20	230	Vucetic and Dobry (1991) Clay PI:20
2	Artifical Fill	1.5	20	230	Vucetic and Dobry (1991) Clay PI:20
3	Sandstone Claystone	1.5	24	297	Vucetic and Dobry (1991) Clay PI:20
4	Sandstone Claystone	1.5	24	364	Vucetic and Dobry (1991) Clay PI:20
5	Sandstone Claystone	1.5	24	431	Vucetic and Dobry (1991) Clay PI:20
6	Sandstone Claystone	1.5	24	498	Vucetic and Dobry (1991) Clay PI:20
7	Sandstone Claystone	1.5	24	565	Vucetic and Dobry (1991) Clay PI:20
8	Sandstone Claystone	1.5	24	632	Vucetic and Dobry (1991) Clay PI:20
9	Sandstone Claystone	1.5	24	699	Vucetic and Dobry (1991) Clay PI:20
10	Sandstone Claystone	1.5	24	765	Vucetic and Dobry (1991) Clay PI:20
11	Sandstone Claystone	1.5	24	832	Vucetic and Dobry (1991) Clay PI:20
12	Sandstone Claystone	1.5	24	899	Vucetic and Dobry (1991) Clay PI:20
13	Sandstone Claystone	1.5	24	966	Vucetic and Dobry (1991) Clay PI:20
14	Sandstone Claystone	1.5	24	1033	Vucetic and Dobry (1991) Clay PI:20
15	Sandstone Claystone	1.5	24	1100	Vucetic and Dobry (1991) Clay PI:20
Bedrock			25	1100	Damping Ratio % 5

**Depth of top slab is 3.00 m, depth of foundation is 18.00 m.*

Table A.11 Site Specific Soil Profile of Tuzla Belediye Station (H=25.50 m)

Layer Number	Layer Name	Thickness (m)	Unit Weight (kN/m³)	Shear Wave Velocity (m/s)	Soil Type
1	Artifical Fill	2	20	223	Vucetic and Dobry (1991) Clay PI:30
2	Sandstone	1.5	26	344	Seed and Idriss (1991) Sand Lower Limit
3	Sandstone	1.5	26	464	Seed and Idriss (1991) Sand Lower Limit
4	Sandstone	1.5	26	499	Seed and Idriss (1991) Sand Lower Limit
5	Sandstone	1.5	26	535	Seed and Idriss (1991) Sand Lower Limit
6	Sandstone	1.5	26	570	Seed and Idriss (1991) Sand Lower Limit
7	Sandstone	1.5	26	605	Seed and Idriss (1991) Sand Lower Limit
8	Sandstone	1.5	26	641	Seed and Idriss (1991) Sand Lower Limit
9	Sandstone	1.5	26	676	Seed and Idriss (1991) Sand Lower Limit
10	Sandstone	1.5	26	711	Seed and Idriss (1991) Sand Lower Limit
11	Sandstone	1.5	26	747	Seed and Idriss (1991) Sand Lower Limit
12	Sandstone	1.5	26	782	Seed and Idriss (1991) Sand Lower Limit
13	Sandstone	1.5	26	817	Seed and Idriss (1991) Sand Lower Limit
14	Sandstone	1.5	26	853	Seed and Idriss (1991) Sand Lower Limit
15	Sandstone	1.5	26	888	Seed and Idriss (1991) Sand Lower Limit
16	Sandstone	1.5	26	923	Seed and Idriss (1991) Sand Lower Limit
17	Sandstone	1.5	26	959	Seed and Idriss (1991) Sand Lower Limit
18	Sandstone	1.5	26	994	Seed and Idriss (1991) Sand Lower Limit
19	Sandstone	1.5	26	1029	Seed and Idriss (1991) Sand Lower Limit
20	Sandstone	1.5	26	1065	Seed and Idriss (1991) Sand Lower Limit
21	Sandstone	1.5	26	1100	Seed and Idriss (1991) Sand Lower Limit
Bedrock			25	1100	Damping Ratio % 5

**Depth of top slab is 2.00 m, depth of foundation is 27.50 m.*

Table A.12 Site Specific Soil Profile of Veysel Karani Station (H=15.00 m)

Layer Number	Layer Name	Thickness (m)	Unit Weight (kN/m^3)	Shear Wave Velocity (m/s)	Soil Type
1	Artifical Fill	3	20	180	Vucetic and Dobry (1991) Clay PI:20
2	Artifical Fill	1.5	20	180	Vucetic and Dobry (1991) Clay PI:20
3	Gravelly Sand Clay	1.5	20	268	Vucetic and Dobry (1991) Clay PI:30
4	Clayey Sand	1.5	20	240	Seed and Idriss (1991) Sand Lower Limit
5	Gravelly Sand Clay	1.5	20	216	Vucetic and Dobry (1991) Clay PI:30
6	Gravelly Sand Clay	1.5	20	312	Vucetic and Dobry (1991) Clay PI:30
7	Gravelly Sand Clay	1.5	20	252	Vucetic and Dobry (1991) Clay PI:30
8	Gravelly Sand Clay	1.5	20	246	Vucetic and Dobry (1991) Clay PI:30
9	Gravelly Sand Clay	1.5	20	246	Vucetic and Dobry (1991) Clay PI:30
10	Gravelly Sand Clay	1.5	20	249	Vucetic and Dobry (1991) Clay PI:30
11	Gravelly Sand Clay	1.5	20	227	Vucetic and Dobry (1991) Clay PI:30
12	Gravelly Sand Clay	1.5	20	252	Vucetic and Dobry (1991) Clay PI:30
13	Gravelly Sand Clay	1.5	20	249	Vucetic and Dobry (1991) Clay PI:30
14	Gravelly Sand Clay	1.5	20	360	Vucetic and Dobry (1991) Clay PI:30
15	Gravelly Sand Clay	1.5	20	255	Vucetic and Dobry (1991) Clay PI:30
16	Gravelly Sand Clay	1.5	20	270	Vucetic and Dobry (1991) Clay PI:30
17	Gravelly Sand Clay	1.5	20	281	Vucetic and Dobry (1991) Clay PI:30
18	Gravelly Sand Clay	1.5	20	350	Vucetic and Dobry (1991) Clay PI:30
19	Gravelly Sand Clay	1.5	20	325	Vucetic and Dobry (1991) Clay PI:30
20	Gravelly Sand Clay	1.5	20	339	Vucetic and Dobry (1991) Clay PI:30
21	Gravelly Sand Clay	1.5	20	360	Vucetic and Dobry (1991) Clay PI:30
22	Gravelly Sand Clay	3	20	275	Vucetic and Dobry (1991) Clay PI:30
23	Gravelly Sand Clay	1.5	20	243	Vucetic and Dobry (1991) Clay PI:30
24	Gravelly Sand Clay	1.5	20	265	Vucetic and Dobry (1991) Clay PI:30
25	Gravelly Sand Clay	1.5	20	309	Vucetic and Dobry (1991) Clay PI:30
26	Claystone	1.5	26	467	Seed and Idriss (1991) Sand Lower Limit
27	Claystone	1.5	26	625	Seed and Idriss (1991) Sand Lower Limit
28	Claystone	1.5	26	784	Seed and Idriss (1991) Sand Lower Limit
29	Claystone	1.5	26	942	Seed and Idriss (1991) Sand Lower Limit
30	Claystone	1.5	26	1100	Seed and Idriss (1991) Sand Lower Limit
Bedrock			25	1100	Damping Ratio % 5

**Depth of top slab is 3.00 m, depth of foundation is 18.00 m.*

B. SHEAR WAVE VELOCITIES OF METRO STATIONS

Table B.1 Equivalent Shear Wave Velocities of Metro Stations

#	Station	Vs_{eq} (m/s)
Station 1	Abdurrahmangazi Metro Station	545.200
Station 2	Aydıntepe Metro Station	559.618
Station 3	Esenyalı Metro Station	448.252
Station 4	Hasanpaşa Metro Station	379.683
Station 5	Kavakpınar Metro Station	343.438
Station 6	Meclis Mahallesi Metro Station	477.239
Station 7	Samandıra Metro Station	282.376
Station 8	Sancaktepe Metro Station	306.347
Station 9	Sarıgazi Metro Station	324.419
Station 10	Sultanbeyli Metro Station	492.534
Station 11	Tuzla Belediye Metro Station	611.981
Station 12	Veysel Karani Metro Station	285.938

Table B.2 Average Shear Wave Velocities in 12 meters of Metro Stations

#	Station	$V_{S,12m}$ (m/s)
Station 1	Abdurrahmangazi Metro Station	418.961
Station 2	Aydıntepe Metro Station	415.184
Station 3	Esenyalı Metro Station	314.179
Station 4	Hasanpaşa Metro Station	246.917
Station 5	Kavakpınar Metro Station	299.324
Station 6	Meclis Mahallesi Metro Station	341.851
Station 7	Samandıra Metro Station	266.098
Station 8	Sancaktepe Metro Station	241.325
Station 9	Sarıgazi Metro Station	252.755
Station 10	Sultanbeyli Metro Station	355.709
Station 11	Tuzla Belediye Metro Station	413.187
Station 12	Veysel Karani Metro Station	219.975

C. FREE FIELD DISPLACEMENTS OF METRO STATIONS FROM LEVEL 1 METHOD

Table C.1 Free Field Displacements (Δ_{ff}) of Metro Stations from Level 1 Method

#	Station Name	PGA	Topslab Displacement (cm)	Foundation Displacement (cm)	$\Delta_{displacement}$ (cm)
Station 1	Abdurrahmangazi Metro Station	0.245	0.1321448	0	0.1321448
Station 2	Aydıntepe Metro Station	0.340	0.1892293	0	0.1892293
Station 3	Esenyalı Metro Station	0.330	0.2855503	0	0.2855503
Station 4	Hasanpaşa Metro Station	0.260	0.2516033	0	0.2516033
Station 5	Kavakpınar Metro Station	0.320	0.4790362	0	0.4790362
Station 6	Meclis Mahallesi Metro Station	0.240	0.1840778	0	0.1840778
Station 7	Samandıra Metro Station	0.240	1.0100829	0	1.0100829
Station 8	Sancaktepe Metro Station	0.250	0.3795458	0	0.3795458
Station 9	Sarıgazi Metro Station	0.235	1.0130185	0	1.0130185
Station 10	Sultanbeyli Metro Station	0.250	0.1798331	0	0.1798331
Station 11	Tuzla Belediye Metro Station	0.370	0.4445915	0	0.4445915
Station 12	Veysel Karani Metro Station	0.260	0.3915204	0	0.3915204

D. FREE FIELD DISPLACEMENTS OF METRO STATIONS FROM LEVEL 2 METHOD

Table D.1 Free Field Displacements (Δ_{ff}) of Abdurrahmangazi Station from Level 2 Method

#	V_S(m/s)	PGA(g)	Disp(m)	Disp(cm)	Ln(V_S,m/sn)	Ln(PGA)	Ln(Disp,cm)
STATION 1 - ABDURRAHMANGAZİ STATION	545.200	0.245	0.000646424	0.0646424	6.301153323	-1.406497068	-2.738884737
	545.200	0.245	0.001251263	0.1251263	6.301153323	-1.406497068	-2.078431652
	545.200	0.245	0.000872956	0.0872956	6.301153323	-1.406497068	-2.438455218
	545.200	0.245	0.000418549	0.0418549	6.301153323	-1.406497068	-3.173546404
	545.200	0.245	0.000735877	0.0735877	6.301153323	-1.406497068	-2.609277387
	545.200	0.245	0.000628062	0.0628062	6.301153323	-1.406497068	-2.767701484
	545.200	0.245	0.000821533	0.0821533	6.301153323	-1.406497068	-2.499168265
	545.200	0.245	0.000766418	0.0766418	6.301153323	-1.406497068	-2.568612659
	545.200	0.245	0.000460308	0.046030778	6.301153323	-1.406497068	-3.078445028
	545.200	0.245	0.00056885	0.056885	6.301153323	-1.406497068	-2.866723593
	545.200	0.245	0.000253136	0.0253136	6.301153323	-1.406497068	-3.676413478
	545.200	0.245	0.000556816	0.0556816	6.301153323	-1.406497068	-2.888105528
	545.200	0.245	0.000848432	0.0848432	6.301153323	-1.406497068	-2.466950432
	545.200	0.245	0.000607041	0.0607041	6.301153323	-1.406497068	-2.801744038
	545.200	0.245	9.94189E-05	0.009941888	6.301153323	-1.406497068	-4.610998332
	545.200	0.245	0.000139714	0.013971368	6.301153323	-1.406497068	-4.270745163
	545.200	0.245	0.000171416	0.017141579	6.301153323	-1.406497068	-4.066248235
	545.200	0.245	0.000172429	0.0172429	6.301153323	-1.406497068	-4.060354814
	545.200	0.245	0.00035931	0.035931	6.301153323	-1.406497068	-3.326154846
	545.200	0.245	0.001777513	0.1777513	6.301153323	-1.406497068	-1.727369897
	545.200	0.245	0.017199485	1.7199485	6.301153323	-1.406497068	0.542294349
	545.200	0.245	0.000490421	0.0490421	6.301153323	-1.406497068	-3.015076166
	545.200	0.245	0.000424451	0.0424451	6.301153323	-1.406497068	-3.159543803
	545.200	0.245	0.000354319	0.0354319	6.301153323	-1.406497068	-3.340142735
	545.200	0.245	0.000468419	0.0468419	6.301153323	-1.406497068	-3.060977177
	545.200	0.245	0.000267496	0.0267496	6.301153323	-1.406497068	-3.621235759
	545.200	0.245	0.000215891	0.0215891	6.301153323	-1.406497068	-3.835566721
	545.200	0.245	6.2435E-05	0.0062435	6.301153323	-1.406497068	-5.076214356
	545.200	0.245	5.4773E-05	0.0054773	6.301153323	-1.406497068	-5.207143
	545.200	0.245	4.8013E-05	0.0048013	6.301153323	-1.406497068	-5.338868564
	545.200	0.245	0.000121404	0.0121404	6.301153323	-1.406497068	-4.411216545
	545.200	0.245	0.000323798	0.0323798	6.301153323	-1.406497068	-3.430220507
	545.200	0.245	0.005734874	0.5734874	6.301153323	-1.406497068	-0.556019313
	545.200	0.245	0.002412564	0.2412564	6.301153323	-1.406497068	-1.421895011
	545.200	0.245	0.000809119	0.0809119	6.301153323	-1.406497068	-2.514394371
	545.200	0.245	0.00073089	0.073089	6.301153323	-1.406497068	-2.616077402
	545.200	0.245	0.0004199	0.04199	6.301153323	-1.406497068	-3.170323784
	545.200	0.245	0.000628299	0.0628299	6.301153323	-1.406497068	-2.767324204
	545.200	0.245	0.000503233	0.0503233	6.301153323	-1.406497068	-2.989287088
	545.200	0.245	0.000339119	0.0339119	6.301153323	-1.406497068	-3.383989294
	545.200	0.245	0.000518221	0.0518221	6.301153323	-1.406497068	-2.95993858
	545.200	0.245	0.000314196	0.0314196	6.301153323	-1.406497068	-3.460323377
	545.200	0.245	0.000396693	0.0396693	6.301153323	-1.406497068	-3.22717769
	545.200	0.245	8.9098E-05	0.0089098	6.301153323	-1.406497068	-4.720603484
	545.200	0.245	0.000282435	0.0282435	6.301153323	-1.406497068	-3.566891936
	545.200	0.245	0.000241384	0.0241384	6.301153323	-1.406497068	-3.723951346
	545.200	0.245	0.000528193	0.05281933	6.301153323	-1.406497068	-2.940878053

Table D.2 Δ_{ff} values of Aydıntepe Station from Level 2 Method

#	V_S(m/s)	PGA(g)	Disp(m)	Disp(cm)	Ln(V_S,m/sn)	Ln(PGA)	Ln(Disp,cm)
STATION 2 - AYDINTEPE STATION	559.618	0.340	0.00066823	0.066823	6.327253894	-1.078809661	-2.705707946
	559.618	0.340	0.001219881	0.1219881	6.327253894	-1.078809661	-2.10383178
	559.618	0.340	0.000617507	0.0617507	6.327253894	-1.078809661	-2.784649968
	559.618	0.340	0.000600131	0.0600131	6.327253894	-1.078809661	-2.813192407
	559.618	0.340	0.000669083	0.0669083	6.327253894	-1.078809661	-2.704432254
	559.618	0.340	0.000887361	0.0887361	6.327253894	-1.078809661	-2.422088483
	559.618	0.340	0.001093768	0.1093768	6.327253894	-1.078809661	-2.212956477
	559.618	0.340	0.000881404	0.0881404	6.327253894	-1.078809661	-2.428824281
	559.618	0.340	0.000435557	0.0435557	6.327253894	-1.078809661	-3.1337147
	559.618	0.340	0.000767966	0.0767966	6.327253894	-1.078809661	-2.566594911
	559.618	0.340	0.000425981	0.0425981	6.327253894	-1.078809661	-3.155945628
	559.618	0.340	0.000673059	0.0673059	6.327253894	-1.078809661	-2.698507379
	559.618	0.340	0.001023923	0.1023923	6.327253894	-1.078809661	-2.278943765
	559.618	0.340	0.000795008	0.0795008	6.327253894	-1.078809661	-2.531988194
	559.618	0.340	0.000126362	0.0126362	6.327253894	-1.078809661	-4.371189568
	559.618	0.340	0.000369776	0.0369776	6.327253894	-1.078809661	-3.297442955
	559.618	0.340	0.0003641	0.03641	6.327253894	-1.078809661	-3.312911817
	559.618	0.340	0.000152659	0.0152659	6.327253894	-1.078809661	-4.182133696
	559.618	0.340	0.000513771	0.0513771	6.327253894	-1.078809661	-2.968562731
	559.618	0.340	0.001734242	0.1734242	6.327253894	-1.078809661	-1.752014663
	559.618	0.340	0.021279809	2.1279809	6.327253894	-1.078809661	0.755173596
	559.618	0.340	0.000676741	0.0676741	6.327253894	-1.078809661	-2.693051742
	559.618	0.340	0.000649503	0.0649503	6.327253894	-1.078809661	-2.734132917
	559.618	0.340	0.009992148	0.9992148	6.327253894	-1.078809661	-0.000785508
	559.618	0.340	0.000429178	0.0429178	6.327253894	-1.078809661	-3.148468621
	559.618	0.340	0.000597168	0.0597168	6.327253894	-1.078809661	-2.818141891
	559.618	0.340	0.000364549	0.0364549	6.327253894	-1.078809661	-3.311679399
	559.618	0.340	0.000427415	0.0427415	6.327253894	-1.078809661	-3.152584934
	559.618	0.340	3.6614E-05	0.0036614	6.327253894	-1.078809661	-5.609909691
	559.618	0.340	0.000162791	0.016279089	6.327253894	-1.078809661	-4.117873848
	559.618	0.340	0.00024853	0.024853	6.327253894	-1.078809661	-3.694776809
	559.618	0.340	0.000375342	0.037534206	6.327253894	-1.078809661	-3.282502603
	559.618	0.340	0.008107646	0.8107646	6.327253894	-1.078809661	-0.209777526
	559.618	0.340	0.004889399	0.488939892	6.327253894	-1.078809661	-0.715515717
	559.618	0.340	0.001021115	0.1021115	6.327253894	-1.078809661	-2.281689925
	559.618	0.340	0.000951748	0.0951748	6.327253894	-1.078809661	-2.352040078
	559.618	0.340	0.000396086	0.0396086	6.327253894	-1.078809661	-3.228709013
	559.618	0.340	0.000481594	0.0481594	6.327253894	-1.078809661	-3.033238937
	559.618	0.340	0.000738287	0.0738287	6.327253894	-1.078809661	-2.606007734
	559.618	0.340	0.000195248	0.0195248	6.327253894	-1.078809661	-3.936069827
	559.618	0.340	0.000538982	0.0538982	6.327253894	-1.078809661	-2.920658197
	559.618	0.340	0.000353356	0.0353356	6.327253894	-1.078809661	-3.342864325
	559.618	0.340	0.000535954	0.0535954	6.327253894	-1.078809661	-2.926292035
	559.618	0.340	0.000330688	0.0330688	6.327253894	-1.078809661	-3.409165039
	559.618	0.340	0.000234151	0.02341511	6.327253894	-1.078809661	-3.754373742
	559.618	0.340	0.000729899	0.0729899	6.327253894	-1.078809661	-2.617434204

Table D.3 Δ_{ff} values of Esenyalı Station from Level 2 Method

#	V_S(m/s)	PGA(g)	Disp(m)	Disp(cm)	Ln(V_S,m/sn)	Ln(PGA)	Ln(Disp,cm)
STATION 3 - ESENYALI STATION	448.252	0.330	0.00233575	0.233575	6.105356133	-1.108662625	-1.454252054
	448.252	0.330	0.002075334	0.2075334	6.105356133	-1.108662625	-1.572462988
	448.252	0.330	0.00099355	0.099355	6.105356133	-1.108662625	-2.309055984
	448.252	0.330	0.001231288	0.1231288	6.105356133	-1.108662625	-2.094524317
	448.252	0.330	0.001078422	0.1078422	6.105356133	-1.108662625	-2.227086231
	448.252	0.330	0.001745918	0.1745918	6.105356133	-1.108662625	-1.745304601
	448.252	0.330	0.001705476	0.1705476	6.105356133	-1.108662625	-1.768740842
	448.252	0.330	0.00250008	0.250008	6.105356133	-1.108662625	-1.386262362
	448.252	0.330	0.002175623	0.2175623	6.105356133	-1.108662625	-1.525270033
	448.252	0.330	0.002336393	0.2336393	6.105356133	-1.108662625	-1.453976806
	448.252	0.330	0.000503557	0.0503557	6.105356133	-1.108662625	-2.988643459
	448.252	0.330	0.001724841	0.1724841	6.105356133	-1.108662625	-1.757450221
	448.252	0.330	0.003486941	0.3486941	6.105356133	-1.108662625	-1.053560245
	448.252	0.330	0.00155223	0.155223	6.105356133	-1.108662625	-1.862892486
	448.252	0.330	0.000345905	0.0345905	6.105356133	-1.108662625	-3.364176201
	448.252	0.330	0.000423728	0.0423728	6.105356133	-1.108662625	-3.161248632
	448.252	0.330	0.000476233	0.0476233	6.105356133	-1.108662625	-3.044433142
	448.252	0.330	0.000316597	0.0316597	6.105356133	-1.108662625	-3.4527107
	448.252	0.330	0.00104693	0.104693	6.105356133	-1.108662625	-2.256723021
	448.252	0.330	0.002331325	0.2331325	6.105356133	-1.108662625	-1.456148318
	448.252	0.330	0.023408092	2.3408092	6.105356133	-1.108662625	0.850496682
	448.252	0.330	0.001491062	0.1491062	6.105356133	-1.108662625	-1.903096475
	448.252	0.330	0.001231439	0.1231439	6.105356133	-1.108662625	-2.094401689
	448.252	0.330	0.009569375	0.9569375	6.105356133	-1.108662625	-0.044017198
	448.252	0.330	0.000873132	0.0873132	6.105356133	-1.108662625	-2.438253625
	448.252	0.330	0.001604202	0.1604202	6.105356133	-1.108662625	-1.829958656
	448.252	0.330	0.001177426	0.1177426	6.105356133	-1.108662625	-2.139254393
	448.252	0.330	0.000720781	0.0720781	6.105356133	-1.108662625	-2.630005026
	448.252	0.330	0.000205016	0.0205016	6.105356133	-1.108662625	-3.887252347
	448.252	0.330	0.00021438	0.021438	6.105356133	-1.108662625	-3.842590231
	448.252	0.330	0.000128716	0.0128716	6.105356133	-1.108662625	-4.352731945
	448.252	0.330	0.000386508	0.0386508	6.105356133	-1.108662625	-3.253187806
	448.252	0.330	0.000978505	0.0978505	6.105356133	-1.108662625	-2.324314475
	448.252	0.330	0.008481285	0.8481285	6.105356133	-1.108662625	-0.164723122
	448.252	0.330	0.004042857	0.4042857	6.105356133	-1.108662625	-0.905633473
	448.252	0.330	0.002439266	0.2439266	6.105356133	-1.108662625	-1.410887919
	448.252	0.330	0.001363391	0.1363391	6.105356133	-1.108662625	-1.992610114
	448.252	0.330	0.001269752	0.1269752	6.105356133	-1.108662625	-2.063763487
	448.252	0.330	0.00135426	0.135426	6.105356133	-1.108662625	-1.999329913
	448.252	0.330	0.002724264	0.2724264	6.105356133	-1.108662625	-1.300386793
	448.252	0.330	0.000741051	0.0741051	6.105356133	-1.108662625	-2.602270923
	448.252	0.330	0.001096239	0.1096239	6.105356133	-1.108662625	-2.210699863
	448.252	0.330	0.000779509	0.0779509	6.105356133	-1.108662625	-2.551676138
	448.252	0.330	0.001314181	0.1314181	6.105356133	-1.108662625	-2.029371435
	448.252	0.330	0.000168703	0.0168703	6.105356133	-1.108662625	-4.0822006
	448.252	0.330	0.000809088	0.0809088	6.105356133	-1.108662625	-2.514432685
	448.252	0.330	0.00087966	0.087966	6.105356133	-1.108662625	-2.430804903
	448.252	0.330	0.001260038	0.1260038	6.105356133	-1.108662625	-2.071443214

Table D.4 Δ_{ff} values of Hasanpaşa Station from Level 2 Method

#	V_S(m/s)	PGA(g)	Disp(m)	Disp(cm)	Ln(V_S,m/sn)	Ln(PGA)	Ln(Disp,cm)
STATION 4 - HASANPAŞA STATION	379.683	0.260	0.00579614	0.579614	5.939335864	-1.347073648	-0.545392914
	379.683	0.260	0.001315973	0.1315973	5.939335864	-1.347073648	-2.028008777
	379.683	0.260	0.002585988	0.2585988	5.939335864	-1.347073648	-1.352477453
	379.683	0.260	0.008616267	0.8616267	5.939335864	-1.347073648	-0.148933165
	379.683	0.260	0.002829153	0.2829153	5.939335864	-1.347073648	-1.262607719
	379.683	0.260	0.005685172	0.5685172	5.939335864	-1.347073648	-0.564723711
	379.683	0.260	0.007581298	0.7581298	5.939335864	-1.347073648	-0.276900668
	379.683	0.260	0.004452283	0.4452283	5.939335864	-1.347073648	-0.809168095
	379.683	0.260	0.00272618	0.272618	5.939335864	-1.347073648	-1.299683731
	379.683	0.260	0.003662702	0.3662702	5.939335864	-1.347073648	-1.004383967
	379.683	0.260	0.007512846	0.7512846	5.939335864	-1.347073648	-0.285970738
	379.683	0.260	0.003759431	0.3759431	5.939335864	-1.347073648	-0.978317477
	379.683	0.260	0.003776952	0.3776952	5.939335864	-1.347073648	-0.973667758
	379.683	0.260	0.014203039	1.4203039	5.939335864	-1.347073648	0.350870863
	379.683	0.260	0.004927384	0.4927384	5.939335864	-1.347073648	-0.707776875
	379.683	0.260	0.003996577	0.3996577	5.939335864	-1.347073648	-0.917146848
	379.683	0.260	0.003269137	0.3269137	5.939335864	-1.347073648	-1.118059057
	379.683	0.260	0.003707481	0.3707481	5.939335864	-1.347073648	-0.992232423
	379.683	0.260	0.006894593	0.6894593	5.939335864	-1.347073648	-0.371847612
	379.683	0.260	0.008090534	0.8090534	5.939335864	-1.347073648	-0.211890357
	379.683	0.260	0.003836426	0.3836426	5.939335864	-1.347073648	-0.958043889
	379.683	0.260	0.008000679	0.8000679	5.939335864	-1.347073648	-0.22305868
	379.683	0.260	0.00519629	0.519629	5.939335864	-1.347073648	-0.654640184
	379.683	0.260	0.004493503	0.4493503	5.939335864	-1.347073648	-0.799952517
	379.683	0.260	0.005848298	0.5848298	5.939335864	-1.347073648	-0.536434414
	379.683	0.260	0.005569051	0.5569051	5.939335864	-1.347073648	-0.585360431
	379.683	0.260	0.006943714	0.6943714	5.939335864	-1.347073648	-0.364748303
	379.683	0.260	0.008052118	0.8052118	5.939335864	-1.347073648	-0.216649931
	379.683	0.260	0.00077439	0.077439	5.939335864	-1.347073648	-2.558264749
	379.683	0.260	0.006500841	0.6500841	5.939335864	-1.347073648	-0.43065354
	379.683	0.260	0.002683655	0.2683655	5.939335864	-1.347073648	-1.315405422
	379.683	0.260	0.00890962	0.890962	5.939335864	-1.347073648	-0.115453501
	379.683	0.260	0.007017776	0.7017776	5.939335864	-1.347073648	-0.354138734
	379.683	0.260	0.002882325	0.2882325	5.939335864	-1.347073648	-1.243987833
	379.683	0.260	0.012341348	1.2341348	5.939335864	-1.347073648	0.210370158
	379.683	0.260	0.003800281	0.3800281	5.939335864	-1.347073648	-0.967510082
	379.683	0.260	0.010300898	1.0300898	5.939335864	-1.347073648	0.029645983
	379.683	0.260	0.003772276	0.3772276	5.939335864	-1.347073648	-0.97490656
	379.683	0.260	0.005935889	0.5935889	5.939335864	-1.347073648	-0.521568287
	379.683	0.260	0.005359213	0.5359213	5.939335864	-1.347073648	-0.623767957
	379.683	0.260	0.000882798	0.0882798	5.939335864	-1.347073648	-2.427243963
	379.683	0.260	0.002658392	0.2658392	5.939335864	-1.347073648	-1.324863664
	379.683	0.260	0.005149045	0.5149045	5.939335864	-1.347073648	-0.663773832
	379.683	0.260	0.009839201	0.9839201	5.939335864	-1.347073648	-0.016210584
	379.683	0.260	0.008602119	0.8602119	5.939335864	-1.347073648	-0.150576525
	379.683	0.260	0.006685063	0.6685063	5.939335864	-1.347073648	-0.402709458
	379.683	0.260	0.006923468	0.6923468	5.939335864	-1.347073648	-0.367668293
	379.683	0.260	0.006771144	0.6771144	5.939335864	-1.347073648	-0.38991504

Table D.5 Δ_{ff} values of Kavakpınar Station from Level 2 Method

#	V_S(m/s)	PGA(g)	Disp(m)	Disp(cm)	Ln(V_S,m/sn)	Ln(PGA)	Ln(Disp,cm)
STATION 5 - KAVAKPINAR STATION	343.438	0.320	0.004666632	0.4666632	5.839006277	-1.139434283	-0.762147481
	343.438	0.320	0.002263957	0.2263957	5.839006277	-1.139434283	-1.485470926
	343.438	0.320	0.006710654	0.6710654	5.839006277	-1.139434283	-0.39888868
	343.438	0.320	0.009217858	0.9217858	5.839006277	-1.139434283	-0.081442403
	343.438	0.320	0.003765528	0.3765528	5.839006277	-1.139434283	-0.976697003
	343.438	0.320	0.006472799	0.6472799	5.839006277	-1.139434283	-0.434976466
	343.438	0.320	0.006392927	0.6392927	5.839006277	-1.139434283	-0.44739287
	343.438	0.320	0.004135504	0.4135504	5.839006277	-1.139434283	-0.882975886
	343.438	0.320	0.006471582	0.6471582	5.839006277	-1.139434283	-0.435164501
	343.438	0.320	0.000717834	0.0717834	5.839006277	-1.139434283	-2.634102027
	343.438	0.320	0.017397296	1.7397296	5.839006277	-1.139434283	0.553729699
	343.438	0.320	0.002951226	0.2951226	5.839006277	-1.139434283	-1.220364416
	343.438	0.320	0.002381082	0.2381082	5.839006277	-1.139434283	-1.435030087
	343.438	0.320	0.013686521	1.368652136	5.839006277	-1.139434283	0.313826413
	343.438	0.320	0.010227376	1.022737605	5.839006277	-1.139434283	0.022482958
	343.438	0.320	0.019141252	1.9141252	5.839006277	-1.139434283	0.649260704
	343.438	0.320	0.020266916	2.0266916	5.839006277	-1.139434283	0.70640471
	343.438	0.320	0.016073771	1.6073771	5.839006277	-1.139434283	0.47460372
	343.438	0.320	0.007932217	0.7932217	5.839006277	-1.139434283	-0.231652525
	343.438	0.320	0.011698904	1.1698904	5.839006277	-1.139434283	0.156910069
	343.438	0.320	0.000136983	0.0136983	5.839006277	-1.139434283	-4.290483541
	343.438	0.320	0.000826383	0.0826383	5.839006277	-1.139434283	-2.493282026
	343.438	0.320	0.00744502	0.744502	5.839006277	-1.139434283	-0.29503974
	343.438	0.320	0.013903495	1.3903495	5.839006277	-1.139434283	0.329555154
	343.438	0.320	0.010073528	1.0073528	5.839006277	-1.139434283	0.0073259
	343.438	0.320	0.011173357	1.1173357	5.839006277	-1.139434283	0.110947012
	343.438	0.320	0.004643612	0.4643612	5.839006277	-1.139434283	-0.767092581
	343.438	0.320	0.006338138	0.6338138	5.839006277	-1.139434283	-0.456000059
	343.438	0.320	0.018008187	1.8008187	5.839006277	-1.139434283	0.588241395
	343.438	0.320	0.001076994	0.1076994	5.839006277	-1.139434283	-2.228411266
	343.438	0.320	0.011999005	1.1999005	5.839006277	-1.139434283	0.182238637
	343.438	0.320	0.009577669	0.9577669	5.839006277	-1.139434283	-0.04315085
	343.438	0.320	0.017988332	1.7988332	5.839006277	-1.139434283	0.587138232
	343.438	0.320	0.019303458	1.9303458	5.839006277	-1.139434283	0.657699158
	343.438	0.320	0.005910214	0.5910214	5.839006277	-1.139434283	-0.525903052
	343.438	0.320	0.000241163	0.0241163	5.839006277	-1.139434283	-3.724867319
	343.438	0.320	0.005947102	0.5947102	5.839006277	-1.139434283	-0.519681051
	343.438	0.320	0.003832325	0.3832325	5.839006277	-1.139434283	-0.959113424
	343.438	0.320	0.013245123	1.3245123	5.839006277	-1.139434283	0.281044316
	343.438	0.320	0.01074468	1.074468	5.839006277	-1.139434283	0.071825655
	343.438	0.320	0.004666557	0.4666557	5.839006277	-1.139434283	-0.762163552
	343.438	0.320	0.006562133	0.6562133	5.839006277	-1.139434283	-0.42126939
	343.438	0.320	0.008709508	0.8709508	5.839006277	-1.139434283	-0.138169791
	343.438	0.320	0.013042174	1.3042174	5.839006277	-1.139434283	0.265603167
	343.438	0.320	0.01372492	1.372492	5.839006277	-1.139434283	0.316628066
	343.438	0.320	0.013039567	1.3039567	5.839006277	-1.139434283	0.265403257
	343.438	0.320	0.011504647	1.1504647	5.839006277	-1.139434283	0.140165948
	343.438	0.320	0.010167885	1.0167885	5.839006277	-1.139434283	0.016649131
	343.438	0.320	0.0238034	2.38034	5.839006277	-1.139434283	0.867243335

Table D.6 Δ_{ff} values of Meclis Mahallesi Station from Level 2 Method

#	V_S(m/s)	PGA(g)	Disp(m)	Disp(cm)	Ln(V_S,m/sn)	Ln(PGA)	Ln(Disp,cm)
STATION 6 - MECLİS MAHALLESİ STATION	477.239	0.240	0.001517401	0.1517401	6.168017114	-1.427116356	-1.88558609
	477.239	0.240	0.001559377	0.1559377	6.168017114	-1.427116356	-1.85829871
	477.239	0.240	0.000766896	0.0766896	6.168017114	-1.427116356	-2.567989173
	477.239	0.240	0.000876254	0.0876254	6.168017114	-1.427116356	-2.434684369
	477.239	0.240	0.000812885	0.0812885	6.168017114	-1.427116356	-2.509750724
	477.239	0.240	0.000967225	0.0967225	6.168017114	-1.427116356	-2.335909225
	477.239	0.240	0.001184557	0.1184557	6.168017114	-1.427116356	-2.133216228
	477.239	0.240	0.00158564	0.158564	6.168017114	-1.427116356	-1.841596982
	477.239	0.240	0.001316797	0.131679727	6.168017114	-1.427116356	-2.027382612
	477.239	0.240	0.001491749	0.1491749	6.168017114	-1.427116356	-1.902635836
	477.239	0.240	0.000307716	0.0307716	6.168017114	-1.427116356	-3.481163092
	477.239	0.240	0.001185799	0.1185799	6.168017114	-1.427116356	-2.132168284
	477.239	0.240	0.001991664	0.1991664	6.168017114	-1.427116356	-1.613614623
	477.239	0.240	0.000973634	0.0973634	6.168017114	-1.427116356	-2.329304909
	477.239	0.240	0.000207769	0.0207769	6.168017114	-1.427116356	-3.873913486
	477.239	0.240	0.000267788	0.0267788	6.168017114	-1.427116356	-3.620144749
	477.239	0.240	0.000319071	0.0319071	6.168017114	-1.427116356	-3.444926723
	477.239	0.240	0.000208924	0.0208924	6.168017114	-1.427116356	-3.868369823
	477.239	0.240	0.000675724	0.0675724	6.168017114	-1.427116356	-2.694555663
	477.239	0.240	0.001731666	0.1731666	6.168017114	-1.427116356	-1.753501142
	477.239	0.240	0.017364985	1.7364985	6.168017114	-1.427116356	0.551870729
	477.239	0.240	0.001006294	0.1006294	6.168017114	-1.427116356	-2.296310817
	477.239	0.240	0.0007665	0.076650012	6.168017114	-1.427116356	-2.568505512
	477.239	0.240	0.007089978	0.7089978	6.168017114	-1.427116356	-0.343902855
	477.239	0.240	0.000536787	0.0536787	6.168017114	-1.427116356	-2.924739004
	477.239	0.240	0.001105765	0.1105765	6.168017114	-1.427116356	-2.20204769
	477.239	0.240	0.000707537	0.0707537	6.168017114	-1.427116356	-2.648550447
	477.239	0.240	0.000464462	0.0464462	6.168017114	-1.427116356	-3.069460625
	477.239	0.240	0.000119754	0.0119754	6.168017114	-1.427116356	-4.424900733
	477.239	0.240	0.000110717	0.0110717	6.168017114	-1.427116356	-4.503362976
	477.239	0.240	8.6321E-05	0.0086321	6.168017114	-1.427116356	-4.752267466
	477.239	0.240	0.000237518	0.0237518	6.168017114	-1.427116356	-3.740096962
	477.239	0.240	0.000627679	0.0627679	6.168017114	-1.427116356	-2.768311483
	477.239	0.240	0.00609363	0.609363	6.168017114	-1.427116356	-0.49534113
	477.239	0.240	0.002783688	0.2783688	6.168017114	-1.427116356	-1.278808426
	477.239	0.240	0.001469413	0.1469413	6.168017114	-1.427116356	-1.917722092
	477.239	0.240	0.000940927	0.0940927	6.168017114	-1.427116356	-2.363474812
	477.239	0.240	0.000923224	0.0923224	6.168017114	-1.427116356	-2.38246848
	477.239	0.240	0.000949081	0.0949081	6.168017114	-1.427116356	-2.354846224
	477.239	0.240	0.001455787	0.1455787	6.168017114	-1.427116356	-1.927038445
	477.239	0.240	0.000511392	0.0511392	6.168017114	-1.427116356	-2.973203953
	477.239	0.240	0.000784735	0.0784735	6.168017114	-1.427116356	-2.544994291
	477.239	0.240	0.000527357	0.0527357	6.168017114	-1.427116356	-2.942462633
	477.239	0.240	0.000822008	0.0822008	6.168017114	-1.427116356	-2.498590245
	477.239	0.240	0.000102682	0.0102682	6.168017114	-1.427116356	-4.578703538
	477.239	0.240	0.000519479	0.0519479	6.168017114	-1.427116356	-2.957513986
	477.239	0.240	0.000575633	0.057563278	6.168017114	-1.427116356	-2.854870449
	477.239	0.240	0.000845058	0.0845058	6.168017114	-1.427116356	-2.470935108

Table D.7 Δ_{ff} values of Samandıra Station from Level 2 Method

#	V_S(m/s)	PGA(g)	Disp(m)	Disp(cm)	Ln(V_S,m/sn)	Ln(PGA)	Ln(Disp,cm)
STATION 7 - SAMANDIRA STATION	282.376	0.240	0.007993448	0.7993448	5.643240402	-1.427116356	-0.223962887
	282.376	0.240	0.002907497	0.2907497	5.643240402	-1.427116356	-1.235292519
	282.376	0.240	0.010428052	1.0428052	5.643240402	-1.427116356	0.04191439
	282.376	0.240	0.018023773	1.8023773	5.643240402	-1.427116356	0.589106516
	282.376	0.240	0.005650465	0.5650465	5.643240402	-1.427116356	-0.57084725
	282.376	0.240	0.018034526	1.8034526	5.643240402	-1.427116356	0.589702939
	282.376	0.240	0.01728622	1.728622	5.643240402	-1.427116356	0.547324559
	282.376	0.240	0.006327447	0.6327447	5.643240402	-1.427116356	-0.457688256
	282.376	0.240	0.008793586	0.8793586	5.643240402	-1.427116356	-0.128562501
	282.376	0.240	0.001862824	0.1862824	5.643240402	-1.427116356	-1.680491477
	282.376	0.240	0.024695387	2.4695387	5.643240402	-1.427116356	0.904031372
	282.376	0.240	0.007915348	0.7915348	5.643240402	-1.427116356	-0.233781433
	282.376	0.240	0.002900659	0.2900659	5.643240402	-1.427116356	-1.23764714
	282.376	0.240	0.014602998	1.460299817	5.643240402	-1.427116356	0.378641769
	282.376	0.240	0.016450045	1.6450045	5.643240402	-1.427116356	0.49774312
	282.376	0.240	0.096228921	9.6228921	5.643240402	-1.427116356	2.264144854
	282.376	0.240	0.082136572	8.2136572	5.643240402	-1.427116356	2.105798281
	282.376	0.240	0.027389117	2.7389117	5.643240402	-1.427116356	1.007560652
	282.376	0.240	0.020546223	2.0546223	5.643240402	-1.427116356	0.720092035
	282.376	0.240	0.021656084	2.1656084	5.643240402	-1.427116356	0.772701338
	282.376	0.240	0.010188744	1.0188744	5.643240402	-1.427116356	0.018698489
	282.376	0.240	0.029453833	2.9453833	5.643240402	-1.427116356	1.080238961
	282.376	0.240	0.012832417	1.2832417	5.643240402	-1.427116356	0.249389454
	282.376	0.240	0.03691121	3.691121	5.643240402	-1.427116356	1.305930206
	282.376	0.240	0.007404991	0.7404991	5.643240402	-1.427116356	-0.300430861
	282.376	0.240	0.011896172	1.1896172	5.643240402	-1.427116356	0.173631575
	282.376	0.240	0.025612318	2.5612318	5.643240402	-1.427116356	0.940488315
	282.376	0.240	0.001845447	0.1845447	5.643240402	-1.427116356	-1.689863568
	282.376	0.240	0.022078028	2.2078028	5.643240402	-1.427116356	0.791997813
	282.376	0.240	0.014713929	1.4713929	5.643240402	-1.427116356	0.386209503
	282.376	0.240	0.118863734	11.8863734	5.643240402	-1.427116356	2.475392652
	282.376	0.240	0.036122775	3.6122775	5.643240402	-1.427116356	1.28433846
	282.376	0.240	0.013757114	1.3757114	5.643240402	-1.427116356	0.318970979
	282.376	0.240	0.003569153	0.3569153	5.643240402	-1.427116356	-1.03025678
	282.376	0.240	0.010284	1.0284	5.643240402	-1.427116356	0.028004196
	282.376	0.240	0.019038282	1.9038282	5.643240402	-1.427116356	0.643866701
	282.376	0.240	0.012546166	1.2546166	5.643240402	-1.427116356	0.226830028
	282.376	0.240	0.006646204	0.6646204	5.643240402	-1.427116356	-0.408539228
	282.376	0.240	0.008869405	0.8869405	5.643240402	-1.427116356	-0.119977379
	282.376	0.240	0.012917456	1.2917456	5.643240402	-1.427116356	0.255994482
	282.376	0.240	0.034098147	3.4098147	5.643240402	-1.427116356	1.22665795
	282.376	0.240	0.017817706	1.7817706	5.643240402	-1.427116356	0.577607589
	282.376	0.240	0.01553232	1.553232	5.643240402	-1.427116356	0.440337921
	282.376	0.240	0.017209451	1.7209451	5.643240402	-1.427116356	0.542873617
	282.376	0.240	0.019977789	1.9977789	5.643240402	-1.427116356	0.692036013
	282.376	0.240	0.056568834	5.6568834	5.643240402	-1.427116356	1.732873105

Table D.8 Δ_{ff} values of Sancaktepe Station from Level 2 Method

#	V_S(m/s)	PGA(g)	Disp(m)	Disp(cm)	Ln(V_S,m/sn)	Ln(PGA)	Ln(Disp,cm)
STATION 8 - SANCAKTEPE STATION	306.347	0.250	0.007124799	0.7124799	5.724717031	-1.386294361	-0.339003578
	306.347	0.250	0.001565058	0.1565058	5.724717031	-1.386294361	-1.854662209
	306.347	0.250	0.003887127	0.3887127	5.724717031	-1.386294361	-0.944914769
	306.347	0.250	0.011663744	1.1663744	5.724717031	-1.386294361	0.153900134
	306.347	0.250	0.005004458	0.5004458	5.724717031	-1.386294361	-0.692255978
	306.347	0.250	0.01212195	1.212195	5.724717031	-1.386294361	0.192432766
	306.347	0.250	0.008814812	0.8814812	5.724717031	-1.386294361	-0.126151605
	306.347	0.250	0.005260128	0.5260128	5.724717031	-1.386294361	-0.642429732
	306.347	0.250	0.007918573	0.7918573	5.724717031	-1.386294361	-0.23337408
	306.347	0.250	0.00394033	0.394033	5.724717031	-1.386294361	-0.931320617
	306.347	0.250	0.012679177	1.2679177	5.724717031	-1.386294361	0.237375949
	306.347	0.250	0.00459214	0.459214	5.724717031	-1.386294361	-0.778238947
	306.347	0.250	0.004594793	0.4594793	5.724717031	-1.386294361	-0.777661387
	306.347	0.250	0.022968927	2.2968927	5.724717031	-1.386294361	0.83155721
	306.347	0.250	0.009019066	0.9019066	5.724717031	-1.386294361	-0.103244312
	306.347	0.250	0.009015936	0.9015936	5.724717031	-1.386294361	-0.103591415
	306.347	0.250	0.00677927	0.677927	5.724717031	-1.386294361	-0.388715666
	306.347	0.250	0.005237654	0.5237654	5.724717031	-1.386294361	-0.646711405
	306.347	0.250	0.0112246	1.12246	5.724717031	-1.386294361	0.115522705
	306.347	0.250	0.015465537	1.5465537	5.724717031	-1.386294361	0.436029036
	306.347	0.250	0.011127801	1.1127801	5.724717031	-1.386294361	0.106861479
	306.347	0.250	0.008091453	0.8091453	5.724717031	-1.386294361	-0.211776774
	306.347	0.250	0.004681308	0.4681308	5.724717031	-1.386294361	-0.759007535
	306.347	0.250	0.010449166	1.0449166	5.724717031	-1.386294361	0.043937074
	306.347	0.250	0.005913922	0.5913922	5.724717031	-1.386294361	-0.525275861
	306.347	0.250	0.010198492	1.0198492	5.724717031	-1.386294361	0.019654773
	306.347	0.250	0.018098198	1.8098198	5.724717031	-1.386294361	0.593227282
	306.347	0.250	0.004817311	0.4817311	5.724717031	-1.386294361	-0.730369204
	306.347	0.250	0.009891351	0.9891351	5.724717031	-1.386294361	-0.010924354
	306.347	0.250	0.007189076	0.7189076	5.724717031	-1.386294361	-0.330022441
	306.347	0.250	0.016450458	1.6450458	5.724717031	-1.386294361	0.497768226
	306.347	0.250	0.010091707	1.0091707	5.724717031	-1.386294361	0.009128904
	306.347	0.250	0.000667779	0.0667779	5.724717031	-1.386294361	-2.706383092
	306.347	0.250	0.017443342	1.7443342	5.724717031	-1.386294361	0.556372936
	306.347	0.250	0.004530146	0.4530146	5.724717031	-1.386294361	-0.791830924
	306.347	0.250	0.012607379	1.2607379	5.724717031	-1.386294361	0.231697184
	306.347	0.250	0.007128631	0.7128631	5.724717031	-1.386294361	-0.338465883
	306.347	0.250	0.006424374	0.6424374	5.724717031	-1.386294361	-0.442485899
	306.347	0.250	0.006894288	0.6894288	5.724717031	-1.386294361	-0.37189185
	306.347	0.250	0.000920693	0.0920693	5.724717031	-1.386294361	-2.385213725
	306.347	0.250	0.005855281	0.5855281	5.724717031	-1.386294361	-0.535241104
	306.347	0.250	0.011743901	1.1743901	5.724717031	-1.386294361	0.160748949
	306.347	0.250	0.014511127	1.4511127	5.724717031	-1.386294361	0.372330641
	306.347	0.250	0.018255547	1.8255547	5.724717031	-1.386294361	0.601883886
	306.347	0.250	0.014532143	1.4532143	5.724717031	-1.386294361	0.373777862
	306.347	0.250	0.008852267	0.885226705	5.724717031	-1.386294361	-0.121911503
	306.347	0.250	0.010542424	1.0542424	5.724717031	-1.386294361	0.052822405

Table D.9 Δ_{ff} values of Sarıgazi Station from Level 2 Method

#	V_S(m/s)	PGA(g)	Disp(m)	Disp(cm)	Ln(V_S,m/sn)	Ln(PGA)	Ln(Disp,cm)
STATION 9 - SARIGAZİ STATION	324.419	0.235	0.007274836	0.7274836	5.782036512	-1.448169765	-0.318163823
	324.419	0.235	0.002042496	0.2042496	5.782036512	-1.448169765	-1.588412504
	324.419	0.235	0.005359032	0.5359032	5.782036512	-1.448169765	-0.623801731
	324.419	0.235	0.013508029	1.3508029	5.782036512	-1.448169765	0.300699156
	324.419	0.235	0.005684426	0.5684426	5.782036512	-1.448169765	-0.564854938
	324.419	0.235	0.013532173	1.3532173	5.782036512	-1.448169765	0.302484942
	324.419	0.235	0.009416365	0.9416365	5.782036512	-1.448169765	-0.06013596
	324.419	0.235	0.005768916	0.5768916	5.782036512	-1.448169765	-0.550100898
	324.419	0.235	0.008674506	0.8674506	5.782036512	-1.448169765	-0.142196714
	324.419	0.235	0.004085489	0.4085489	5.782036512	-1.448169765	-0.895143666
	324.419	0.235	0.014985127	1.4985127	5.782036512	-1.448169765	0.404473083
	324.419	0.235	0.004104044	0.4104044	5.782036512	-1.448169765	-0.890612264
	324.419	0.235	0.005319565	0.5319565	5.782036512	-1.448169765	-0.63119356
	324.419	0.235	0.023294259	2.32942594	5.782036512	-1.448169765	0.845621859
	324.419	0.235	0.008967176	0.8967176	5.782036512	-1.448169765	-0.109014294
	324.419	0.235	0.015128721	1.5128721	5.782036512	-1.448169765	0.414009897
	324.419	0.235	0.007721392	0.7721392	5.782036512	-1.448169765	-0.258590434
	324.419	0.235	0.006519312	0.6519312	5.782036512	-1.448169765	-0.427816244
	324.419	0.235	0.012073504	1.2073504	5.782036512	-1.448169765	0.188428207
	324.419	0.235	0.015953187	1.5953187	5.782036512	-1.448169765	0.467073528
	324.419	0.235	0.014539306	1.4539306	5.782036512	-1.448169765	0.374270648
	324.419	0.235	0.010457181	1.0457181	5.782036512	-1.448169765	0.044703826
	324.419	0.235	0.009951047	0.9951047	5.782036512	-1.448169765	-0.004907321
	324.419	0.235	0.011175435	1.1175435	5.782036512	-1.448169765	0.111132973
	324.419	0.235	0.012047629	1.2047629	5.782036512	-1.448169765	0.186282784
	324.419	0.235	0.006470123	0.6470123	5.782036512	-1.448169765	-0.435389974
	324.419	0.235	0.010624202	1.0624202	5.782036512	-1.448169765	0.060549513
	324.419	0.235	0.021229398	2.1229398	5.782036512	-1.448169765	0.752801826
	324.419	0.235	0.005075381	0.5075381	5.782036512	-1.448169765	-0.678183497
	324.419	0.235	0.00951403	0.951403	5.782036512	-1.448169765	-0.049817542
	324.419	0.235	0.010704892	1.0704892	5.782036512	-1.448169765	0.06811574
	324.419	0.235	0.021930114	2.1930114	5.782036512	-1.448169765	0.785275668
	324.419	0.235	0.008996211	0.8996211	5.782036512	-1.448169765	-0.105781604
	324.419	0.235	0.005550865	0.5550865	5.782036512	-1.448169765	-0.588631322
	324.419	0.235	0.017921895	1.7921895	5.782036512	-1.448169765	0.583438057
	324.419	0.235	0.005708721	0.5708721	5.782036512	-1.448169765	-0.560590087
	324.419	0.235	0.015512136	1.5512136	5.782036512	-1.448169765	0.439037592
	324.419	0.235	0.010496432	1.0496432	5.782036512	-1.448169765	0.048450297
	324.419	0.235	0.00620829	0.620829	5.782036512	-1.448169765	-0.476699597
	324.419	0.235	0.008983573	0.8983573	5.782036512	-1.448169765	-0.107187406
	324.419	0.235	0.009806192	0.9806192	5.782036512	-1.448169765	-0.01957107
	324.419	0.235	0.01575095	1.575095	5.782036512	-1.448169765	0.454315588
	324.419	0.235	0.01605056	1.605056	5.782036512	-1.448169765	0.473158647
	324.419	0.235	0.015300532	1.5300532	5.782036512	-1.448169765	0.425302506
	324.419	0.235	0.013828078	1.3828078	5.782036512	-1.448169765	0.32411607
	324.419	0.235	0.01036349	1.036349	5.782036512	-1.448169765	0.03570396
	324.419	0.235	0.014678118	1.4678118	5.782036512	-1.448169765	0.38377272

Table D.10 Δ_{ff} values of Sultanbeyli Station from Level 2 Method

#	V_S(m/s)	PGA(g)	Disp(m)	Disp(cm)	Ln(V_S,m/sn)	Ln(PGA)	Ln(Disp,cm)
STATION 10 - SULTANBEYLİ STATION	492.534	0.250	0.001005627	0.1005627	6.199564074	-1.386294361	-2.296973865
	492.534	0.250	0.001235317	0.1235317	6.199564074	-1.386294361	-2.091257476
	492.534	0.250	0.000797393	0.0797393	6.199564074	-1.386294361	-2.528992716
	492.534	0.250	0.000656488	0.0656488	6.199564074	-1.386294361	-2.723435957
	492.534	0.250	0.000629192	0.0629192	6.199564074	-1.386294361	-2.765903915
	492.534	0.250	0.000706163	0.0706163	6.199564074	-1.386294361	-2.650494283
	492.534	0.250	0.001016083	0.1016083	6.199564074	-1.386294361	-2.286630054
	492.534	0.250	0.001091871	0.1091871	6.199564074	-1.386294361	-2.214692355
	492.534	0.250	0.000642145	0.0642145	6.199564074	-1.386294361	-2.745526237
	492.534	0.250	0.000940416	0.0940416	6.199564074	-1.386294361	-2.364018041
	492.534	0.250	0.000296989	0.0296989	6.199564074	-1.386294361	-3.516645271
	492.534	0.250	0.000809435	0.080943483	6.199564074	-1.386294361	-2.514004113
	492.534	0.250	0.001309129	0.1309129	6.199564074	-1.386294361	-2.033223062
	492.534	0.250	0.00075334	0.075334	6.199564074	-1.386294361	-2.585823719
	492.534	0.250	0.00013088	0.013088	6.199564074	-1.386294361	-4.336059499
	492.534	0.250	0.000212161	0.0212161	6.199564074	-1.386294361	-3.852994952
	492.534	0.250	0.000255987	0.0255987	6.199564074	-1.386294361	-3.66521371
	492.534	0.250	0.000167207	0.0167207	6.199564074	-1.386294361	-4.091107806
	492.534	0.250	0.000495063	0.0495063	6.199564074	-1.386294361	-3.005655345
	492.534	0.250	0.0017349	0.17349	6.199564074	-1.386294361	-1.751635318
	492.534	0.250	0.017842784	1.7842784	6.199564074	-1.386294361	0.579014076
	492.534	0.250	0.000744673	0.0744673	6.199564074	-1.386294361	-2.597395176
	492.534	0.250	0.00059208	0.059208	6.199564074	-1.386294361	-2.826698611
	492.534	0.250	0.007466483	0.7466483	6.199564074	-1.386294361	-0.292161021
	492.534	0.250	0.000413104	0.0413104	6.199564074	-1.386294361	-3.186640995
	492.534	0.250	0.000731881	0.0731881	6.199564074	-1.386294361	-2.61472244
	492.534	0.250	0.000379475	0.0379475	6.199564074	-1.386294361	-3.271551653
	492.534	0.250	0.000323195	0.0323195	6.199564074	-1.386294361	-3.432084516
	492.534	0.250	7.5349E-05	0.0075349	6.199564074	-1.386294361	-4.888209718
	492.534	0.250	5.4279E-05	0.0054279	6.199564074	-1.386294361	-5.21620296
	492.534	0.250	7.5031E-05	0.0075031	6.199564074	-1.386294361	-4.892439011
	492.534	0.250	0.000196552	0.0196552	6.199564074	-1.386294361	-3.929413345
	492.534	0.250	0.000447528	0.0447528	6.199564074	-1.386294361	-3.106601266
	492.534	0.250	0.006337361	0.6337361	6.199564074	-1.386294361	-0.456122657
	492.534	0.250	0.002759172	0.2759172	6.199564074	-1.386294361	-1.287654458
	492.534	0.250	0.001139228	0.1139228	6.199564074	-1.386294361	-2.172234253
	492.534	0.250	0.000846472	0.0846472	6.199564074	-1.386294361	-2.469263248
	492.534	0.250	0.000532754	0.0532754	6.199564074	-1.386294361	-2.932280593
	492.534	0.250	0.000647002	0.0647002	6.199564074	-1.386294361	-2.737990986
	492.534	0.250	0.000773333	0.0773333	6.199564074	-1.386294361	-2.559630627
	492.534	0.250	0.000344904	0.0344904	6.199564074	-1.386294361	-3.367074255
	492.534	0.250	0.000603025	0.0603025	6.199564074	-1.386294361	-2.808381717
	492.534	0.250	0.000399193	0.0399193	6.199564074	-1.386294361	-3.220895363
	492.534	0.250	0.000577019	0.0577019	6.199564074	-1.386294361	-2.852465177
	492.534	0.250	5.6846E-05	0.0056846	6.199564074	-1.386294361	-5.169994515
	492.534	0.250	0.000351922	0.0351922	6.199564074	-1.386294361	-3.346930812
	492.534	0.250	0.000273594	0.0273594	6.199564074	-1.386294361	-3.598695116
	492.534	0.250	0.000641994	0.0641994	6.199564074	-1.386294361	-2.745761414

Table D.11 Δ_{ff} values of Tuzla Belediye Station from Level 2 Method

#	V_S(m/s)	PGA(g)	Disp(m)	Disp(cm)	Ln(V_S,m/sn)	Ln(PGA)	Ln(Disp,cm)
STATION 11 - TUZLA BELEDİYE STATION	611.981	0.370	0.002443954	0.2443954	6.416700729	-0.994252273	-1.408967873
	611.981	0.370	0.001898116	0.1898116	6.416700729	-0.994252273	-1.661723278
	611.981	0.370	0.001037245	0.1037245	6.416700729	-0.994252273	-2.266016933
	611.981	0.370	0.002403602	0.2403602	6.416700729	-0.994252273	-1.425616647
	611.981	0.370	0.000890279	0.0890279	6.416700729	-0.994252273	-2.418805475
	611.981	0.370	0.001799952	0.1799952	6.416700729	-0.994252273	-1.714825095
	611.981	0.370	0.003098366	0.3098366	6.416700729	-0.994252273	-1.171710217
	611.981	0.370	0.002709629	0.2709629	6.416700729	-0.994252273	-1.305773368
	611.981	0.370	0.000858971	0.0858971	6.416700729	-0.994252273	-2.454605211
	611.981	0.370	0.002172622	0.2172622	6.416700729	-0.994252273	-1.52665036
	611.981	0.370	0.00143418	0.143418	6.416700729	-0.994252273	-1.941991836
	611.981	0.370	0.001735311	0.1735311	6.416700729	-0.994252273	-1.751398445
	611.981	0.370	0.002698365	0.2698365	6.416700729	-0.994252273	-1.309939059
	611.981	0.370	0.002571485	0.2571485	6.416700729	-0.994252273	-1.35810154
	611.981	0.370	0.000701643	0.0701643	6.416700729	-0.994252273	-2.656915644
	611.981	0.370	0.001366072	0.1366072	6.416700729	-0.994252273	-1.990645625
	611.981	0.370	0.001271551	0.1271551	6.416700729	-0.994252273	-2.062347678
	611.981	0.370	0.000885066	0.0885066	6.416700729	-0.994252273	-2.424678153
	611.981	0.370	0.001735979	0.1735979	6.416700729	-0.994252273	-1.751013574
	611.981	0.370	0.002381344	0.2381344	6.416700729	-0.994252273	-1.434920059
	611.981	0.370	0.018046424	1.8046424	6.416700729	-0.994252273	0.590362456
	611.981	0.370	0.001926529	0.1926529	6.416700729	-0.994252273	-1.646865155
	611.981	0.370	0.001778317	0.1778317	6.416700729	-0.994252273	-1.726917682
	611.981	0.370	0.007249046	0.7249046	6.416700729	-0.994252273	-0.321715219
	611.981	0.370	0.001420246	0.1420246	6.416700729	-0.994252273	-1.951754997
	611.981	0.370	0.002499712	0.2499712	6.416700729	-0.994252273	-1.386409568
	611.981	0.370	0.001489414	0.1489414	6.416700729	-0.994252273	-1.904202339
	611.981	0.370	0.001772942	0.1772942	6.416700729	-0.994252273	-1.729944779
	611.981	0.370	0.000182589	0.0182589	6.416700729	-0.994252273	-4.003102647
	611.981	0.370	0.000664818	0.0664818	6.416700729	-0.994252273	-2.710827053
	611.981	0.370	0.000880049	0.088004898	6.416700729	-0.994252273	-2.43036281
	611.981	0.370	0.001295031	0.1295031	6.416700729	-0.994252273	-2.04405046
	611.981	0.370	0.00689566	0.689566	6.416700729	-0.994252273	-0.371692865
	611.981	0.370	0.008204566	0.8204566	6.416700729	-0.994252273	-0.197894264
	611.981	0.370	0.002920255	0.2920255	6.416700729	-0.994252273	-1.230914152
	611.981	0.370	0.003281318	0.3281318	6.416700729	-0.994252273	-1.114339922
	611.981	0.370	0.001014984	0.1014984	6.416700729	-0.994252273	-2.287712244
	611.981	0.370	0.001602206	0.1602206	6.416700729	-0.994252273	-1.831203663
	611.981	0.370	0.002335771	0.2335771	6.416700729	-0.994252273	-1.454243064
	611.981	0.370	0.001159359	0.1159359	6.416700729	-0.994252273	-2.154717827
	611.981	0.370	0.000815562	0.0815562	6.416700729	-0.994252273	-2.506462926
	611.981	0.370	0.001714495	0.1714495	6.416700729	-0.994252273	-1.763466516
	611.981	0.370	6.359E-05	0.006359	6.416700729	-0.994252273	-5.057884147
	611.981	0.370	0.001400706	0.1400706	6.416700729	-0.994252273	-1.965608698
	611.981	0.370	0.000741773	0.0741773	6.416700729	-0.994252273	-2.601297106
	611.981	0.370	0.002584797	0.258479744	6.416700729	-0.994252273	-1.352937946

Table D.12 Δ_{ff} values of Veysel Karani Station from Level 2 Method

#	V_S(m/s)	PGA(g)	Disp(m)	Disp(cm)	Ln(V_S,m/sn)	Ln(PGA)	Ln(Disp,cm)
STATION 12 - VEYSEL KARANİ STATION	285.938	0.260	0.002639632	0.2639632	5.655776653	-1.347073648	-1.331945579
	285.938	0.260	0.007983429	0.7983429	5.655776653	-1.347073648	-0.225217075
	285.938	0.260	0.00574141	0.574141	5.655776653	-1.347073648	-0.554880268
	285.938	0.260	0.002066595	0.2066595	5.655776653	-1.347073648	-1.576682768
	285.938	0.260	0.011234694	1.1234694	5.655776653	-1.347073648	0.116421576
	285.938	0.260	0.007230356	0.7230356	5.655776653	-1.347073648	-0.324296819
	285.938	0.260	0.003553595	0.3553595	5.655776653	-1.347073648	-1.034625326
	285.938	0.260	0.005632707	0.5632707	5.655776653	-1.347073648	-0.573994949
	285.938	0.260	0.001368128	0.1368128	5.655776653	-1.347073648	-1.989141711
	285.938	0.260	0.019311051	1.9311051	5.655776653	-1.347073648	0.65809243
	285.938	0.260	0.004857326	0.4857326	5.655776653	-1.347073648	-0.722097012
	285.938	0.260	0.003036367	0.3036367	5.655776653	-1.347073648	-1.191923358
	285.938	0.260	0.01315408	1.315408	5.655776653	-1.347073648	0.274146884
	285.938	0.260	0.011301135	1.1301135	5.655776653	-1.347073648	0.12231807
	285.938	0.260	0.034800375	3.4800375	5.655776653	-1.347073648	1.24704307
	285.938	0.260	0.03172576	3.172576	5.655776653	-1.347073648	1.154543876
	285.938	0.260	0.017248338	1.7248338	5.655776653	-1.347073648	0.545130698
	285.938	0.260	0.014965686	1.4965686	5.655776653	-1.347073648	0.403174888
	285.938	0.260	0.012912223	1.2912223	5.655776653	-1.347073648	0.255589289
	285.938	0.260	0.005392556	0.5392556	5.655776653	-1.347073648	-0.617565609
	285.938	0.260	0.020250512	2.0250512	5.655776653	-1.347073648	0.705594984
	285.938	0.260	0.009942964	0.9942964	5.655776653	-1.347073648	-0.005719928
	285.938	0.260	0.018724779	1.8724779	5.655776653	-1.347073648	0.627262634
	285.938	0.260	0.000377105	0.0377105	5.655776653	-1.347073648	-3.277816709
	285.938	0.260	0.004986222	0.4986222	5.655776653	-1.347073648	-0.695906584
	285.938	0.260	0.019259031	1.9259031	5.655776653	-1.347073648	0.655395001
	285.938	0.260	0.009722391	0.9722391	5.655776653	-1.347073648	-0.028153517
	285.938	0.260	0.008160063	0.8160063	5.655776653	-1.347073648	-0.203333203
	285.938	0.260	0.019319865	1.9319865	5.655776653	-1.347073648	0.658548748
	285.938	0.260	0.024327169	2.4327169	5.655776653	-1.347073648	0.889008699
	285.938	0.260	0.008322484	0.8322484	5.655776653	-1.347073648	-0.183624325
	285.938	0.260	0.006957793	0.6957793	5.655776653	-1.347073648	-0.362722767
	285.938	0.260	0.004814375	0.4814375	5.655776653	-1.347073648	-0.730978859
	285.938	0.260	0.008153347	0.8153347	5.655776653	-1.347073648	-0.204156575
	285.938	0.260	0.006905634	0.6905634	5.655776653	-1.347073648	-0.370247493
	285.938	0.260	0.002181936	0.2181936	5.655776653	-1.347073648	-1.522372537
	285.938	0.260	0.003458567	0.3458567	5.655776653	-1.347073648	-1.061730752
	285.938	0.260	0.008316931	0.8316931	5.655776653	-1.347073648	-0.184291776
	285.938	0.260	0.014725065	1.4725065	5.655776653	-1.347073648	0.386966051
	285.938	0.260	0.012712478	1.2712478	5.655776653	-1.347073648	0.239998938
	285.938	0.260	0.012693199	1.2693199	5.655776653	-1.347073648	0.238481245
	285.938	0.260	0.009584525	0.9584525	5.655776653	-1.347073648	-0.042435274
	285.938	0.260	0.010339094	1.0339094	5.655776653	-1.347073648	0.033347151
	285.938	0.260	0.024051716	2.4051716	5.655776653	-1.347073648	0.877621252